Pakistan Journal of Engineering and Technology, PakJET
Multidisciplinary | Peer Reviewed | Open Access
Volume: 2, Number: 1, Pages: 1- 8, Year: 2019

Recognition of Off-Line Hand-Written Alphabets Using Knowledge-Based Computational Intelligence

Muhammad Haseeb [1] and Ghulam Abbas [*,1]

[1] Electrical Engineering Department, The University of Lahore, Lahore 54000, Pakistan

[*] Corresponding author: Ghulam Abbas (e-mail: ghulam.abbas@ee.uol.edu.pk)

***Abstract*—The handwritten character recognition is considered an active recognition problem under the field of image processing and pattern recognition. Both areas of research have gained so much popularity in few last years due to technology advancements and necessity of time. The handwritten character recognition also becomes popular due to globalization and technology improvements. In previous time, the information was stored in written form only. To utilize that information, one needs such an advanced method which can do this task efficiently and without reliance on human. This work provides such a simplified and accurate method for the recognition of handwritten characters. A system is proposed to recognize characters using convolutional neural network (CNN) and is evaluated on a benchmark dataset named as EMNIST to show the performance of the proposed technique. The proposed system gains the accuracy of 97.62% which is better than various existing methods.**

***Index Terms*—Convolutional neural network, handwritten character recognition, EMNIST dataset.**

I. Introduction

Automatic recognition of characters is an important area and significant development in this area is already performed, although there is much scope to carry the research further. Successful models are deployed to recognize printed text for English and many other languages where the problem needs much attention for some languages. Handwritten character recognition is a similar area where the characters are not consistent and are written in cursive manner. There are two type of approaches to solve the problem of handwritten character recognition: one is online handwritten character recognition in which the writing strokes are noted and text is recognized; the other one is offline mode which is more complex as it involves the scanning of the handwritten text and then recognition of this text. Handwritten character recognition has many applications especially in digitization of historical documents and records, postal address and other such information. The task of offline handwritten character recognition has some complexities such as localization and recognition of handwritten text, and segmentation of characters in continuous text. Recognition of text can be important in helping visually impaired persons [1]. Such a system can be of help in provision of addition information to an autonomous navigation system. Moreover, text in natural images can provide rich information about the underlying scenes or images.

The current research focuses on unsupervised feature learning. There are few feature-learning algorithms which extract low-level representations of underlying data [2], [3] and provide an alternative to hand-engineered features. These types of algorithms have achieved success in some visual recognition tasks [4]. In text recognition task, the model in [5] has achieved good performance in text localization and character recognition. The model relies on scalable and simple feature-learning architecture which does not depend on hand-crafted features or prior knowledge. The task of feature learning and character recognition is performed using convolutional neural network (CNN). CNNs are layered neural networks which have good representational capacity and are applied to various problems such as object recognition [6], handwritten text recognition [7], and character recognition [8].

The proposed method is experimented using scanned images which are not noise-free and the neural network is used for recognition of character. The characters which are used for recognition are English alphabets. Surf Feature Extraction method is used to perform the complete recognition along with Neural Network. The proposed algorithm provides usable results in terms of PSNR and MSE (which are used for evaluation of the technique) as compared to existing methodologies for the task of character recognition. The overall work is based on character recognition with reduced noise and enhancement of image quality with different levels of noise and eventually makes the technique suitable for both

image processing and pattern recognizing tasks.

II. Neural Networks

A. Neural Networks' Background

Neural networks try to solve the problem with a different approach inspired from human visual cortex. The neural network is formed with several neurons, cascaded in progressive layers with multiple interconnections. These neural networks are provided with a large number of handwritten characters with labels, referred as training set, and automatically form rules by adjusting the weights of neural connections for recognition of handwritten characters. The recognition accuracy of the neural network increases by increasing the number of training examples.

B. Neural Networks' Architecture

Neural networks have different parts and each of them can be described with their specific name. The leftmost layer of neural network shown in Fig. 1 is named input layer and the neurons in this layer are called input neurons. All the inputs to the neural network are provided through input neurons only. The rightmost layer of the neural network is called the output layer and neurons contained in this layer are called output neurons. The neural network contains only one output neuron but it could be more than one, depending on the number of output states. The middle layers of the neural networks are called hidden layers because these neurons are neither accessible at input nor at output. The term hidden layer sounds mysterious but it is called so only because it is not visible to input or the output. Neural network shown in Fig. 1 has two hidden layers but it can have single or multiple layers depending on complexity.

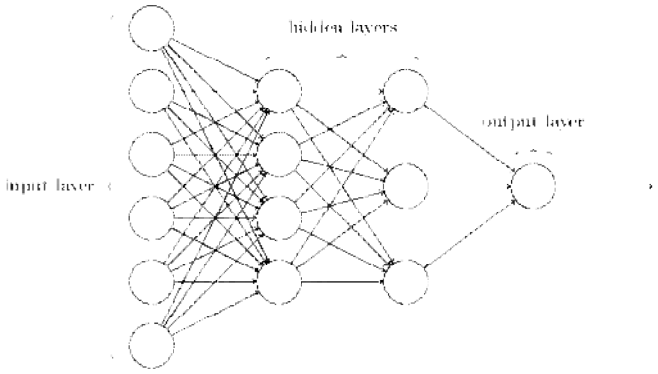

Fig. 1. Architecture of neural network with two hidden layers.

The number of input and output neurons depends on the input variables and the output states respectively. For example, if we want to determine whether the character is "*C*" or not. If the input image size is 32 by 32 pixels with grayscale intensities, there would be a total of 32×32=1024 neurons in the input layers encoding the grayscale intensities from zero to one. The output layer will contain only one neuron with values greater than or less than 0.5, indicating "*C*" if the value is greater than 0.5 and "not a *C*" in case the value is less than 0.5.

III. Convolutional Neural Networks

The feed forward neural networks have input and output layers along with single or multiple hidden layers. All the neurons in each subsequent layer are fully connected to each neuron in next layer as shown in Fig. 2. The problem with such network is that fully connected layers do not make much sense in character recognition. The reason is that they do not take into account the spatial structure of pixels, i.e. the pixels which are adjacent and far away from one another have similar value. The concept of spatial structure is needed to be incorporated in such a way that instead of starting from a series of input neurons, we have a matrix of input neurons. This concept results in the development of convolutional neural networks (CNNs). CNNs use a special architectural design which has particular adaptability for image classification. The use of this special architectural design makes them faster to train. This strategy is useful in training of many-layered networks (deep) which are especially useful at image classification.

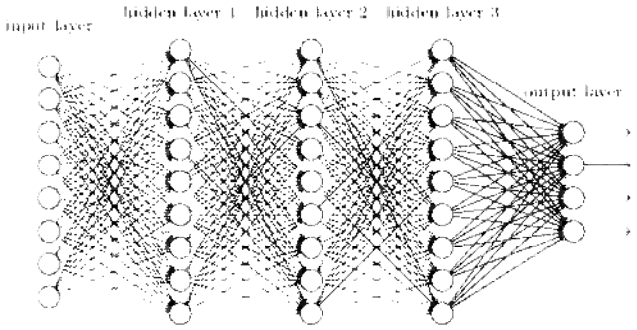

Fig. 2. Fully-connected feed forward neural network.

CNNs are based on three basic ideas: pooling, shared weights and local receptive fields.

A. Local Receptive Fields

To be more exact, every neuron in the main shrouded layer associates with a little locale of the information neurons, say, for instance, a 5×5 area, relating to 25×25 entered pixels. In this way, for a specific shrouded neuron, we may have associations that resemble as shown in Fig. 3.

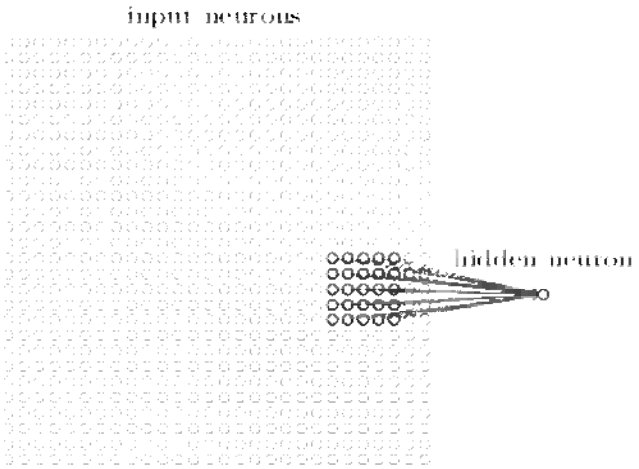

Fig. 3. Local receptive field of 5×5.

That region of the input image is known as the local receptive field for the hidden neuron. It is a little window on the input pixels. Every association learns a weight. Furthermore, the hidden neuron also calculates a bias. We, at that point, slide the local receptive field over the whole input image. For every local receptive field, there is an alternate hidden neuron in the primary hidden layer. The local receptive field is slided to right by one neuron (i.e. one pixel) and it is connected to another neuron in the hidden layer. Then we slide the local receptive field over by one pixel to the right, to connect to a second hidden neuron (see Fig. 4).

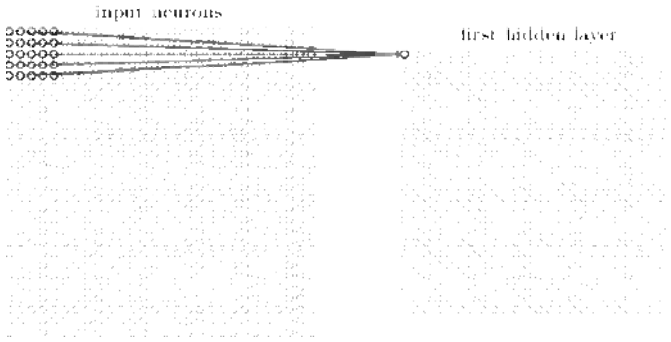

Fig. 4. Connection of local receptive field with hidden neurons.

Continuation of the same operation yields first hidden layer. When we have a 28×28 neurons in the input image, and length of local receptive field five, there will be 24×24 neurons in the first hidden layer. This is on the grounds that we can just move the local receptive field crosswise over or downward, before crashing into the right-hand side or base of the input image. The movement of local receptive field in this image is 1 pixel but it could be increased as per the requirement. This is called stride length and researchers have experimented with different stride lengths to observe the behavior of deep convolution CNN.

B. Shared Weights and Biases

In this demonstration, the local receptive field has a size of 5×5 weights connected to hidden neurons. It is worth mentioning that the weight and biases are shared and same weights and biases are used for all 24×24 neurons in the first hidden layer. Mathematically, for all i and j_{th} hidden neurons, the output is:

$$\sigma\left(b+\sum_{i=0}^{4}\sum_{j=0}^{4}w_{l,m}\alpha_{i+l,j+m}\right) \tag{1}$$

In (1), σ is the sigmoid activation function; b is the bias value shared with other pixels; w is the array of shared weights; α denotes the input activation at a specified position represented by i, j.

This phenomenon of shared weights and biases means that first hidden layer detects exactly the same feature. The notion of the feature is to extract hidden layer from local receptive field. This learned feature may be an edge or corner in the image which could occur anywhere in the image and can be used as a useful feature. CNNs are adjusted well in respect of translation invariance. The map which gets translated from input image to hidden layer is sometimes called as feature map. The feature map can be more than one in most of the cases and each feature learns a specific image feature. Fig. 5 shows 20 different feature maps learned during first hidden layer. Each small image indicates a 5×5 weight of local receptive layer.

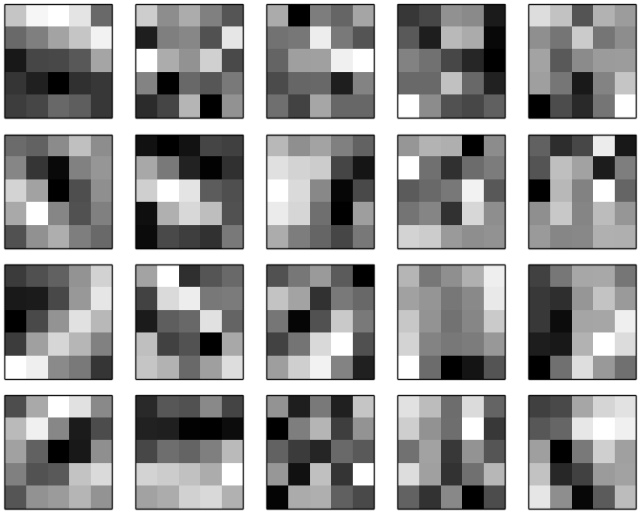

Fig. 5. 20 feature maps of 5×5 learned by convolution net.

C. Pooling Layers

Convolution neural network's basic unit is convolution layer described previously. Pooling layer is also an integral layer which is used just after the convolutional layer. This layer simplifies the information from the previous convolutional layer. A pooling layer simplifies the output from the convolutional layer. For example, a unit of pooling layer can take a 2×2 block and condense the information into a single neuron. Some common pooling operation may be max-pooling or average-pooling in which the output takes the maximum or average of 2×2 input block, same as demonstrated in Fig. 6.

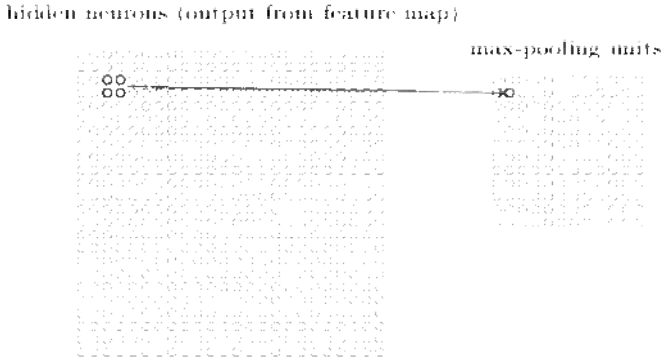

Fig. 6. Max-pooling operation on 2×2 block.

Pooling layer results in further reduction in size of convolution layer's output. For a 24×24 layer produced from the convolutional layer, the pooling layer of size 2×2 produces an output of 12×12 neurons as shown in Fig. 7.

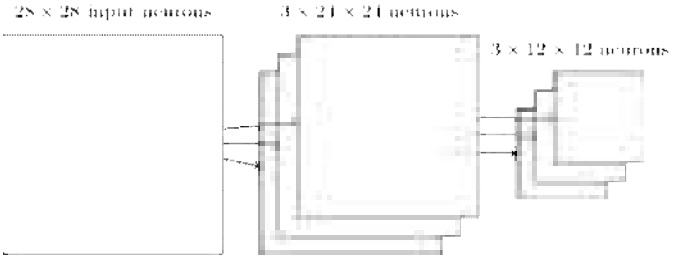

Fig. 7. Structure of cascaded convolution neural network's layer after pooling operation.

Putting all the configurations in final form results into a convolution neural network of Fig. 8. The output of pooling layer is connected to sigmoid neurons placed in vertical fashion which may be less than the total neurons in the previous layer. This layer is a fully-connected layer, i.e. every neuron is connected with all the neurons in the sigmoid layer. The final (output) layer is a softmax layer which provides a normalized output for output. The number of neurons in the output layer depends on the total number of classes, and the neuron of softmax layer with highest normalized value describes the correct class of the image.

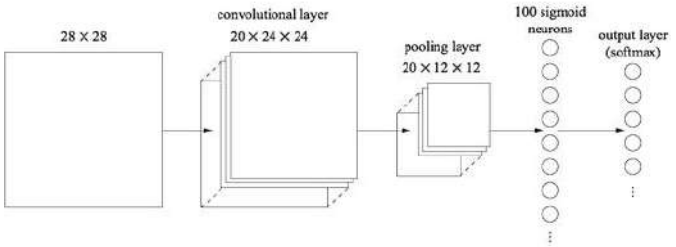

Fig. 8. Simplified structure of a convolution neural network for handwritten characters recognition.

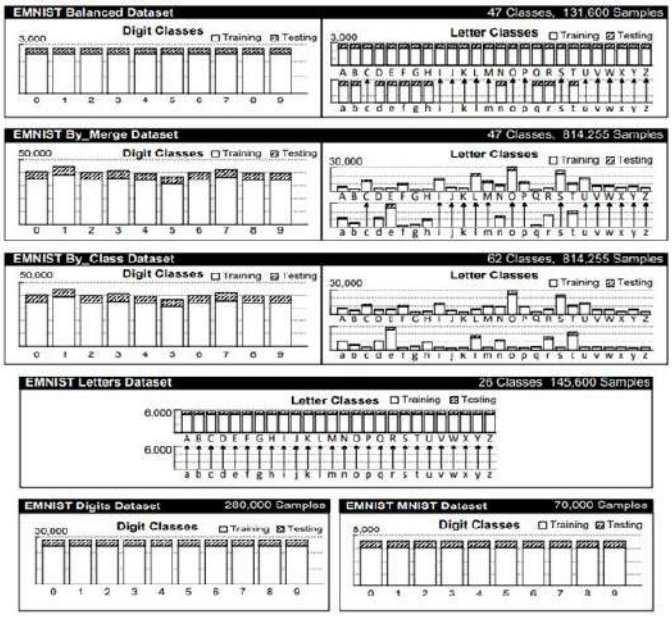

Fig. 9. Visual representation of the EMNIST dataset.

IV. Methodology

A. Handwritten Character Recognition

Despite the inherent differences between the text detection and character recognition tasks, structurally identical network architectures for both the text detector and character classifier are used. State-of-the-art performance is to be achieved on the EMNIST dataset.

B. Dataset

For the task of handwritten character recognition large number of handwritten character images are required and the plenty of datasets are available online to use. To evaluate the performance of the proposed work, the EMNIST dataset [9], which is the derived form of NIST special database 19, is used. This dataset contains handwritten character images in form of six different splits as shown in Fig. 9.

C. Hand Character Recognition Steps

Various steps involved in recognizing the hand-written characters are depicted in Fig. 10.

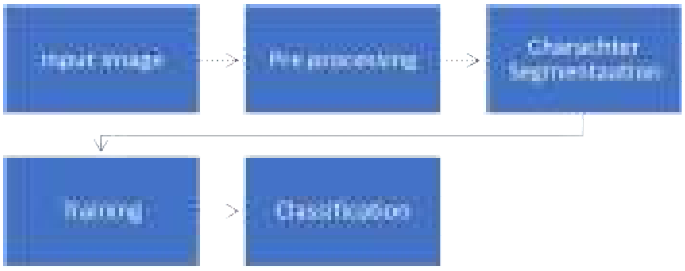

Fig. 10. Hand character recognition steps.

1) Preprocessing

The first task for hand character recognition is preprocessing of the input image. First, an image input is given to the system and then skew correction of the image is performed to get the correct alignment. After converting RGB image into grayscale, we have used Otsu algorithm for black and white image conversion. Conversion of image is performed using Otsu algorithm [10]. The next task is to remove the noise from black & white image and for that first image is inverted and then 3×3 median filter is applied. The morphological operations have their own importance in recognition task and in this scenario, we have used 60 pixels as a threshold and images less than 60 pixels are removed. Further, we need clear stroke of image and that is done by applying morphological thinning filter.

2) Character Segmentation

The next task is to segment the single character as a single image and for that first connected regions are selected ranging from 200-30000 pixels. Then character extraction is achieved by applying horizontal thresholding and a single character is stored as an image. As EMNIST dataset has images of 28×28 pixels, the input image is also resized by 28×28 after applying centralization of image. All above steps are applied during testing phase and the system learns from data.

3) Training

When dealing with neural networks, training is an important phase as the whole performance of the system relies on how your system is trained. In short, the performance is as better as your training of the data. For the present scenario, the EMNIST dataset is already trained but we need to explain the process for testing of system as whenever a new input comes, how it will learn from the system.

a) Architecture of Neural Network

Neural network basically has input, hidden and output layer and in the present study we have used a seven-layered neural network in which:

- First layer is of 28×28 pixel input layer or of 784 neurons (28×28=784).
- The second layer is 2-dimensional convolutional layer with local receptive field of 5×5 pixels and extracts 20 features, and rectified linear unit is used as an activation function.
- The next layer is 2-dimensional max-pooling layer of 2×2 with stride length of 2 pixels.
- The fourth layer is the fully connected layer of 62 elements neurons.
- Then there is the softmax layer which helps into mapping of the input to the real or correct value.
- The sixth layer is classification layer and classifies the input as a correct character.
- The last is the output layer which shows the recognized character.

b) Training Parameters

Stochastic Gradient Descent: The stochastic gradient descent is basically gradient vector and the purpose of using this is learning of neural network as it provides suitable weights and biases which are helpful in minimizing the cost of network. It works by recurrently calculating the gradient ΔC which is further passed in opposite direction, falling down, as shown in Fig. 11 [11]. Training options used for our work are shown in Fig. 12.

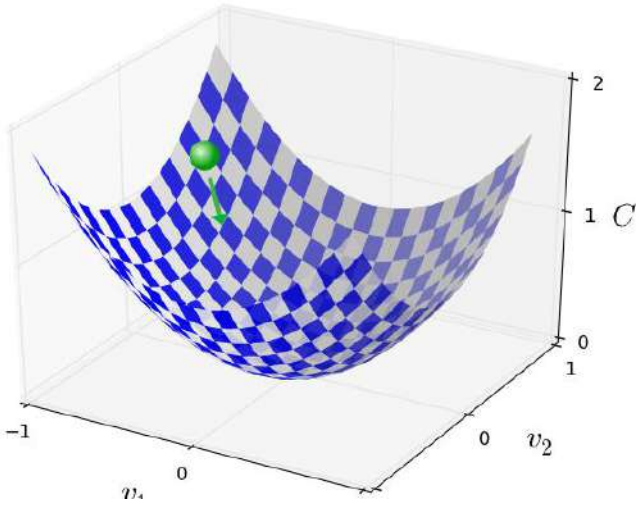

Fig. 11. Slope of stochastic gradient descent.

```
options =

  TrainingOptionsSGDM with properties:

                     Momentum: 0.9000
                 InitialLearnRate: 1.0000e-04
        LearnRateScheduleSettings: [1×1 struct]
                 L2Regularization: 1.0000e-04
          GradientThresholdMethod: 'l2norm'
                GradientThreshold: Inf
                        MaxEpochs: 20
                    MiniBatchSize: 128
                          Verbose: 1
                  VerboseFrequency: 50
                    ValidationData: []
               ValidationFrequency: 50
                ValidationPatience: 5
                          Shuffle: 'once'
                   CheckpointPath: ''
             ExecutionEnvironment: 'auto'
                      WorkerLoad: []
                       OutputFcn: []
                           Plots: 'none'
                 SequenceLength: 'longest'
             SequencePaddingValue: 0
```

Fig. 12. Training options.

Epochs: In neural network while training of data, we need to update the weights and for that purpose we need a parameter to define the number of iterations of training vector before updating a weight value. The maximum number of epochs used is twenty (20). Progression of epochs is shown in Fig. 13.

```
Training on single CPU.
Initializing image normalization.
|=========================================================================================|
|  Epoch  |  Iteration  |  Time Elapsed  |  Mini-batch  |  Mini-batch  |  Base Learning  |
|         |             |   (hh:mm:ss)   |   Accuracy   |     Loss     |      Rate       |
|=========================================================================================|
|       1 |           1 |       00:00:00 |       2.34% |       5.4756 |    1.0000e-04 |
|       1 |          50 |       00:00:02 |      70.31% |       1.0910 |    1.0000e-04 |
|       1 |         100 |       00:00:05 |      76.56% |       0.9263 |    1.0000e-04 |
|       1 |         150 |       00:00:07 |      76.56% |       0.8804 |    1.0000e-04 |
|       1 |         200 |       00:00:10 |      79.69% |       0.6904 |    1.0000e-04 |
|       1 |         250 |       00:00:13 |      85.94% |       0.4960 |    1.0000e-04 |
|       1 |         300 |       00:00:15 |      81.25% |       0.5008 |    1.0000e-04 |
|       1 |         350 |       00:00:18 |      82.81% |       0.5121 |    1.0000e-04 |
|       1 |         400 |       00:00:21 |      89.84% |       0.3411 |    1.0000e-04 |
|       1 |         450 |       00:00:24 |      89.06% |       0.2709 |    1.0000e-04 |
|       1 |         500 |       00:00:26 |      92.97% |       0.2707 |    1.0000e-04 |
|       1 |         550 |       00:00:29 |      94.53% |       0.2032 |    1.0000e-04 |
|       1 |         600 |       00:00:32 |      95.31% |       0.1603 |    1.0000e-04 |
|       1 |         650 |       00:00:35 |      88.28% |       0.4730 |    1.0000e-04 |
|       1 |         700 |       00:00:38 |      85.16% |       0.4002 |    1.0000e-04 |
|       1 |         750 |       00:00:41 |      91.41% |       0.3464 |    1.0000e-04 |
|       1 |         800 |       00:00:44 |      87.50% |       0.3873 |    1.0000e-04 |
|       1 |         850 |       00:00:47 |      87.50% |       0.4149 |    1.0000e-04 |
|       1 |         900 |       00:00:49 |      91.41% |       0.2744 |    1.0000e-04 |
```

Fig. 13. Training of data.

Learning Rate: The learning rate of network is kept 0.0001.

4) Classification

After the training of the data, next is to use it for system evaluation which means to correctly classify the input image with what handwritten character it is. The 80% of the data is used for training and the 20% is used for the testing task. It means that the 20% data is used to classify and, the collected classification measure is the achieved accuracy of our handwritten character recognition system.

V. Results and Discussion

After explaining the complete methodology used for handwritten character recognition, we are in a state to explain the results achieved through the process and also the

evaluation measures used. The proposed system uses convolutional neural network for character recognition task. By performing all the essential steps, our system correctly identifies the characters as shown in Figs. 14 to 21.

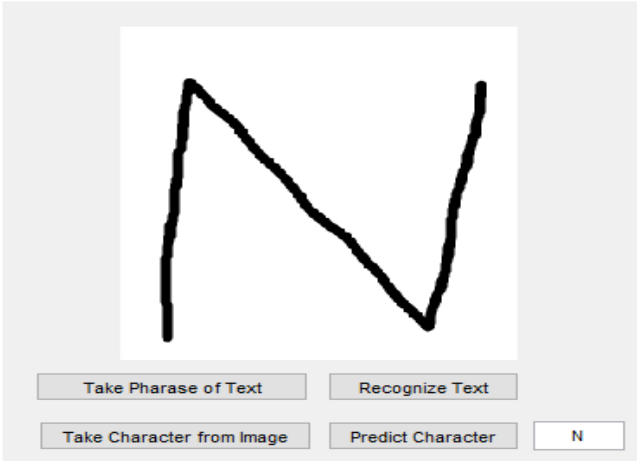

Fig. 14. Single character recognition (1).

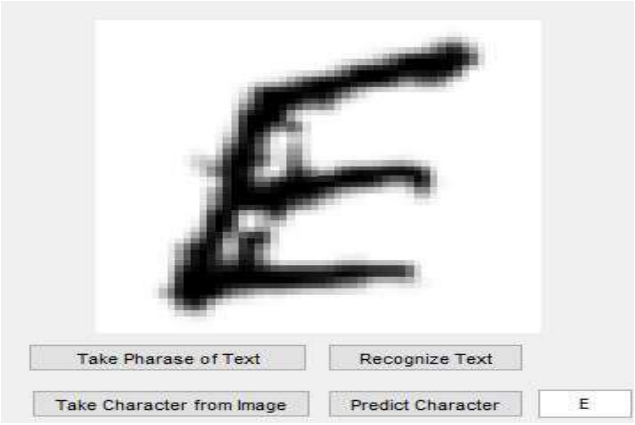

Fig. 15. Single character recognition (2).

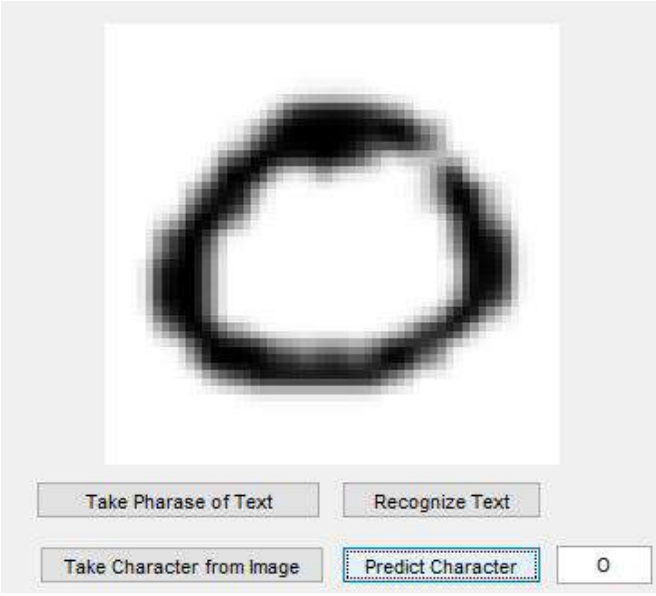

Fig. 16. Single character recognition (3).

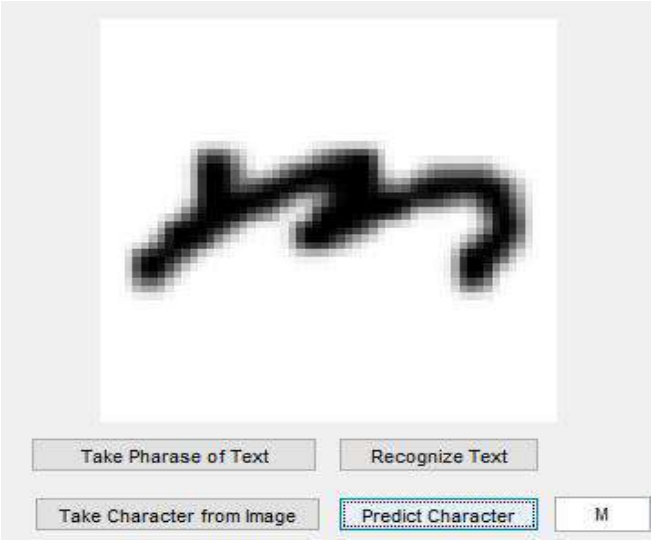

Fig. 17. Single character recognition (4).

Fig. 18. Single character recognition (5).

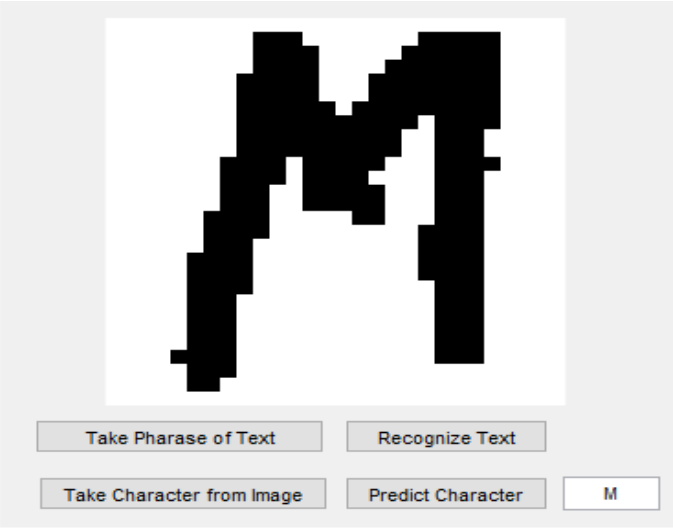

Fig. 19. Single character recognition (6).

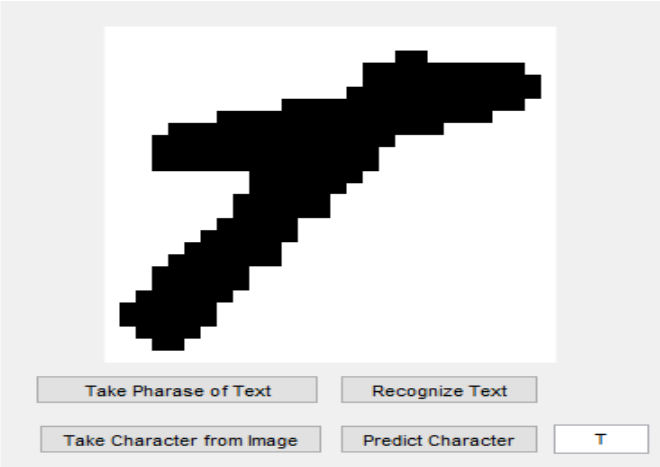

Fig. 20. Single character recognition (7).

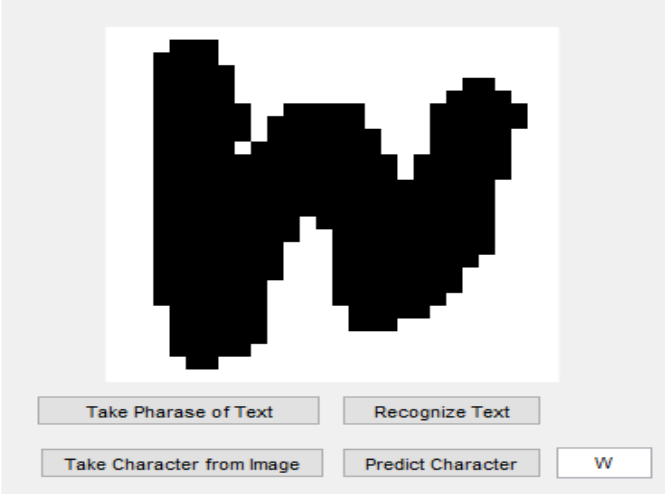

Fig. 21. Single character recognition (8).

Not only the single characters are identified through the system but also the phrase is also correctly recognized as shown in Figs. 22 to 24. The main difference between single character and phrase recognition is that for single character recognition we need the character segmentation but in case of phrase recognition we have to skip segmentation step.

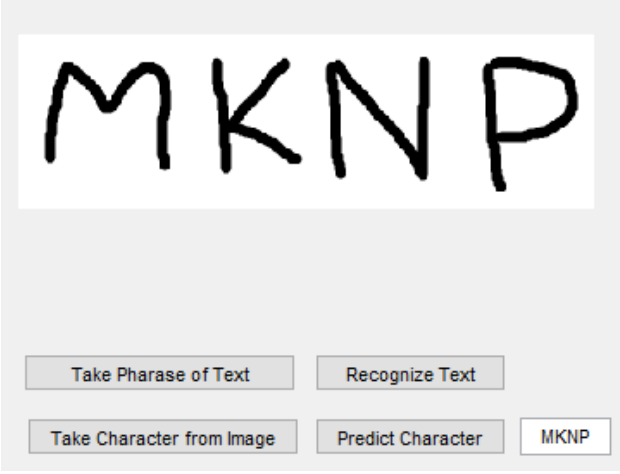

Fig. 22. Phrase recognition (1).

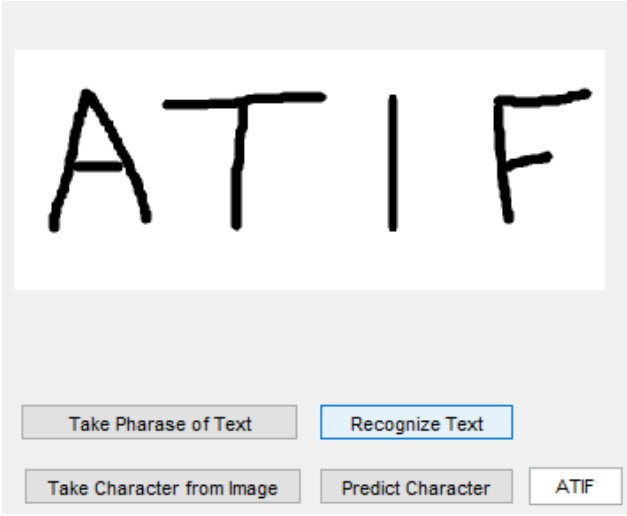

Fig. 23. Phrase recognition (2).

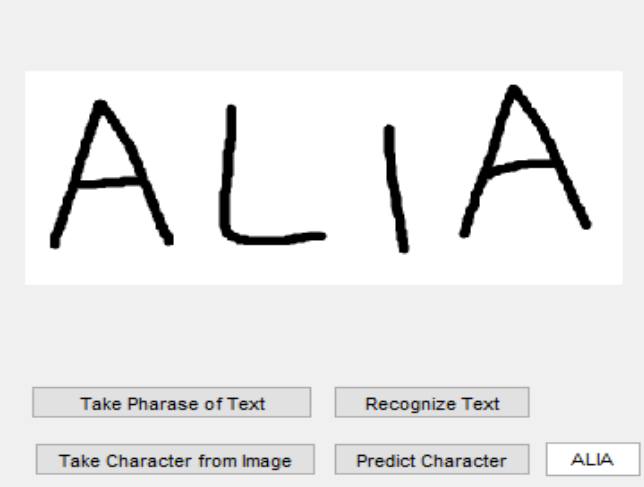

Fig. 24. Phrase recognition (3).

This study is mainly carried out for handwritten character recognition problem using convolutional neural network, which means to train your computer to perform the task automatically instead of human dependence. The convolutional neural networks are famous these days due to their outstanding performance on almost every kind of problem. For the present case, we have used a seven layered network which takes input of 28×28 pixel image. The recognition problem depends on the type of characters you are dealing with. Say for example if we only have to recognize single digit then we can simply use ten output neurons which is required to match the digit from 0 to 9. Furthermore, task is slightly different when the recognition subject is different but the main functionality of the system remains same throughout the process. In training parameters, we have used stochastic gradient descent method during the learning of neural network which is commonly used among researchers for learning of neural network. The mini batch size during training is 128.

To evaluate the performance of our system we need to define some kind of evaluation measure and the %Accuracy is the widely used measure to compare or analyze the system

performance. The accuracy can be calculated as:

$$\%Accuracy = \frac{Correctly\ recognized\ samples}{Total\ number\ of\ samples\ in\ dataset} \times 100 \qquad (2)$$

The proposed system is tested using EMNIST dataset and on the given dataset our system has achieved best accuracy of 97.62% which means our system performs significantly better and also outperforms various major methods.

VI. CONCLUSIONS

The task of recognition is so far an active research area due to its high demand and dependence of human writing scripts. Even if every type of structural, topological and statistical measures of characters are obtained, even then still the work of recognition is left due to a lot of variation in languages, their writing styles and also the writing mood of a person. Hand character recognition system is the capability of a system to take input of a written image to recognize it automatically. The input is normally used in the form of a scanned image of required character. The hand-written characters are recognized successfully in this work using CNN. This network uses different layer for the task completion and the purpose of these layers is to reduce the processing. The performance of the system on the dataset was as good as of humans in a lot of cases which have made these networks a real use of the time. But also, it is tough to recognize small characters which are written in smaller fronts because the parameters for such characters and their recognition need other careful implementation. The recognition of handwritten character is done using its scanned image of 28×28 pixels. Our proposed system works on seven-layered convolutional neural network, and characters are initially separated through using segmentation technique. Through the proposed system, we can recognize individual characters as well as phrases. The performance of the system is evaluated using accuracy measure on EMNIST dataset which is a most popular dataset for training and testing of machine learning applications. The overall proposed system after training and testing has proved its worth. For the recorded observations, the system achieves accuracy of 97.62% which makes the proposed method usable for hand character recognition tasks.

REFERENCES

[1] R. Ani, E. Maria, J. J. Joyce, V. Sakkaravarthy and M. A. Raja, "Smart Specs: Voice assisted text reading system for visually impaired persons using TTS method," *2017 International Conference on Innovations in Green Energy and Healthcare Technologies (IGEHT)*, Coimbatore, 2017, pp. 1-6.

[2] J. Pradeep, E. Srinivasan and S. Himavathi, "Diagonal based feature extraction for handwritten character recognition system using neural network," *2011 3rd International Conference on Electronics Computer Technology*, Kanyakumari, 2011, pp. 364-368.

[3] R. Verma and R. Kaur, "An Efficient Technique for character recognition using Neural Network & Surf Feature Extraction," *International Journal of Computer Science and Information Technologies*, vol. 5, no. 2, pp. 1995-1997, 2014.

[4] M. I. Jubair and P. Banik "An Approach to Extract Features from Document Image for Character Recognition," *Global Journal of Computer Science and Technology*, 2013.

[5] M. A. Rahiman and M. S. Rajasree, "Printed Malayalam Character Recognition Using Back-propagation Neural Networks," *2009 IEEE International Advance Computing Conference*, Patiala, 2009, pp. 197-201.

[6] V. P. Agnihotri, "Offline Handwritten Devanagari Script Recognition," *Information Technology and Computer Science*, vol. 8, pp. 37-42, 2012.

[7] R. Alaasam, B. Kurar, M. Kassis and J. El-Sana, "Experiment study on utilizing convolutional neural networks to recognize historical Arabic handwritten text," *2017 1st International Workshop on Arabic Script Analysis and Recognition (ASAR)*, Nancy, 2017, pp. 124-128.

[8] C. Wu, W. Fan, Y. He, J. Sun and S. Naoi, "Handwritten Character Recognition by Alternately Trained Relaxation Convolutional Neural Network," *2014 14th International Conference on Frontiers in Handwriting Recognition*, Heraklion, 2014, pp. 291-296.

[9] G. Cohen et al, "EMNIST: an extension of MNIST to handwritten letters," *arXiv preprint arXiv:1702.05373*, 2017.

[10] M. Yongli and H. Zhikai, "The study of segmentation of rubbings image based on OTSU&histogram differential algorithm," *2017 International Conference on Computer, Information and Telecommunication Systems (CITS)*, Dalian, 2017, pp. 171-175.

[11] R. Johnson and T. Zhang, "Accelerating stochastic gradient descent using predictive variance reduction," *Advances in neural information processing systems*, 2013.

Pakistan Journal of Engineering and Technology, PakJET
Multidisciplinary | Peer Reviewed | Open Access
Volume: 2, Number: 1, Pages: 9- 17, Year: 2019

Demand side Management for SMART Grid

Hasnain Atif[1] and Hafiz Tehzeeb ul Hassan[*,1]

[1] Electrical Engineering Department, The University of Lahore, Lahore 54000, Pakistan

[*] Corresponding author: Ghulam Abbas (e-mail: tehzeebul.hassan@ee.uol.edu.pk)

***Abstract*—**In this paper, we are going to suggest a prominent feature of smart Grid i.e. Demand side management. Smart grid is up to date facility used for bi-communication system of Generation, transmission and consumption. The fundamental principle of smart grid is demand response analysis. For supposition, we focus on three type of frequently used load which are base, continuous and discrete load. A sufficient volume of load in the form of diversified appliance of different power rating would be considered. Our main objective is the reduction of peak to average ratio enhances the efficiency of smart grid. For this, a revived scheme of electricity consumption pattern is required keeping in consideration reliability, feasibility and user preference. Subsequently, it will decrease the electricity production and consumption cost. Increasing the number of appliances would complicate the problem to some extent so making it more challenging. In theoretical work small numbers of appliances are taken. Genetic algorithm would be used to solve this specific problem. Simulation results would show the prove that there is an ultimate reduction in the cost by using the algorithm.

Index Terms—Genetic algorithm; Load scheduling; Smart grid; Energy management; Demand side management.

I. INTRODUCTION

Integration of latest communication and control techniques in the traditional grid system for the efficient way of transmission and distribution of electricity is called smart grid. Two main objectives are reduction in electricity cost by effective load management technique and decline in global warming by subsequent reduction in carbon emission. Demand side management is the prominent feature of smart grid for load management. Another unique feature of smart grid is dynamic pricing through the use of smart meter and automatic metering techniques; load in accordance to dynamic pricing scheme can be managed easily.

Dynamic pricing scheme are widely used to bring efficiency in grid system. Through pricing signal, user is enabled to modify its schedule. Keeping in consideration the next pricing scheme. This integration of dynamic pricing and user response. Primarily serve the reduction in peak to average ratio (PAR).For this different pricing scheme like Day-ahead pricing. Times of use, peak hour pricing or Real Time Pricing are used. All of these are expected nature except Real Time Pricing (RTP).

It is also very effective from market point of view. Change in the consumption pattern alters the electricity prices accordingly. Thus, the whole system brings the economy of production. The desired pattern of the load shape and the power network is achieved by the modification of consumer pattern through demand side management. Consequently the load, with the user will. Is shifted from peak hour to off-peak hours, to reduce the cost.

Normally we apply six methods to shape loads of different types. These are peak clipping, valley filling, load shedding, flexible load shape, strategic conservation and strategic load growth.in peak clipping and valley filling method load is reduced by shifting it from peak to valley .by manipulating demand at consumer end, load demand is reduced in strategic conservation [1] method. Contrary to it, in strategic load growth [1-3] method demand is produced in off-peak hour that is at valley.in strategic load growth demand is modified only for those customer whose consent has attained and are ready to take part in DSM modeling. In case of load shedding we shift the load from peak hour to off-peak hour through scheduled load shedding

II. RELATED WORK

In [4] the role of communication technologies resources in the development of demand side management of a smart grid is discussed. Communication technologies are different from

traditional computation in a way that they can easily map the applications separately. In Demand side management (DSM) we generally focus on the economic efficiency of the given system. A novel cost oriented optimization model is proposed to map the cloud computing resources in the cost efficient way. Uncertain factors are also considered in this research work which may include load prediction and unavailability of computing instances.

In [5] the price based and reward based approaches are used to propose the demand side management scheme of the cyber-physical smart distribution system. The fundamental objective is to maximize the profit. This research work also left consumers to choose economic criteria. The proposed frame work is being evaluated using IEEE 37 bus test system.

In [6] the contribution of renewable energy source along the demand side management (DSM) scheme of the grid is studied. Day ahead optimization process is used to reduce the monetary expenses of the consumers. The proposed algorithm is tested in a realistic scenario.

One of the key factor of demand side management (DSM) scheme is discussed in [7]. Demand response is a key factor of demand side management. In demand response strategy the consumer described its load plan to the supplier discussed the price scheme with the consumers.

Both parties are the beneficiaries in this scenario. it reduces the overall bill thus an incentive for consumer. It also helps to lessen the peak to average ratio which is beneficial for the supplier. As the additional power sources are not required and the fuel cost can be saved.

In [8] the monitoring of energy meters by using 'Internet of Things'(IoT) is discussed. In this way supplier can buy surplus energy from consumer. In this work dynamic pricing problem is achieved by a convex optimization problem. In this research work it is proved that the energy is distributed in the system in an efficient way.

In [9] an instantaneous load billing scheme attracts the consumer to shift their load from peak hour to the off-peak hours. Condition for the existence of Nash equilibrium is also analyzed through this paper. In this research work there is no concept of central unit. Consumer share information with their neighbor by using distributed synchronous agreement based algorithm and gossip based algorithm.

In [10] a smart architecture is proposed to manage the load in smart buildings. The architecture is composed of the layered structure. Hence it allows the seamless integration of diverse techniques for optimal scheduling and dynamic pricing. The results are generated by using Matlab and the efficiency of the proposed work is confirmed.

In [11] in order to maintain coordination between consumer and supplier a new energy price scheme is put forward. We minimize the difference between the value and the cost of energy by an entirely new objective function.. The main objective is to minimize the peak to average ratio (PAR). The performance is finally evaluated through computer based simulations.
In [12] to evaluate demand side management (DSM) a methodology is proposed based on elasticity and time of use pricing concepts.

In [13] an optimization problem is suggested to minimize the price of consumption. An algorithm is proposed in a way that if minimizes the consumer's wait time and by doing so it enhances the consumer's comfort level.

In [14] the overload problem in thermal generation is addressed by hybrid distribution methodology. In this research work for power flow management, demand distribution along with demand response is controlled. The control action is evaluated through companies.

In [15] an instantaneous load billing scheme is adopted to attract the consumers. The objective function is implemented by analyzing the conditions for the existence of Nash equilibrium.

In [16] the concept of zero energy building is discussed. Renewable energy is supplied by using solar panel which also has the connection with grid. A control system controls the electrical technical building system.

In [17] the paid scheme of the user depends upon the energy profit of the consumer. Distributers put their maximum effort to diminish the difference between the instantaneous energy demand and average demand of the power system. By the game theory methodology user voluntarily cut down their consumption cost.

The minimization of peak to average ratio (PAR) of the load is accomplished by real time pricing scheme [18]. The user and the distributor communicate with each other to find the optimal prices. By doing this, the supplier can overcome the uncertainty of the load attached by the consumer and user can estimate the price of the energy consumed by the attached load.

In [19] the importance of smart grid (SG) over the traditional grid is described. Smart grids have some features which are not present in traditional grids like intelligence, adaption and flexibility to reduce the effect of outages in the society. An optimized methodology is discussed in this paper which increases the robustness of the smart grid (SG).

III. PROBLEM FORMULATION

Different types of appliance have different energy consumption. Each appliance shares the information of its type with energy management controller (EMC) which the schedule them accordingly. Price signal is supposed real time in nature, we multiply the hourly price signal with the energy utilized by the consumer at that time slot. So, the cost of energy consumption is given by following expression

Minimize

$$\sum_{t=1}^{24}\sum_{a=1}^{n}\sum_{b=1}^{m}\rho_{ab}(t)\times \text{ṅ}_{ab}(t)\times\omega(t) \ldots.1$$

Subject to

$$\sum_{t=1}^{24}\sum_{a=1}^{n}\sum_{b=1}^{m}\rho_{ab}(t)\times \text{ṅ}_{ab}(t)\leq \text{ɀ}(t).....2$$

$$\sum_{t=1}^{24}\sum_{a=1}^{n}\sum_{b=1}^{m}\rho_{ab}(t)=OPT_{ab}.....3$$

$$\beta_a\leq 24-OPT_a \qquad \forall\ DL \ldots\ldots\ldots\ldots 4$$

$$\beta_a^s\leq\beta_a\leq\beta_a^s+OPT_a \quad \forall\ CL.....5$$

$$\beta_a=\beta_a^s \qquad \forall\ BL \ldots\ldots 6$$

$$\nabla_{Scheduled}<\nabla_{Unscheduled}.....7$$

$$\partial_{Scheduled}^{T}=\partial_{Unscheduled}^{T}.....8$$

$$\epsilon_{min}\leq\ \epsilon\leq\epsilon_{max} \ldots\ldots\ldots\ldots\ldots\ldots\ldots 9$$

$$\partial(t)-\ \epsilon(t)>0 \ldots\ldots\ldots\ldots\ldots\ldots\ldots\ldots 10$$

$$\rho\in\{0,1\}.....11$$

$OPT_{ab}=duty\ cycle$

$\text{ṅ}_{ab=}$ Power utilized by the appliance a of type b
$\rho_{ab=}$ ON/OFF state of appliance a of type b
$\omega(t)=price\ during\ time\ interval\ t$
ɀ(t)= max. Power limit at time interval t
$\beta=peak\ load$
$\epsilon=energy\ from\ RES$

Equation 2 represents that the energy consumption at that time is less than the maximum power limit at time interval 't' resulting reduction in peak to average ratio. The length of operational time will be equal to ON/OFF state of appliance is represented by equation 3. Equation 4 shows that the discrete load can be scheduled in any time slot of the whole day. Equation 5 shows that for continuous load duty cycle is not interruptible. It means, once a load is connected, it cannot be removed unless it completes its duty cycle. Equation 6 shows that for basic load, there is continuous duty cycle throughout the day consequently we cannot apply demand side management (DSM) scheme here or load cannot be shifted.
Equation 7 shows that the peak of scheduled load is less than the peak of unscheduled load. Equation 8 shows that total load connected remain same whether applying algorithm or without algorithm. Equation 9 shows that the energy from renewable source will be greater than minimum load energy and less than maximum load energy. It means some power needed from wapda. Equation 10 shows that the difference between total connected load and renewable energy source will be positive. It means we cannot sale energy to wapda but we buy energy from wapda while equation 11 shows that the state of appliance whether it is in ON state or OFF state.

IV. PROPOSED ALGORITHM FOR DSM

Chromosomes of the population represent a viable solution to our problem i.e. it would be our main concern. Chromosomes represent the array of bits whose length is equal to number of appliances. Status of each bit demonstrates whether the appliance is ON/OFF. The number of controllable appliance which represents the length of chromosome is represent by 'N'. Following are the major steps of Genetic Algorithm (GA).

Initial Population:

It is the first step towards Genetic Algorithm. User preference is the factor upon which the variation of dimension of initial population depends upon. There is a direct relation by the accuracy of solution and the number of population. However, increasing the population brings more complication to the algorithm. Suppose the initial population is M×N where 'M' is the population size and 'N' is the number of appliance.

Fitness Evaluation:

At this stage, fitness evaluation is done for each chromosome. For the purpose of representation, we suppose a chromosome [1 0 1 0 1 0 0] in which the status of 1st, 3rd and 5th is ON whereas the 2nd, 4th and 6th is OFF according to objective function. The appliance which has the ON-status in the array would be multiplied with their respective energy consumption. The result is then accumulated and overall electricity bill is calculated. For the next evaluation, we select that particular chromosome pattern which has the minimum electricity cost. Fitness function is calculated by the following expression

$$\text{Fitness}=\sum_{t=1}^{24}\sum_{a=1}^{n}\sum_{b=1}^{m}\rho_{ab}(t)\times \text{n}_{ab}(t)\times\omega(t)$$

Selection:

We use the random population only to initialize the process then the selected pattern is used for the further reference. New population can be generated by the process of crossover and mutation, new offspring is obtained from parent chromosome. Once again the fitness evaluation is performed here. Various methods can be applied for this selection but for this specific model, we will use tournament based selection method.

Crossover and Mutation:

Crossover and mutation can be done by various methods. Here we apply binary mutation and single point crossover. This is because of the discrete nature of our scheduling problem. Convergence point is the point where algorithm gets its optimal solution. Crossover and mutation are the two step which determine the point of convergence

Rate of crossover is directly proportional to the speed of convergence whereas there is an inverse relationship between the mutation rate and speed of convergence.

Elitism:

It is not necessary that we obtain the solution after the procedure of mutation and convergence. It might be possible that we get the optimal solution at the 1st step by random generation of the population. There is also probability that we lost optimal solution after the step of crossover and mutation. In this way elitism make it possible to keep the solution for the next population.

In this way, till the end result, it not only does the comparison but maintain its status. Following is suggested Demand Side Management (DSM) algorithm. The algorithm of DSM is as follows.

Table 1: Parameter of GA

Parameters	Value
N	6
Maximum generation	500
Size of population	200
P_C **(Crossover Rate)**	0.7
P_m **(Mutation Rate)**	0.3

V. CHARACTRISTIC OF THE SG

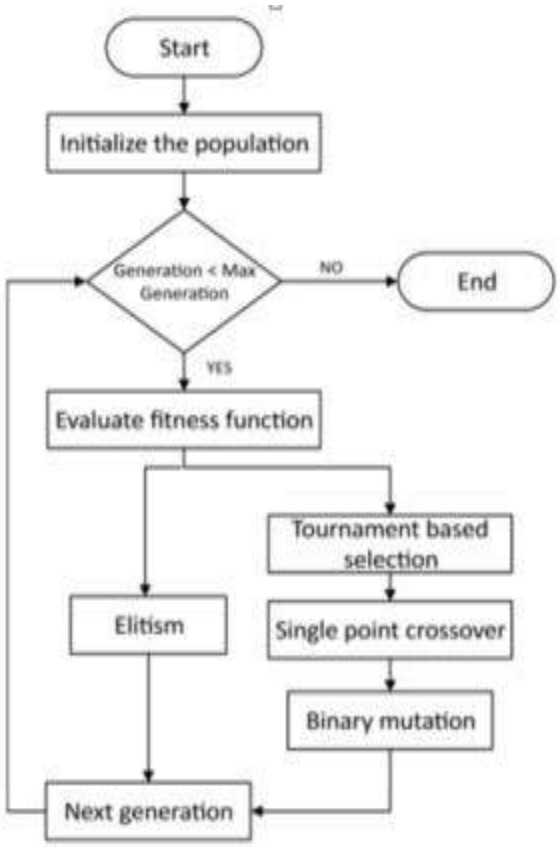

Figure 1: Flow Chart

There are different types of loads which can be controlled. Following are there details.

A. Domestic Area

In this case, we will consider a domestic consumer consisting of various type of load. In table 2 there are various load parameters; real time price signal is taken from [20] as shown in figure. Generally, We observe small duty cycle and low rating of power consumption at domestic level. Following is chart of appliances with different rating category in table 2.

Table 2: Parameters and Energy

Load Type	Loads	OPT(t)	Energy consumption (KWh)
Base Load	Load 1	20	1.6
	Load 2	24	0.6
Discrete Load	Load 3	5	3.6
	Load 4	4	1.5
Continuous Load	Load 5	11	6.5
	Load 6	8	1.7

VI. SIMULATION RESULTS

Different simulation results offer wide scope of manipulation of data and DSM application. Thus it will optimize the cost and PAR. In addition SG pricing scheme is same for different types of users. When offered price is low, scheduled load is maximum through RTP signal thus reduction in bill of electricity.it is evident that by efficient load shedding regular basis electricity bill is reduced from 1685 $ to 1535$ per day resulting 8.90% reduction on daily basis. While the reduction in peak load from 2.735 KW to 1.835KW resulting in about 32.90% reduction in peak load Number of appliances that are controllable at residential are more than that of commercial. Thus RTP is more effectively applied at residential level as is evident from results.

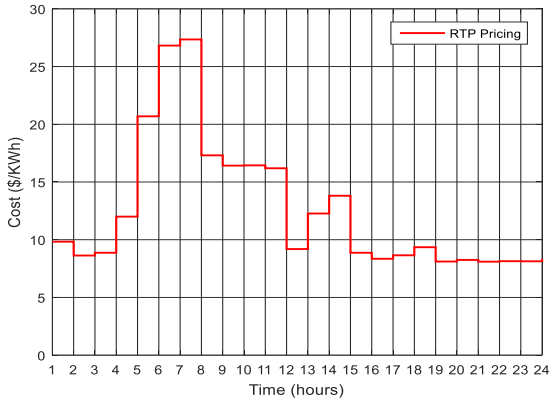

Figure 2: Real Time Price signal

Figure 3 elaborate the waiting time of appliances. Continuous load comprises of those particular appliances which have specific duty cycle and their duty cycle is not interruptible. It means, once a load is connected, it cannot be removed unless it completes its duty cycle. Those appliances whose duty cycle can be interrupted comes in the domain of discrete load. In this way, we can schedule continuous load at any time slot throughout the day subject to completion of its duty cycle which is equal to switched 'ON' time of appliance. Consequently, continuous load has maximum wait time. Discrete load has the waiting time in between of those two.

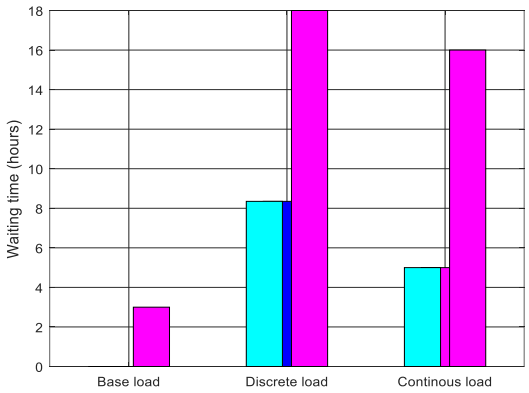

Figure 3: waiting time of multiple load

The profile of cost on daily basis consumption is shown in fig. 4. It can be clearly seen that after scheduling , bill has reduced. This has been achieved by managing the load rather than load shedding. The consumption remains same irrespective of scheduled and unscheduled load. The only thing is to bring modification in consumption profile and alternative energy source has not been utilized so far. However we have categorized the appliance. Base load (BL) is not

scheduled in appliance scheduling because this load is turned 'ON' throughout the day.

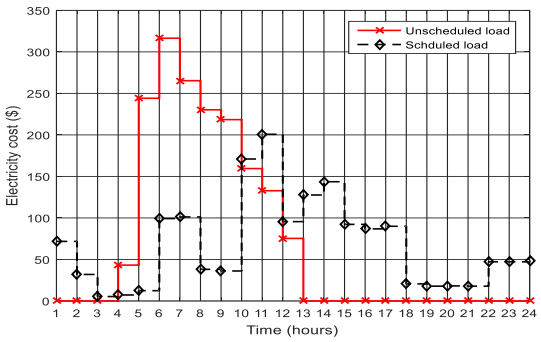

Figure 4: cost of energy consumption

Bill is reduced from 1685 $ to1535 $ which is roundabout 8.90 % reduction in the electrical charges. This reduction which contributes an important part in grid stability because of reduction in peak to average (PAR) results as shown in figure 6, there is a cost reduction owning to less reliance on peak power plants of power providers as shown in figure 5.. Energy consumption which contributes an important part in regulating the electricity prices by the regulatory authority. Reduction in peak to average ratio brings the reduction in the price value of the next schedule.

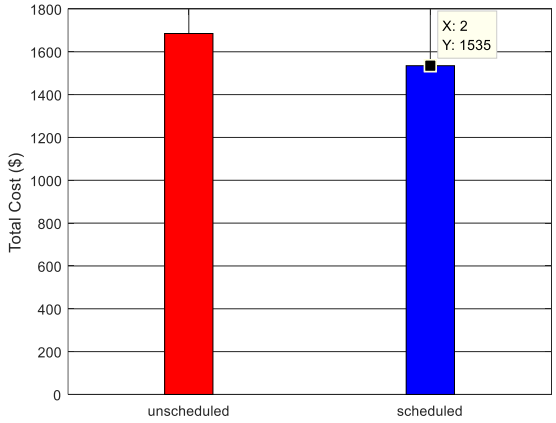

Figure 5: Total electricity bill

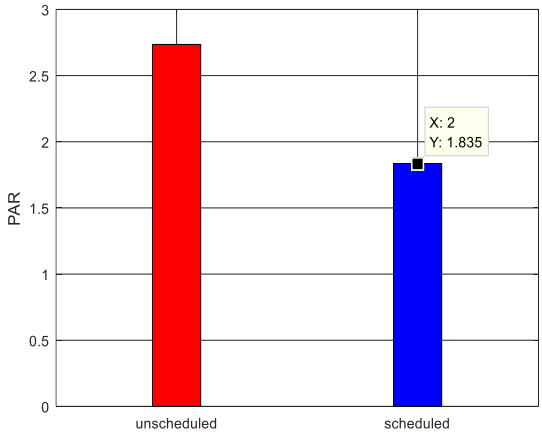

Figure 6: Peak to average ratio

Figure 7 shows Renewable energy source hourly generation with and without consideration efficiency. Also the radiation and temperature affects the generation which is maximum at day time and goes to zero at night. I general the efficiency band of solar generation is taken in between 18% to 22 %.and its consumption profile is shown in figure 8. From the figure we can see that Demand side management (DSM) controller played an important role in bringing the economy and efficiency in the system. The demand side management (DSM) controller's job is to modify the consumer's profile by giving response to Real time price signal which brings the reduction in overall electricity bill. It can also be seen that controller reduce the peas by managing the load.

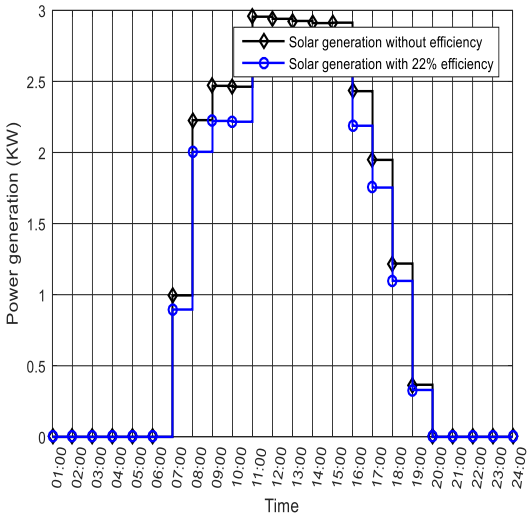

Figure 7: Generation of Renewable Energy

Controller also shares the burden of load with renewable energy sources by integrating them with system. Thus a further reduction in bill is achieved.

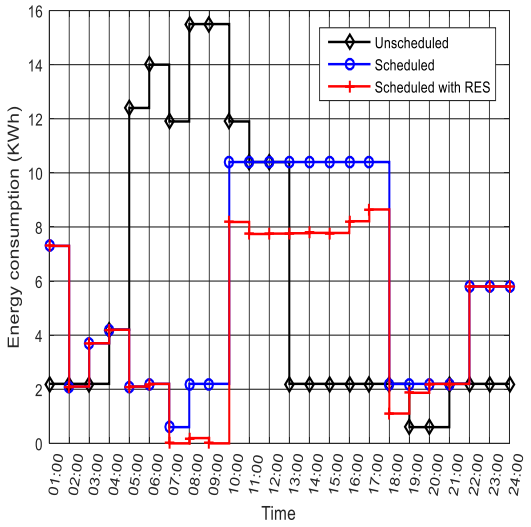

Figure 8: Schedule of Energy Consumption with RES

The whole procedure influences the end user to install the Renewable energy source at domestic level brings the stability and economy in the system which ultimately improve the efficiency. Daily consumption is shown in figure 9 which further strengthen the stance of reduction in consumption.
The reduction is achieved only by managing the time slots and shifting the peak hour's load to off peak hour load. Load shedding or other conventional method of reducing the load has not been utilized here. Only there has been some modification in consumption schedule keeping in consideration the user flexibility. By scheduling the consumption there has been valuable reduction and further reduction is achieved by the rescheduling through Renewable energy source.

The overall reduction with and without taking in account Renewable energy source is shown in figure 10. Scheduling without renewable energy source reduces cost from 2267 $ to 1568 $ which is roundabout 30.83 % reduction in electricity charges. Now, if we reschedule with Renewable energy source method, the reduction is from 2267 $ to 1231 $ which is equivalent to 45.7 % reduction in electricity charges. It is more than 21.5 % reduction as compared to scheduling by not considerable the Renewable energy source method. Thus, there is a considerable more reduction in bill if we integrate Renewable energy source with demand side management (DSM) as shown in the results.

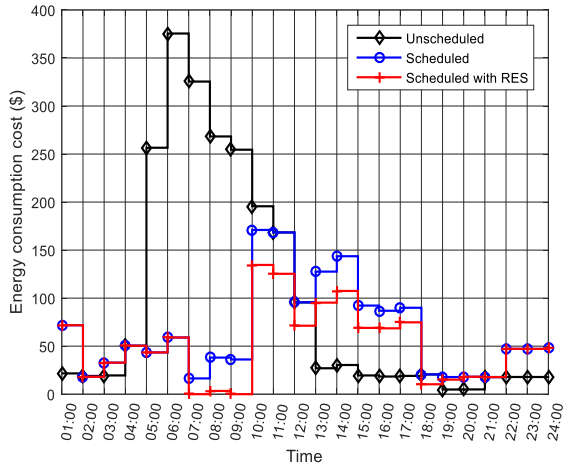

Figure 9: Cost Schedule of Energy Consumption with RES

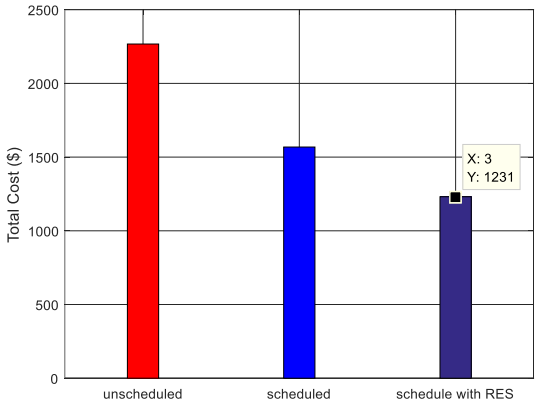

Figure 10: Total bill by using RES

Further, it can be shown that there is reduction in peak to average ratio which is approximately 35.03 % after the scheduling and with the combination of Renewable energy source. This reduction which contributes an important part in grid stability because of reduction in peak to average (PAR) results, there is a cost reduction owning to less reliance on peak power plants of power providers as shown in figure 11. Energy consumption which contributes an important part in regulating the electricity prices by the regulatory authority. Reduction in peak to average ratio also reduces the price value for the next time slot.

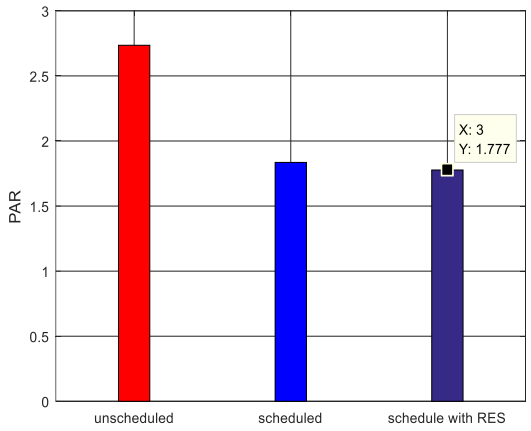

Figure 11: Peak to Average ratio

The table 5.2 represents different scenario of peak to average ratio while table 5.3 elaborate the cost of consumption for different scenario.

Table 3: Comparison in Peak to Average Ratio

Case	Unscheduled load	Scheduled load	Schedule with RES
Case 1	2.735	1.835	-
Case 2	2.735	1.835	1.777

Table 4: Comparison in Consumption cost

Case	Unscheduled load	Scheduled load	Schedule with RES
Case 1	1685	1535	-
Case 2	2267	1568	1231

Table 5.4

Table 5: Comparison of Cost reduction % and Peak to Average Ratio

Case	Reduction in cost %	Reduction in PAR
Case 1	0 8.90%	32.90%
Case 2	45.7%	35.03%

VII. CONCLUSION

In this research, a demand side management (DSM) algorithm has been proposed for energy management at the domestic level. The main focus was peak to average ratio (PAR) and electricity cost reduction by load scheduling. For simulation results, three types of load with various energy and operating constraints along with the integration of Renewable energy source has been discussed. First step of algorithm is to check the Renewable energy source availability up to its optimal level. In case of unavailability or incompatibility with demand scheduling is done by generating real time price signal by processor.

In the final results, the performance index of algorithm has been shown with ultimately reduction in consumption and cost. From statistically point of view, there has been 8.90 % reduction in cost without utilizing Renewable energy source and 45.7 % by integrating Renewable energy source with system.

In addition 32.90 % reduction in peak to average ratio has been achieved without taken in account Renewable energy source and 35.90 % by considering the Renewable energy source in the system.

Table 5.3

Table 6: Comparison in Consumption cost

Case	Un schedu led load	Scheduled load	Schedule with RES	Cost Reduction %	PAR Reduction %
Case 1	1685	1535	-	8.90%	32.90%
Case 2	2267	1568	1231	45.7%	35.03%

REFERENCES

[1]. I. K. Maharjan, Demand Side Management: Load Management, Load Proling, Load Shifting, Residential and Industrial Consumer, Energy Audit, Reliability, Urban, Semi-Urban and Rural Setting. Saar-brcken, Germany: LAP (Lambert Acad. Publ.), 2010.

[2]. D. P. Kothari, Modern Power System Analysis. New Delhi, India: Tata McGraw-Hill, 2003.

[3]. C. W. Gellings, Demand-Side Management: Concepts and Methods. Liburn, GA: Fairmont, 1988

[4]. Cao, Z., Lin, J., Wan, C., Song, Y., Zhang, Y. and Wang, X., 2017. Optimal cloud computing resource allocation for demand side management in smart grid. *IEEE Transactions on Smart Grid*, *8*(4), pp.1943-1955.

[5]. Reddy, K.S., Panwar, L., Panigrahi, B.K., Kumar, R. and Yu, H., 2017. Demand side management with consumer clusters in cyber-physical smart distribution system considering price-based and reward-based scheduling programs. *IET Cyber-Physical Systems: Theory & Applications*, *2*(2), pp.75-83.

[6]. Atzeni, I., Ordóñez, L.G., Scutari, G., Palomar, D.P. and Fonollosa, J.R., 2013. Demand-side management via distributed energy generation and storage optimization. *IEEE Transactions on Smart Grid*, *4*(2), pp.866-876.

[7]. Chai, B., Chen, J., Yang, Z. and Zhang, Y., 2014. Demand response management with multiple utility companies: A two-level game approach. *IEEE Transactions on Smart Grid*, *5*(2), pp.722-731.

[8]. Chiu, T.C., Shih, Y.Y., Pang, A.C. and Pai, C.W., 2017. Optimized day-ahead pricing with renewable energy demand-side management for smart grids. *IEEE Internet of Things Journal*, *4*(2), pp.374-383.

[9]. Chen, H., Li, Y., Louie, R.H. and Vucetic, B., 2014. Autonomous demand side management based on energy consumption scheduling and instantaneous load billing: An aggregative game approach. *IEEE Transactions on Smart Grid*, *5*(4), pp.1744-1754.

[10]. Costanzo, G.T., Zhu, G., Anjos, M.F. and Savard, G., 2012. A system architecture for autonomous demand side load management in smart buildings. *IEEE Transactions on Smart Grid*, *3*(4), pp.2157-2165.

[11]. Fadlullah, Z.M., Quan, D.M., Kato, N. and Stojmenovic, I., 2014. GTES: An optimized game-theoretic demand-side management scheme for smart grid. *IEEE Systems journal*, *8*(2), pp.588-597.

[12]. Galvis, J.C. and Costa, A., 2016. Demand side management using time of use and elasticity price. *IEEE Latin America Transactions*, *14*(10), pp.4267-4274

[13]. Liu, Y., Yuen, C., Huang, S., Hassan, N.U., Wang, X. and Xie, S., 2014. Peak-to-average ratio constrained demand-side management with consumer's preference in residential smart grid. *IEEE Journal of Selected Topics in Signal Processing*, *8*(6), pp.1084-1097.

[14]. Luo, T., Dolan, M.J., Davidson, E.M. and Ault, G.W., 2015. Assessment of a new constraint satisfaction-based hybrid distributed control technique for power flow management in distribution networks with generation and demand response. *IEEE Transactions on Smart Grid*, *6*(1), pp.271-278.

[15]. Chen, H., Li, Y., Louie, R.H. and Vucetic, B., 2014. Autonomous demand side management based on energy consumption scheduling and instantaneous load billing: An aggregative game approach. *IEEE Transactions on Smart Grid*, *5*(4), pp.1744-1754

[16]. Martirano, L., Habib, E., Parise, G., Greco, G., Manganelli, M., Massarella, F. and Parise, L., 2017. Demand Side Management in Microgrids for Load Control in Nearly Zero Energy Buildings. *IEEE Transactions on Industry Applications*, *53*(3), pp.1769-1779.

[17]. Nguyen, H.K., Song, J.B. and Han, Z., 2015. Distributed demand side management with energy storage in smart grid. *IEEE Transactions on Parallel and Distributed Systems*, *26*(12), pp.3346-3357

[18]. Qian, L.P., Zhang, Y.J.A., Huang, J. and Wu, Y., 2013. Demand response management via real-time electricity price control in smart grids. *IEEE Journal on Selected areas in Communications*, *31*(7), pp.1268-1280.

[19]. Yousefi-khangah, B., Ghassemzadeh, S., Hosseini, S.H. and Mohammadi-Ivatloo, B., 2017. Short-term scheduling problem in smart grid considering reliability improvement in bad weather conditions. *IET Generation, Transmission & Distribution*, *11*(10), pp.2521-2533.

[20]. Logenthiran, T., Srinivasan, D. and Shun, T.Z., 2012. Demand side management in smart grid using heuristic optimization. *IEEE transactions on smart grid*, *3*(3), pp.1244-1252

Pakistan Journal of Engineering and Technology, PakJET
Multidisciplinary | Peer Reviewed | Open Access
Volume: 2, Number: 1, Pages: 18- 24, Year: 2019

An Econometric Analysis of Energy Consumption in Pakistan

Hafiz Muhammad Zubair*[1], Muhammad Imran[1], Adeel Qadir[1], Umer Akram[1] and Muhammad Tariq[1]

[1] Mechanical Engineering Department, The University of Lahore, Lahore, Pakistan
*Corresponding Author: Hafiz Muhammad Zubair (muhammad.zubair@me.uol.edu.pk)

Abstract- The ratio of energy generation and consumption plays a key role in economic growth of a country. In Pakistan, main sources of energy generation are primarily contingent on traditional fuels; substantial proportion of which is imported. Not only its import is linked with GDP, but it also affects the nation indirectly by causing unexpected inflation. By having knowledge of energy consumption, imported conventional fuels must gradually be replaced with locally available alternate preferably from non-conventional domain of energy resources in order to maintain economic growth. This present work is therefore compares the relationship between energy consumption and economic growth. Energy model Long-Range Energy Alternatives Planning System (LEAP) has been used in various scenarios to find out energy demand for 2013 and has predicted the demand till year 2040. The analysis thus uncovers new postulates for think tanks to find out best alternates headway of energy sector to overcome energy deficiency in coming years.

Keywords-Energy Outlook, Energy Planning, Modeling, Scenario Analysis, LEAP

I. INTRODUCTION

Energy sector plays a key role on the progress of any nation and depends extremely on its utilization. It was prominently identified during the embargo oil crisis in 1970's. Reports generated on World crisis.net clearly indicate that oil importing countries could face high inflation in situation of oil supply deficit [1]. In results, it would have great impact on their economy. The energy sector is related to energy demand, supply, technologies market potential, technological progress, society and the environment. All variables and parameters are considered for efficient energy planning. No doubt, energy plays a key role in commercial, residential, transportation, agriculture as well as for industrial use in industry. It plays a key role as a final product to meet power needs and demands i.e. for consumption of refrigeration, transportation, cooking, etc. [2]. The amount of energy required for producing a unit depends on technology which is adopted by end-user [3].

Consumers usually select technical and economic feasibility for the utilization of energy, based on energy planning research [4]. They are affected by different policies in place based on energy planning research. Renewable energy development must be encouraged in energy development program. Theoretically all the natural resources with different time scales are said to be renewable. But if the time period is very small then they are called renewable energy resources as bio gas and bio mass. Naves and Leal have studied and examined three important sustainable development standards: social, economic as well as environment [2]. For clean environment, the important criteria is the reduction in emission of greenhouse gasses (GHG), decreasing in air pollution and more concerns for continuous depletion of natural resources in world. On the other hand, economic standards considers mainly the reduction of fossil fuels because of huge demand and giving more emphasis on needs to work on sustainable energy by promoting local investments and energy efficiency projects which would reduce inflation as well as promote businesses on small scales. Indirectly, it would reduce burden on state to meet the energy requirements on small as well as on large scales. Most importantly, social criterion demands the health improvement and the job criteria.

The world's trend is entirely now towards the globalization. There are many issues which need to be addressed but scholars focus more on energy. Most countries are facing energy crisis and their economy is affected remarkably due to energy shortage. In this era, countries are hunting for sustainable as well as other alternative energy resources. The concept of Macro-economic growth focuses more on labor as well as capital.

Character of energy resources did not be considered which are devouring momentous role on economic growth in addition to production [5], [6].

Pakistan has been gifted with lot of energy resources like coal, natural gas, sunshine, water, wind and geothermal resources. Unfortunately these natural resources are never consumed, as most of them are still not in useful stage. According to Alternative Energy Development Board (AEDB) of Pakistan, up to 2003, these sustainable energy resources were not utilized [7]. Pakistan could control over energy crisis by owing to humble investment in energy sector. Poor energy facilities in Pakistan are major resistance to economic growth as well as to

development. Now Pakistan has more focus on national energy resources to facilitate nation with cheap energy. The objective is to increase per capita of energy consumption as well as to enhance the GDP of country.

II. ENERGY CONSUMPTION AND ECONOMIC GROWTH

Since with industrial revolution, energy has been spread exponentially. At present time, by studying the energy consumption per capita, economic growth of any state can be explored. Still energy distribution is not uniform. In the developed countries energy consumption per capita is much larger as compared to developing or under developed countries especially African countries. Therefore, relationship between the economic development and energy consumption vary from country to country and nation to nation. In some countries relation between two variables is constant and in some state relation is not in same rhythm. Much written and discussed on the relationship between energy consumption and economic development in 21st century due to the rapid depletion of energy resources. Energy policy makers provided significant role to understand energy consumption and economy of the country. Historic trend facilitate an important role. In general, configuration of historic energy consumption performs the future energy structure. Forecasting of energy consumption of any nation or state's plans and policies can be developed. In early decades economic progress of any country rely on growth ratio of energetic consumption which should be superior of GDP. But owing to technical variation and structural modification, GDP is preferred as compared to energy consumption growth ratio of economic development of any nation.

Cumulating the consequences from various source of research, energy consumption and economic constraints are categorized into three types which are: (i) No causality (ii) Unidirectional causality (iii) Bidirectional causality [8]. Unidirectional causality is divided into two sub types, one explore that income is outcome of energy consumption second manifests that energy's consumption effects on income [9],[10]. According to numerous schools of thoughts connection between energy consumption and economic are classified into four hypotheses [11]. Growth hypothesis suggests that energy consumption has predominant role on economic uplift. It advocates capital and labor as input factor of production. If energy consumption is slowdown, ultimately it will reduce GDP growth [12], [13]. Contrary to this, conservative hypothesis delivers that policies of low energy usage have no harsh impacts on economy. In addition to this, energy consumption should be excluded from economic growth so that economic growth may not suffer extremely [14], [15]. This hypothesis shows that GDP of the nation state is independent of energy consumption. But there exists a little relationship where a country attains a smooth development. Moreover, Neutral hypothesis suggests that there is no relation between energy consumption and economic parameters. It further clarifies that energy cost is small as compared to GDP, so it doesn't significant on GDP. Bidirectional hypothesis, also known as "feedback", states that economic growth rate and energetic consumption effects on each other which has influence on energy related policies [15], [16]. Bidirectional relation manifests that improvement of energy efficiency measures, scaling down of energy from conventional energy resources and enhances usage of traditional (renewable) energy resources to keep the environment favorable. Resultantly, it would reduce the greenhouse gasses (GHG). Conventional energy fuels (oil and gas) fulfill 80% of world energy consumption. In Pakistan, fossil fuels cover approximately 65% of the total economic energy demand during 2012. It is expected that if this energy carry on, total world energy demand will be increased by over 50% before 2030. In the end of 20th century (1995), oil prices were near to $10 per barrel and now comparatively it has been increased practically 100 times i.e. about $110 per barrel at the end of May 2014 [17]. The import of crude oil in Pakistan was 40.9 million barrel in March 2013 and in March 2014 was 44.9 million barrel. In this situation environment protection is much crucial for livings on the earth. Due to increase in cost and environment concerns, world is shifted towards traditional energy. Less cost is required for this sustainable clean energy. This energy is linked with regional areas development, social community progress, as this renewable energy is available in less developed regions. This can bring down the poverty level in under developed regions. So, economic growth of the country boost up.

III. ECONOMIC STRUCTURE OF PAKISTAN

The economy of Pakistan has been facing abundant exterior and national shocks since 2007 which influence on each sector of society. The economic growth has been critically affected by the devastation caused by the rains and floods, the security hazards in the country and the growing energy demand. The economy of Pakistan, however, has shown bit growing trend at the rate of 2.9% per annum normally as shown in Fig.1.

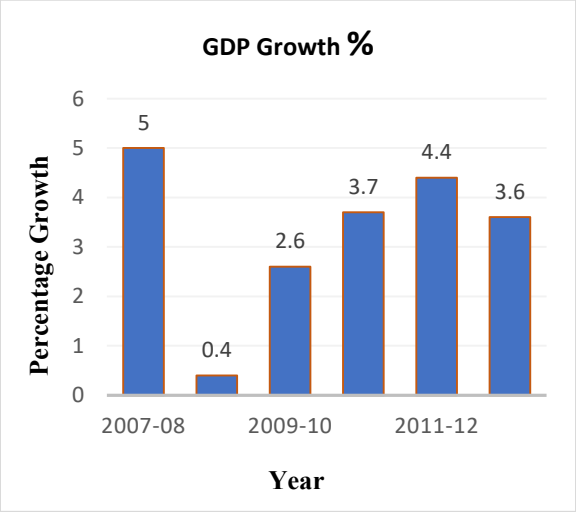

Fig. 1. % GDP Growth Rate of Pakistan from 2007-08 to 2012-13

Energy disasters have been found most deterioration element for economic growth. In fact this does not let us to realize our true economic potential. Power outages have resulted in decrease of annual GDP by 2%. GDP is not progressing any more, which is half of Pakistan's real economic potential of about 6.5% per annum but growth is less than the requirement for constant increase in employment rate and for tumbling poverty. In 2012-13, GDP was estimated 3.6% which encompasses 2.8% in Large Scale Manufacturing (LSM), 3.7% in service and 3.3% in agriculture. Comparing with GDP in previous year 2011-12, GDP of agriculture has fallen 3.5 to 3.3 percent, services 5.3 to 3.7% owing to continuous rains and flood victims. But Large Scale Manufacturing (LSM) growth has increased from 1.2% to 2.8% in current year [18].

In 20th century, 1960, the GDP in Pakistan was $3710 million and now in calendar year 2013, the worth of GDP was 236620 million USD which contributes 0.38% towards the world economy. Average GDP of Pakistan is $56300 million since 1960. On the other hand, in 2013 GNP of Pakistan was smaller than GDP of Pakistan which is 11175600 million PKR.

IV. ENERGY FORECASTING MODELS

Energy models are designed and produced considering the demand of nation. Energy models are categorized in different ways. (i) Univariate against multivariate (ii) Static against dynamic model (iii) Time series techniques ranging verses hybrid models. Energy software models are used to observe the factor of integrating sustainable energy in several systems of energies. Chen and Kung have manifested a model which has features to improve forecasting accuracy using quantitative and qualitative experiences [19]. Energy software models are developed definite to nation liable on market situation and economic. Procedural and economic forecasting model, the integrated Energy planning model, works on alteration sectors and interruption of energy consumption. The core purpose of model is stable energy demand with energy supply and variable used in models are GDP, rural and urbanization rate, growth rate of population, industrial product share as well as number of house hold. For residential energy consumption, Conditional demand analysis (CDA) was analyzed and accurate results obtained by with engineering and network based model [20].

From last two eras, energy consumption is increasing regularly. Worldwide, May energy policy maker and management are trying to overcome shortage of electricity and improving infrastructure, where numerous techniques have been used which anticipate the electricity demand. In Hong Kong, Yuk Yee Yan studied a model, residential consumption model, which is based on climatic variable [21]. In New Zealand, Mohamed and Bodger presented an electricity forecasting model using multiple linear regression model which depend on demographic and economic variables [22]. Al-Ghandoor et al. studied a time series Multivariate linear regression model to isolate basic factor of electricity consumption of Jordanian industrial sector [23]. Liu, Shahbaz and Lean suggested a multivariate model which describes short run as well as long run correlation between urbanization and energy consumption [24]. Similarly, for Srilanka, projection of electricity demand was presented based on time series analysis and this time series model presented forecasting of electricity consumption which makes estimate on the basis of key income and price elasticity [25].

Software (LEAP, MARKAL and TIMES) are used for energy modeling as well as in forecasting. At Boston, institute of Stockholm Environment developed software tool, bottom-up-type, Long range Energy Alternatives Planning System (LEAP). LEAP energy model is adopted in forecasting of energy at national, state, regional and global level. Window based LEAP model is used for energy outlooks, integrating resource planning, strategic analysis of sustainable energy futures, climate change (GHG) mitigation strategies, energy balance and environment inventories. Depending on data of national energy balance, both energy supply and demand are planned for various Mexican end use zones. Energy demand transformation program in LEAP model simulates oil refining, charcoal production, coal mining, natural gas, electricity generation, transmission and distribution, etc.

LEAP integrated energy model has been applied for planning, forecasting and analysis of energy at national and international level Iran [26], China [27], Korea [28], Thailand [29], Rawalpindi and Islamabad [30].

In Taiwan, for long range energy demand and supply, environment change (GHG) emissions analysis, LEAP system software is used. For different type of conditions, various scenarios have been developed [31]. In India LEAP energy model is developed, which is used for modeling the total energy consumption from household of Delhi and accompanying emissions. Various technologies and policies have been analyzed [32]. In Mexico LEAP system model is applied to analyze feasibility of transportation using biogas and electricity generation zone. Different scenarios relaying on moderate and high uses are analyzed. Efficient use of biogas especially in rural sectors is concentrated [33]. In Pakistan (2010), Shabbir and Ahmad worked on LEAP system for Rawalpindi and Islamabad to calculate supply and demand associated transportation emissions [30].

Energy technology systems Analysis Program, an International Energy Agency, developed dynamic technique, bottom up MARKAL model as a least cost linear programming model. Fishbone and Abilock developed numerous equations for Initial MARKAL energy model and several developments have been made on advance level for depth analysis [34]. For different policy changing, Scenarios using 'What if' context and carbon mitigation analysis, MARKAL model can be adapted.

Shanghai used MARKAL system model to develop scenarios under several policy situations [35]. MARKAL model helps in studying how to control pollutant emissions while considering different energy policies.

Planning commission of Pakistan found integrated energy model by using TIMES encompasses the entire energy system which includes resource supplies, power plants and refineries, transmission and distribution systems for fuel and electricity.

V. METHODOLOGY AND DATA USED

LEAP software is adopted to attain main manifests of this research. The key value of LEAP software is that low initial data input is required. The main objective of implement of LEAP in this research is to evaluate and forecast of energy consumption in Pakistan for the duration of 2013 to 2040 because this software relies on simpler accounting principle. In LEAP software, the first depletion year and monetary year in basic parameters of LEAP are taken 2014. In LEAP model only two year values are required one is base year values and other is future year values. For this purpose, different scenarios are constructed. In this research two scenarios were built, one is called current account scenario and second is called business as usual scenario. All such scenarios show the evolvement of energy systems. Most of the researches manipulate forecasting period of twenty to fifty years.

Primarily and also the secondary data has been collected from Pakistan energy year book 2013, economic survey of Pakistan 2012-13, World Bank national statistical report and Pakistan integrated energy model prepared by International resources group for Asian development bank.

In the LEAP, on tree the first notable class is key assumption. Under this class demographic, time series, microeconomic exogenous variables are applied that impact on energy forecasting. These exogenous variables not considered anywhere else in the LEAP resources, transformation and demand tree. Key assumptions used in this study for Pakistan are:

Population 184.30 million people and growth rate is 3.5%. GDP 236.62 billion US$ and growth rate is 4.14%. GNP 110 billion US$ and its growth rate is 6.2%.

In Base Case (Current Scenario) demand analysis is developed. Demand analysis in tree of the LEAP software is distributed into several sectors like household, commercial, industrial, transportation and agriculture. Table 1 shows energy consumption in tons of oil equivalent, TOE, of five sectors and their annual cumulative growth rate (ACGR). ACGR is used in business as usual (BAU) scenario, which is also called modified case, in order to forecast energy consumption in future years.

Table 1: Energy Consumption of Various Sectors in Toe [Xxxvi]

Sector	**2012-13 (TOE)**	**ACGR**
Household	10119014	4.7%
Commercial	1644845	2.5%
Industrial	14256099	-3.2%
Transportation	12713300	1.9%
Agriculture	659986	-3.9%

In 2012-13, total electricity generation in Pakistan was 96122 GWH. The share of hydro is 31.1%, nuclear 4.7%, gas 28.2%, coal 0.1% and oil is 35.9 percent of total electricity generation of Pakistan. These data set is used in electricity generation subsector of transformation in the tree of the LEAP in current account scenario. Total gross electricity generation from nuclear is 750 MW, Hydro 6773 MW and from thermal is 15289 MW.

In BAU scenario, estimated energy produced from different energy sources till the end of 2040 year is given in table 2. For long time future developments in energy sectors, these assumptions are also included in energy policies of Pakistan.

Table 2: Modified Case Assumptions Used In Bau Scenario [Xxxvii]

Energy Resources	Assumed Install Capacity in 2040 (Mega Watt)
Coal	20000 MW
Wind	6000 MW
Solar	2500 MW
Nuclear	15000 MW
Hydro	20000 MW
Biogas	1500 MW

VI. RESULTS AND DISCUSSION

This studied model has been instigated on settlement of two scenarios which consist of transformation, demand analysis and key assumptions. In various scenarios energy demand was evaluated for the current as well as for any future year at any particular technology branch as product of energy intensity and activity level equation discussed in LEAP software help.

$$D(b,s,t) = EI \times TA \quad \text{---------- (I)}$$

Where D is the demand and B stand for technology branch, s for scenario and t represent from base year to any future year. EI represent energy intensity and TA stands for activity level.

DEMAND - As discussed that 2013 was taken as a base year and 2040 as end year forecast of energy consumption in Pakistan. Table 3 depicts the energy consumption in subsector of demand analysis which are household, commercial, industrial, transportation and agriculture developed by LEAP. These subsectors are further divided into various fuel branches and end uses. The fuel branches involve natural gas, liquefied petroleum gas (LPG), electricity, coal, diesel, kerosene, biomass, biogas, wood and agriculture residues.

Table 3: Demand Analysis of Energy Consumption in Million Giga Joules Using Leap

Branches	2015	2040	Total
Household	20.9	115.1	345.1
Commercial	1.4	5.7	18.9
Industrial	66.8	16.3	214.6
Transportation	68.6	669.6	1530.8
Agriculture	0.4	0.4	2.5
Total	158.0	807.1	2111.8

HOUSEHOLD - Energy demand of household is fragmented into two categories urban and rural and further divided into two parts electrified and non-electrified. Fig. 2 describes complete data of urban as well as rural energy demand till forecasted year 2040. Urban population consists of 38.56 million people and remainder belongs to rural areas. It is rough estimated that 100 % of rural and urban population use natural gas for cooking.

94% of urban population are electrified that use electricity for refrigeration, lighting and other appliances. Rural population consists of fraction it is electrified. Percentage for air conditioning and refrigeration for urban and rural household is 60 and 15 percent and increase steadily till the end forecasted year 2040. In some urban household LPG, wood and biomass is used, but their percentage is not much considerable.
While in rural household LPG, wood, agriculture residues and animal dung is used however their share in cooking percentage is almost negligible.

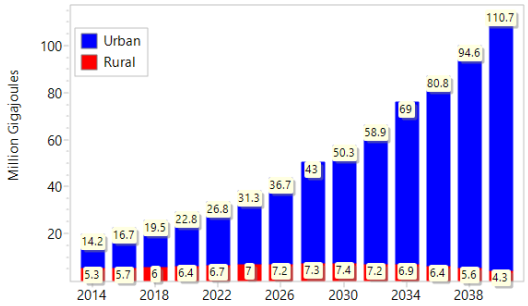

Fig. 2. Household Energy Demand

COMMERCIAL SECTOR - Commercial sector consumes 4.1 percent of total energy for year 2012-13 which is almost equal to the last year's energy consumption that is 4 percent. Its annual compound growth rate has been slowed down from 2.9 percent to 2.5 percent as compared to fiscal year. Fig. 3 is developed by LEAP software which shows that for 2040, energy consumption is three times more than that of energy utilized in 2015. Energy demand will bring the consumption high for water heating, cooking, air conditioning and other appliances.

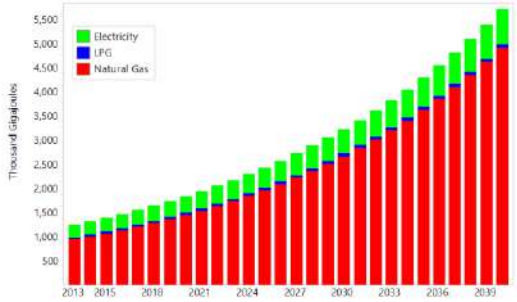

Fig. 3. Energy Demand for Commercial Sector by LEAP

INDUSTRIAL SECTOR - For economic development of any country, industrial sector plays primary role. Since 2006, woefully, energy deterioration results hitting badly on industrial sector's performance of Pakistan. Especially CNG is supplied to transportation sector. Energy consumption in industrial sector of Pakistan relay on oil, natural gas, electricity and coal but mostly industrial output of Pakistan depends on natural gas. Therefore, most of industry in Pakistan is shifting into other Asian countries owing to acute shortage of natural gas. Energy consumption in industrial sector has been declined from 16804.303 thousand TOE in 2007-08 to 14256.099 thousand TOE in 2012-13. According to energy year book 2013, annual cumulative growth rate (ACGR) of industrial sector energy consumption is -3.2 percent containing oil ACGR 5 percent, gas ACGR -3 %, electricity 1.5 % and coal ACGR -7.5 percent. Fig. 4 represents energy demand of various fuels in industrial sector.

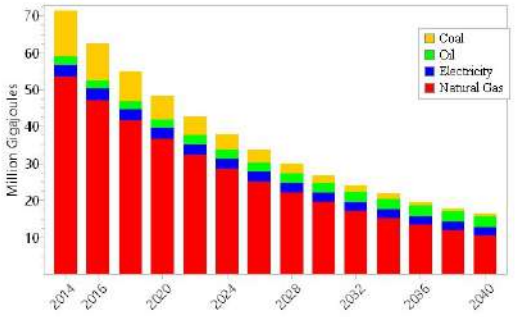

Fig. 4. Energy demand of industrial sector

TRANSPORTATION - Economy of Pakistan also relies on subsector transport which plays a vital role and overall it contributes about 23.74 percent share in services area.

Table 4: Various Fuels Consumption in Transportation Sector [Xxxvi]

Fuel	Energy Consumption (TOE)	%	Growth Rate
Electricity	0	-	-
Natural Gas	2345331	18.447	6.8%
Kerosene	185	0.001	-1.8%
Non Energy	4006604	31.515	12%
Diesel	6361181	50.035	-4.3%
Total	12713301	-	-

Table 4 illustrates the various fuels consumptions that are being used in transport sector as a base year (2013) values. In BAU scenario, the growth rate of these fuels is used as a forecast of energy consumption in transport section. The growth rate of category non-energy, which encloses aviation fuel, motor spirit, High Speed Blending Component (HOBC) and E-10, is 12% which is alarming situation for divesting the natural resources. Diesel in the primarily constituent that is used in transport sector. Diesel contains furnace oil, light diesel oil and high speed diesel. Fig. 5 shows various fuel consumptions by transportation for 2013 to 2040.

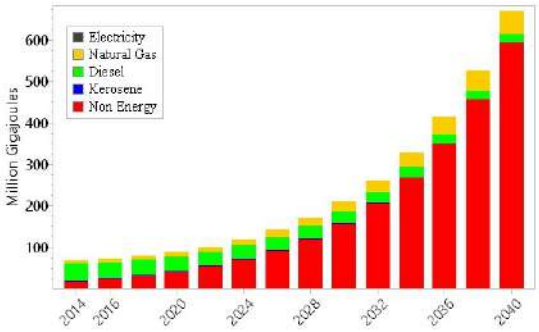

Fig. 5. Energy demand in Transport Sector developed by LEAP

AGRICULTURE - About 61.44 Percent of Pakistan's population belongs to rural areas and depends directly or indirectly on agriculture sector. In economic activity of Pakistan agriculture sector plays a role of back bone and it accounts for nearly 24% of GDP of Pakistan that is largest contribution.

Table 5: Fuels Consumption in Toe of Agriculture Sector [Xxxvi]

Source	2007-08	2012-13
Oil (TOE)	113889	33158
Electricity (TOE)	689948	626827

Table 5 demonstrates major sources of energy in agriculture sector in Pakistan for 2007-08 and 2012-13. It clearly depicts that it depends on electricity and oil. Tube wells and tractors both run by electricity and oil respectively. More over for harvesting, ploughing and other resources, oil is used. On the other hand, according to economic survey of Pakistan, agriculture's growth rate has been fell down to 2.1% in 2013-14 which was .6% more in last year i.e. 2.7%. Fig. 6, developed by LEAP, demonstrates consumption of energy in agriculture between years 2013 to 2040.

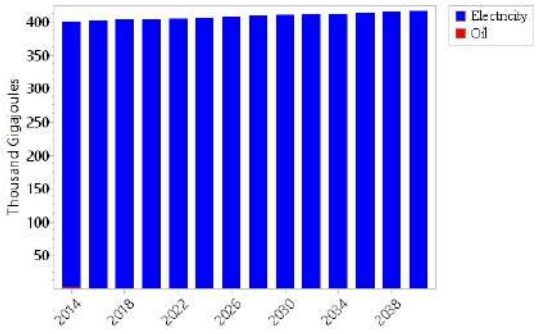

Fig. 6. Energy demand in Agriculture Sector

TRANSFORMATION: ELECTRICITY GENERATION - Fig. 7 depicts of electricity generation variation from base year 2013 to till end forecasted year 2040 developed from LEAP. Fossil fuels play predominant role in Pakistan electricity generation. In current year, share of fossil fuels in electricity generation is 64.1 percent which will be slowed down to 46.8 percent in end year 2040 and will be shifted to nuclear, hydro and some renewable resources such as solar, wind, biogas.

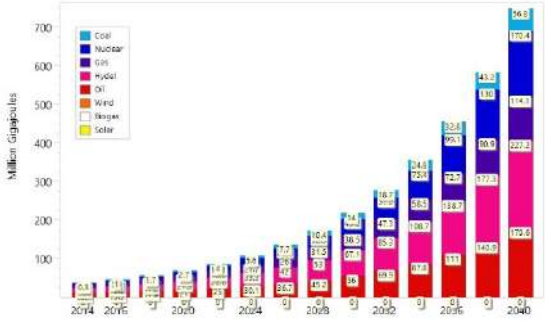

Fig. 7. Electricity Generation Variation from 2013 to 2040.

VII. CONCLUSION

Core upshot of the said research is to discuss the assorted factors which are directly or indirectly involved in planning to pawn the predicament of energy crises. It is hooray to move that consumption of energy is significant, vow economic progress along with the auxiliary components in Pakistan. In future upsurge in energy demand involves factual tenacity of aggregate of energy. As energy is prime need for growing economy, however, economic of Pakistan is devastating owing to scarcity of energy. Pakistan has huge potential of wind and solar energy. Sindh and Baluchistan have wide area which suits best for the utilization of Wind energy in power generation. Its capacity is about 150,000MW all over the country whereas 50,000MW is available at average wind speed of 7 m/s. On the other hand, large area in Pakistan does support for the solar energy generation, but these two green energy sources are not playing significant role in power generation.

REFERENCES

[1] Yongli Wang, Yudong Wang. 2019. Planning and operation method of the Regional Integrated Energy System considering economy and environment. Energy, pp34.
[2] Simone Ferrari , Federica Zagarella, 2019. Assessment of tools for urban energy planning, Energy 7(9), pp.) 544-551.
[3] J.Randolph, G.M. Masters., 2008. Energy for sustainability: Technology, planning, policy. Washington: Island Press.
[4] I.S.Chaudhry, N. Safdar,F.Farooq., 2012. Energy Consumption and Economic Growth: Empirical Evidence from Pakistan. Pakistan Journal of Social Sciences (PJSS), 32(2), pp. 371-382.
[5] D.I. Stern., 2004. Economic Growth and Energy. Encyclopedia of Energy, Volume 2, pp. 35-51.
[6] Z.Huang, H. Yu, Z. Peng, M. Zhao., 2015. Methods and tools for community energy planning: A review. Renewable and Sustainable Energy Reviews, Volume 42, pp. 1335-1348.
[7] Yuan Liu, Hongwei Lu, Jing Shen, Li He., 2017. Optimization-based provincial hybrid renewable and non-renewable energy planning – A case study of Shanxi, China: Energy Policy, 37(7), pp. 2745-2753
[8] A.Belke, F.Dobnik,C.Dreger., 2011. Energy consumption and economic growth: New insights into the cointegration relationship. Energy Economics, 33(5), pp. 782-789.
[9] U. Soytas, R. Sari., 2009. Energy consumption, economic growth, and carbon emissions: Challenges faced by an EU candidate member. Ecological Economics, 68(6), pp. 1667-1675.
[10]E. Yıldırım, D. Sukruoglu, A. Aslan., 2014. Energy consumption and economic growth in the next 11 countries: The bootstrapped autoregressive metric causality approach. Energy Economics, Volume 44, pp. 14-21.
[11]G. Sajal., 2009. Electricity supply, employment and real GDP in India: evidence from cointegration and Granger-causality tests. Energy Policy, 37(8), pp. 2926-2929.
[12]J. H. Yuan, J. G. Kang,C. H. Zhao, Z. G. Hu., 2008. Energy consumption and economic growth: Evidence from China at both aggregated and disaggregated levels. Energy Economics, 30(6), pp. 3077-3094.
[13]V. Costantini, C. Martini., 2010. The causality between energy consumption and economic growth: A multi-sectoral analysis using non-stationary cointegrated panel data. Energy Economics, 32(3), pp. 591-603.
[14]O. Ilhan., 2010. A literature survey on energy-growth nexus. Energy Policy, 38(1), pp. 340-349.
[15]J. E. Payne., 2009. On the dynamics of energy consumption and output in the US. Applied Energy, 86(4), pp. 575-577.
[16]S. E. Wasti, M. Shoaib., 2013. PakistanN Eonomic Survey 2012-13. s.l.:Government of Pakistan Ministry of Finance.
[17]S. E. Wasti, D. I. Ahmad., 2012-13. Pakistan Economic Survey:Growth and Investment. s.l.:Government of Pakistan Ministry of Finance.

[18] K. Chen, S. H. Kung., 1984. Synthesis of qualitative and quantitative approaches to long-range forecasting. Technological Forecasting and Social Change, 26(3), pp. 255-266.
[19] M. A. Koksal, V. I. Ugursal., 2008. Comparison of neural network, conditional demand analysis, and engineering approaches for modeling end-use energy consumption in the residential sector. Applied Energy, 85(4), pp. 271-296.
[20] Y. Y. Yee.., 1998. Climate and residential electricity consumption in Hong Kong. Energy, 23(1), pp. 17-20.
[21] Z. Mohamed, P. Bodger., 2005. Forecasting electricity consumption in New Zealand using economic and demographic variables. Energy, 30(10), pp. 1833-1843.
[22] S. Ghosh, K. Kanjilal., 2014. Long-term equilibrium relationship between urbanization, energy consumption and economic activity: Empirical evidence from India. Energy, Volume 66, pp. 324-331.
[23] H. Amarawickrama, L. C. Hunt., 2008. Electricity demand for Sri Lanka: a time series analysis. Energy, 33(5), pp. 724-739.
[24] K. Amirnekooei, M.M. Ardehali, A. Sadri., 2012. Integrated resource planning for Iran: Development of reference energy system, and long-term energy environment Plan. Energy, 46(1), pp. 374-385.
[25] B. Guo, Y. Wang, A. Zhang., 2003. China'S Energy Future:Leap Tool Application In China. s.l.:East Asia Energy Futures (EAEF)/Asia Energy Security Project.
[26] H. C. Shin, J. W. Park,H. S. Kim, E. S. Shin., 2005. Environmental and economic assessment of landfill gas electricity generation in Korea using LEAP model. Energy Policy, 33(10), pp. 1261–1270.
[27] T. Limanond, S. Jomnonkwao, A. Srikaew., 2011. Projection of future transport energy demand of Thailand. Energy Policy, 39(5), p. 2754–2763.
[28] R. Shabbir, S. S. Ahmad., 2010. Monitoring urban transport air pollution and energy demand in Rawalpindi and Islamabad using leap model. Energy, 35(5), pp. 2323–2332.
[29] Y. Huang, Y. J. Bor, C. Y. Peng., 2011. The long-term forecast of Taiwan's energy supply and demand: LEAP model application. Energy Policy, 39(11), pp. 6790–6803.
[30] Kumar, S.C Bhattacharya, H.L. Pham., 2003. Greenhouse gas mitigation potential of biomass energy technologies in Vietnam using the long range energy alternative planning system model. Energy, 28(7), pp. 627–654.
[31] J. Islas, F. Manzini, O. Masera., 2007. A prospective study of bioenergy use in Mexico. Energy, 32(12), pp. 2306–2320.
[32] L. G. Fishbone, H. Abilock., 1981. Markal, a linear-programming model for energy systems analysis: technical description of the BNL version. Energy Research, 5(4), pp. 353–375.
[33] C. Changhong, W. Bingyan, F. Qingyan, C. Green, D. G. Streets., 2006. Reductions in emissions of local air pollutants and co-benefits of Chinese energy policy: a Shanghai case study. Energy Policy, 34(6), pp. 754–762.
[34] Basit., 2013. Pakistan Energy Year Book 2013. s.l.:Ministry of Petroleum & Natural Resources Hydrocarbon Development Institute of Pakistan.

Pakistan Journal of Engineering and Technology, PakJET
Multidisciplinary | Peer Reviewed | Open Access
Volume: 2, Number: 1, Pages: 25- 30, Year: 2019

Development of Organic Rankine Cycle for Microcogeneration by using Scroll Compressor

Raees Ahmad[*1], Imran Ahmed[1], Asif Mumtaz[1], Umer Akram[1]

[1]Mechanical Engineering Department, The University of Lahore, 1-KM Thokar Niaz baig, Raiwind Road, Lahore, Pakistan
*Corresponding author: Raees Ahmad (email: raees.ravian@me.uol.edu.pk)

Abstract— **ORCs are being used in low grade heat recovery applications. The Model prepared is a 1 kW ORC comprising of four main parts: evaporator, Scroll expander, condenser and feed pump. Main restriction, while designing ORC model, was to choose working fluid. Working fluid will be a refrigerant whose properties will be modified to the working conditions in which the heat recovery is carried out. A refrigerant R134a (a gas used for Household refrigeration system) has been selected as working media due to its required performance, high safety and frequent availability in Pakistan. An investigational study has been carried out on an ORC, recovering heat from hot water at a temperature ranging from 130-140°C. The scroll compressor will be used in reverse as a volumetric scroll expander to extract work from the system. Physical Model of every equipment of the test bench has been validated. The ORC test bench has been commissioned and testing has been performed under different working conditions to understand its behavior broadly. In the last section of this work, future work has been proposed for better optimization of the ORC test bench.**

Index Terms— Organic Rankine Cycle, Scroll Compressor, Microgeneration, Development of System, Power Generation.

I. INTRODUCTION

A survey had been conducted by World Energy Council in 2015 which shows that the most important need of the hour globally is to devise ways and methods for increasing energy efficiency and utilizing renewable energy resources (1). The ever increasing thirst for energy for industrialized and under developing countries alike are driving the need for action. Waste heat recovery (WHR) systems can be part of the solution for increasing energy efficiency and generating renewable power. A key technology used to generate power from heat is the conventional steam Rankine cycle (RC) which is used where high temperature (>340 °C) heat is available (2). Unfortunately, not all heat sources produce sufficiently high temperature heat required to drive a conventional steam Rankine cycle.

The development of lower boiling point organic working fluids has provided an avenue for increased applications of RCs to heat sources at relatively lower temperature. Organic Rankine cycles (ORC), work with fluids that are organic in nature instead of water, and utilize heat at temperatures around 65 °C. Sources of heat for ORCs may be either waste sources or dedicated sources.

The technologies to build ORC systems were available as early as 1976. The economics of ORCs weren't favorable until the use of modified off the shelf refrigeration components and there are still technological and economic challenges to wide acceptance of the ORC technology to smaller applications in the less than 100 kW range. Smaller systems are important as there are many more sources of waste heat in this range of operation. To that end, the effort in this work was undertaken to create an environment to conduct research on sub-100 kW ORCs and collect preliminary results for the configuration of working fluid and expander. Section II describes the working principal of Organic Rankin Cycle (ORC) and summarizes the key points in waste heat recovery by means of ORC.

II. HOW ORGANIC RANKINE CYCLE WORKS

The Organic Rankine Cycle (ORC) as compared to conventional Rankine Cycle can work at very low temperatures, thanks to the organic fluids with low boiling points. Although the efficiency of an ORC is typically between 10% and 20%, yet the properties of the organic fluid has a great impact on the overall performance of ORC cycle.

The working process (as shown in Fig. 1) is completed in four (or five) consecutive steps:

- An organic fluid that is in liquid state at relatively low pressure, gains pressure by using a feed pump.
- This fluid under high pressure will be vaporized by a heat source. The superheated vapor will be expanded trough a turbine.
- An optional regenerator can be added between expander exhaust and condenser supply. This results in heat exchange between the two streams (inlet to evaporator and exit from expander) of working fluid which contributes towards overall efficiency of ORC.
- The working fluid will be condensed and flows back to the feed pump supply.

The working code/principal of an ORC is thus alike to the conventional Rankine cycle with working fluid as water. The main difference between the two cycles is the choice of working fluids; ORC utilizes organic working fluids which have low boiling points, thus making it possible to operate the cycle at relatively low temperatures.

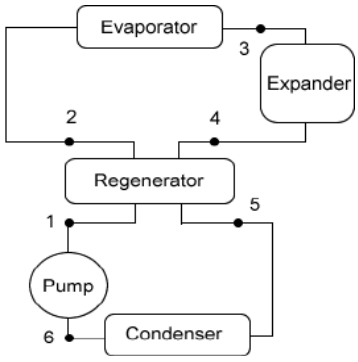

FIGURE 1. Components of an organic Rankine cycle

The main objective of this research work is to model an efficient useful application based on Organic Rankine Cycle by finding possibilities of design amendments for minimizing the cost and enhancing the efficiency. The experimental model of ORC has been developed with low cost and operational results have been obtained accordingly. This is an attempt to introduce ORCs in Pakistan which is an advance concept of power generation as compared to conventional Rankine Cycle, so that it may contribute towards meeting the growing energy demands in future.

III. Principal Steps in Modeling of ORC Cycle

The prime portion of the in hand research work is devoted to the finding out the best suitable application(s) for heat recovery, with their pros and cons, deficiencies, and potential usages. A comparison is performed among several working fluids to find the best suitable & environment friendly ones. As the expander/scroll compressor has a vital significance, so a reasonable portion of the thesis/research work is devoted to its study.

Scroll compressors have a lot of advantages over the conventional reciprocating compressor. They have less moving parts which tends to have higher reliability. The gas flow is often constant which leads to lower noise. Also there are no inlet and outlet valves which may contribute towards producing noise. Scroll compressor also generate low vibrations as compared to reciprocating compressor which is an important factor for the reliability of our experimental model. The working model is then explained, with detailed summary of each component and its measurement devices. The experimental procedure is elucidated with all the practical obstructions and the suggested remedies.

Thorough analysis of the measurements has been put forwarded, in order to enlighten the difficulties perceived in the test(s).

IV. Literature Review

Organic working fluids have been developed which have high molecular weight and specific heat, that has low ozone depletion potential called ODP as well as low global warming potential called GWP and low flammability. Extensive researches have already been carried out on the effect of working fluid selection as it applies to Rankine cycles [1-7]. Working fluids studied include water, ammonia, chlorofluorocarbons, hydro fluorocarbons, hydro chlorofluorocarbons, carbon dioxide and lot of other organic materials. Plenty of working fluids have too much attractive thermo physical properties, but are quickly ruled as unfavorable due to certain reasons like flammability, toxicity, lack of availability, cost factor, requirement of high working pressures and reason of phasing-out due to environmental considerations.

Efficiency of an ORC system mainly depends on the efficiency of expander [8,9]. Selecting expander for specific operating temperatures, expansion ratio and working fluid is very much important. Generally, expanders are of two types: turbo expanders as well as positive displacement (PD) expander. Former type is mostly used in large scale power plants while PD machines are used in smaller power plants. Turbo expanders can attain the rotating speeds as much high as 50,000 RPM and have performance efficiencies range up to 60 to 90%

Positive displacement machines operate at slower speeds and exhibit higher expansion ratios than turbo expanders of same size. The slower speed eliminate the need of higher cost rotating components and decrease the manufacturing costs in areas such as balancing. Due to these factors cost of expander for PD machines is less as compared to turbo

expanders. PD expanders have lower peak efficiencies than turbo expanders, but work well through a range of operating conditions. As concluded by Badr et el. [10], PD expanders are best choice for small waste heat systems.

The expression “waste heat recovery” basically expresses the factor of utilization of any sort of heat rejected to the environment. Viable heat sources are numerous in breadth and number of installations. Examples include industrial processes, exhaust from gas turbines, IC engines, and return flows from steam boilers and furnaces etc [11]. A thorough review of applications of industrial waste heat recovery is provided by Johnson and Choate [12]. Waste heat can be converted to electricity using a thermodynamic cycle by exchanging the heat directly to working fluids.

Organic Rankine cycles produce electricity /power from various heat sources with low temperature range like geothermal, biomass and from solar concentrators [13–16]. ORC technology is being used by companies such as Ormat, Turboden, General Electric, Pratt and Whitney, Koehler-Ziegler, Infinity Turbine, Electratherm, GMK, Adoratec [17, 18]. Sizes of Organic Rankine cycle application are in range from under 1 kW [19], to multi-unit applications producing several megawatts [20]

V. Experimental Procedures

Working fluid chosen for the present test bench is R-134a. The source of heat is comprised of hot air/saturated steam flowing at temperature range from 130-140 C0 with pressure at 6 bars from a already installed boiler in Heat & IC Engine Laboratory at University of Lahore. The expander selected is an scroll compressor of HONDA Car which is modified to be run in expander mode. Speed (RPM) of expander will be measured by means of tachometer. The condenser is fed with tap water for cooling of refrigerant gas after passing through the expander in direct cooling method whereas in indirect cooling method a separate radiator has been used wherein working fluid is further cooled by using small 12 V Fan.

For measurements of pressures and temperature of the cycle at different states pressure gauges and Thermometers and pressure transducers have been used at certain specific points on piping system. Figure 2 gives the overall schematic view of the test bench designed for development of organic Rankine cycle for micro cogeneration by using scroll compressor.

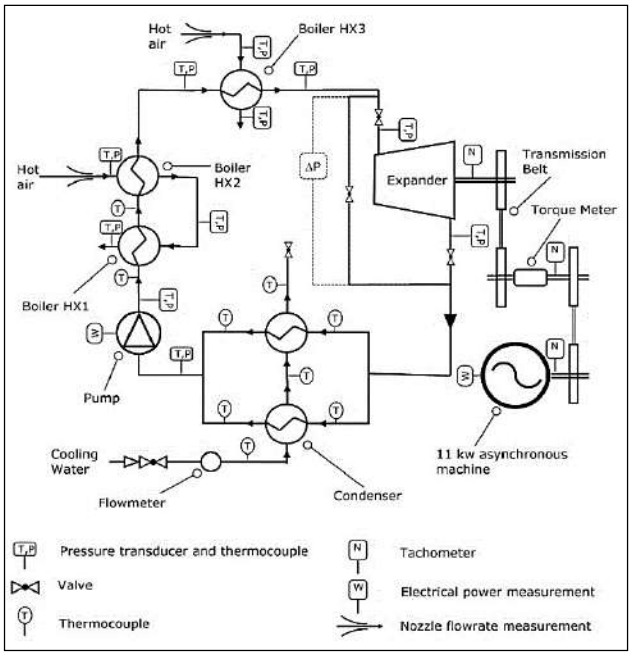

FIGURE 2. Schematic View of the Rankine Cycle test bench

During commissioning of ORC test bench three variables are of main interest whereas rest of all to be held constants, but in actual it was not so easy to do this. During commissioning/testing of ORC test bench variations in flow rate of organic fluid and water temperature at the entry point of condenser were observed.

FIGURE 3. ORC Test Bench.

Before starting the commissioning of ORC test Bench all the valves were actuated in open Positions as shown in ORC Test Bench Single Line Diagram. The positions of all the valve are adjusted so that from the heat source it directs the entire mass flow rate of water /steam through evaporator of ORC test bench during testing.

The condenser temperature was tried to controller as low as possible by putting ice in the bucket and in addition fan of radiator condenser was also put in operation to maintain the temperature of working fluid at 25 °C. During testing, it was visually noted how long fan of radiator was on duty during any data collection point so that overall system efficiency calculations could be made. Particulars of the boiler are tabled below:

TABLE 1.
PARTICULARS OF BOILER

Status of Boiler:	Functional
Fuel Use:	Natural /Sui Gas (Connection is available)
Operation Time:	04 Hours
Safety Certificates:	Already get from the supplier and additional Pressure Relief Valves are available and Functional and shutdown automatically in case of emergency.
Maximum Pressure achievable	80 Psi Almost 6 Bar
Maximum Temperature of Steam achievable	130-140 C0

VI. RESULTS AND DISCUSSION

During commissioning of the ORC test bench a lot of difficulties were faced in the form of leakage of organic fluid or working fluid through seals of pump, variable temperature of the cooling water at entry point of condensers etc however only one test day was successful in running a turbine /scroll expander.

After doing the successful commissioning of the test bench, boiler was operated to get the steam with temperature 100 C0 at 06 bars. With the aforementioned improved quality of the steam passed through the evaporator. It was noted that purity of the organic fluid at the exit of evaporator as well as entry point of scroll expander was quite improved and eventually speed of the expander/turbine was improved which was measured by the tachometer.

Rotational Speed of Scroll expander/ turbine was reached up to approximately 300 RPM only due to reduced/controlled flow rate and mixed quality of the working medium. The turbine could not spin fast enough to run "where it wanted to" with a 1:1 turbine to generator belt ratio without risking damage to the generator. Leakage through the seals of pump would not let the pump develop the differential pressure required to operate at the designed pressures. To counter the issue (1) above, operating conditions of boiler were improved by increasing the temperature and pressure of the steam to be passed through evaporator. Issue (2) from above was solved by replacing the Positive displacement pump by small compressor/pump of the air conditioner so that the pump can be capable of producing differential pressure of at least 10 bars.

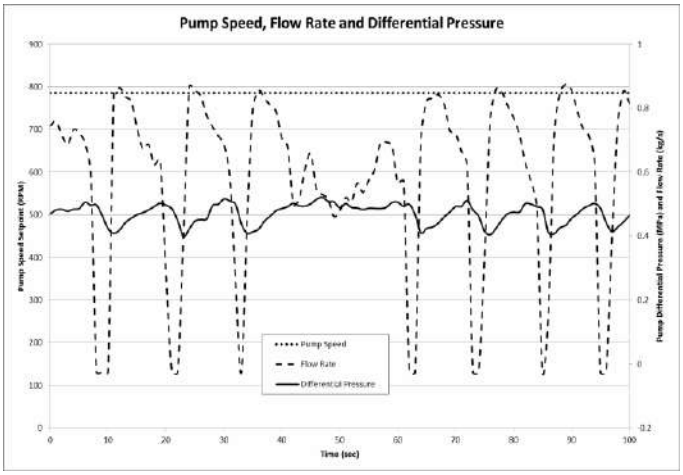

Figure 4. Pump Speed, Flow Rate and Differential Pressure. Note differential pressure peaking at 0.5 MPa and flow rate dropping repeatedly while pump speed is constant. This indicates the pressure relief valve was opening repeatedly.

After doing the trial test of the test bench on November 05 2018, boiler was operated to get the steam with temperature 140 C0 at 08 bars. With the aforementioned improved quality of the steam passed through the evaporator. It was noted that quality of the working fluid at the exit of evaporator and entry point of scroll expander was quite improved and eventually speed of the expander/turbine was improved which was measured by the tachometer.

Following results were observed after experimental analysis:

- Leakage of working fluid R134a was removed and pump was producing required differential pressure of at least 08 bars.
- Rotational Speed of Scroll expander/ turbine was reached up to approximately 800 RPM
- The Working fluid R134 inlet temperature to the evaporator was not stable during testing.
- It was shown the exit pressure at the condenser was within 0.007 MPa of the inlet to the pump.
- A system relative efficiency to turbine RPM plot was obtained.

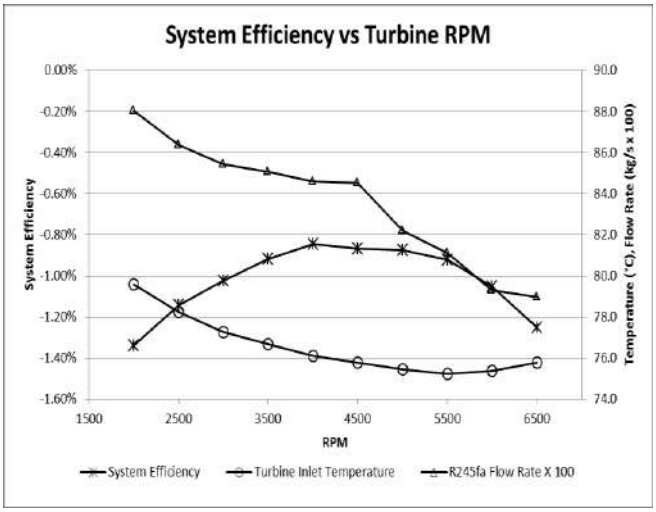

Figure 5. System efficiency versus turbine RPM.

Based upon the above mentioned results of experimental setup of ORC, it can be said that the ORC test bench model is operational and can be used to carry out further experiments. There were some errors in the beginning which were removed. All the components and overall model possess great potential for learning and this can be an initial attempt to introduce the advance energy-efficient concept of ORC in Pakistan.

VII. CONCLUSIONS

ORCs can be a great avenue towards energy contribution for countries like Pakistan. This study shows that how ORC models can be developed within the country that are fully operational, as concluded by the operational results carried out by ORC test bench. This experimental setup has been developed and operated within Pakistan and no component or device was imported for this purpose. This indicates a great possibility that such advance technologies can be employed and implemented indigenously, only the necessary awareness is required. Thus it can promise a great potential for future concerns.

Due to a lack of required testing facilities during this work, it is recommended that additional data be taken from the SANDEN manufacturer of the scroll expander. Sanden's next generation scroll compressors is designed to accomplish exceptional robustness. The scroll compression mechanism provides smooth, silent operation and high efficiency. It has swept volume of 77.1 cm3. It has shown great potential as a robust expander for tests on steam. The preliminary results from this work while operating the turbine on an organic fluid are promising. The turbine should be completely characterized through a realistic range of inlet and outlet conditions and rotational speeds.

Power meters need to be installed on the feed pump, generator and condenser to do the accurate system efficiency calculations. Also, a torque senor should be installed on the turbine to allow calculation of actual turbine power output without including belt drive and power conversion losses.

One of the overarching goals for the test bed is to conduct research on different expanders and working fluids while working at varying condenser conditions. Especially interesting would be to study the performance of variable displacement expanders with varying condenser temperatures and pressures.

A final recommendation for future work on the ORC test bench is to arrange a low RPM generator which can be connected to scroll expander to produce electricity. The low RPM generator can be easily available from local market of Pakistan. After connecting the aforementioned low RPM generator ORC efficiency test bench can be slightly improved by modifying the different equipment of test bench.

REFERENCES

[1] Hung T. C., Wang S. K., Kuo C. H., Pei B. S., and Tsai K. F., 2010, “A Study of Organic Working Fluids on System Efficiency of an ORC Using Low-grade Energy Sources,” Energy, 35(3), pp. 1403-1411.

[2] Liu B.-T., Chien K.-H., and Wang C.-C., 2004, “Effect of Working Fluids on Organic Rankine Cycle for Waste Heat Recovery,” Energy, 29(8), pp. 1207-1217.

[3] Radermacher R., 1989, “Thermodynamic and Heat Transfer Implications of Working Fluid Mixtures in Rankine Cycles,” International Journal of Heat and Fluid Flow, 10(2), pp. 90-102.

[4] Saleh B., Koglbauer G., Wendland M., and Fischer J., 2007, “Working Fluids for

[5] Low-temperature Organic Rankine Cycles,” Energy, 32(7), pp. 1210-1221.

[6] Badr O., Probert S. D., and O’Callaghan P. W., 1985, “Selecting a Working Fluid for a Rankine-Cycle Engine,” Applied Energy, 21(1), pp. 1-42.

[7] Ganic E. N., and Wu J., 1980, “On the Selection of Working Fluids for OTEC Power Plants,” Energy Conversion and Management, 20(1), pp. 9-22.

[8] Marcuccilli F., and Thiolet D., 2010, “Optimizing Binary Cycles Thanks to Radial Inflow Turbines,” World Geothermal Congress 2010, Bali, Indonesia.

[9] Facao J., and Oliveira A. C., 2009, “Analysis of Energetic, Design and Operational Criteria When Choosing an Adequate Working Fluid for Small ORC Systems,” 2009 International Mechanical Engineering Congress & Exposition, Paper #IMECE2009- 12420, ASME, Lake Buena Vista, FL, USA.

[10] Quoilin S., and Lemort V., 2009, “Technological and Economical Survey of Organic Rankine Cycle Systems,” 5th European Conference Economics and Management of Energy in Industry, Algarve, Portugal.

[11] Oomori H., and Ogino S., 1993, “Waste Heat Recovery of Passenger Car Using a Combination of Rankine Bottoming Cycle and Evaporative Engine Cooling System,” Paper# 930880, SAE International, Detroit, MI.

[12] Johnston J. R., 2001, "Evaluation of Expanders for Use in a Solar-powered Rankine
[13] Cycle Heat Engine," thesis, The Ohio State University, Columbus, OH.
[14] Badr O., O'Callaghan P. W., and Probert S. D., 1984, "Performances of Rankine- cycle Engines as Functions of Their Expanders' Efficiencies," Applied Energy, 18(1), pp. 15-27.
[15] Biddle R., November, "Exploiting Wasted Heat: New Approaches to Electricity Generation from Wasted Heat," Refocus, 6(6), pp. 34-37.
[16] Holdmann G., Test Evaluation of Organic Rankine Cycle Engines Operating on Recovered Heat from Diesel Engine Exhaust, Alaska Center for Energy and Power.
[17] Patel P. S., and Doyle E. F., 1976, "Compounding the Truck Diesel Engine with an Organic Rankine-Cycle System," Automotive Engineering Congress and Exposition, Paper #760343, SAE International, Warrendale, PA.
[18] Srinivasan K. K., Mago P. J., and Krishnan S. R., 2010, "Analysis of Exhaust Waste Heat Recovery from a Dual Fuel Low Temperature Combustion Engine Using an Organic Rankine Cycle," Energy, 35(6), pp. 2387-2399.
[19] Johnson K. M., Testimony on the U.S. Department of Energy's (DOE's) Programs for Developing Water-efficient Environmentally-sustainable Energy-Related Technologies.
[20] Zimmerle D., and Cirincione N., 2011, "Analysis of Dry Cooling for Organic Rankine Cycle Systems," 5th International Conference on Energy Sustainability, Paper.

Pakistan Journal of Engineering and Technology, PakJET
Multidisciplinary | Peer Reviewed | Open Access
Volume: 2, Number: 1, Pages: 31- 35, Year: 2019

Field Testing & Strength Evaluation of Khushhal Garh Rail cum Road Bridge

M.A. Chaudhry[1,*], A.M. Zafar Khan[1], Z.A. Siddiqi[1]

[1]Department of Civil Engineering, The University of Lahore

*Corresponding author: M.A. Chaudhry (email: drmahboob@uol.edu.pk)

***ABSTRACT*—Old age steel bridges mostly have various problems facing potentially catastrophic result. There is complex array of issues with the railway wrought iron bridges regarding their residual life. Road Cum Rail Bridge near Khushhal Garh is of wrought iron & crosses the River Indus. This bridge is 775 ft. long and consist of four deck truss spans i.e. a 303'-0" anchor arm, a 104'-8" east cantilever (Jand end) , a 261'-0" slung and a 104'-8" west cantilever span (Kohat end). The west cantilever is anchored deep into the rock by means of guys. The upper end of the guys is attached to the top boom while the lower end is connected to anchors of size 10'x 7'-6"x 4'. Roadway is supported on bottom booms of the trusses and railway track is on the top chords. The bridge was opened to traffic on 27th November, 1907. In the course of time this bridge showed some signs of distress, in December 2006, it was decided by the Pakistan Railways Authorities to carry out strength evaluation of this bridge.The task was awarded to a joint venture, Pakistan Railways Advisory and Consultancy Services (PRACS) and Multi-Dimensional Consultants (MDC, Lahore, to conduct field studies, carry out computed model analysis & suggest measures for the repair & rehabilitation of this bridge if required. For field testing, 30 strain gauges were installed at different critical locations of main members of truss. Tensile and compressive strain variation under standard test train were recorded and analyzed. Maximum tensile & compressive stresses in main members were assessed. 22.5 Ton axle group III engine were used with PR standard test train for the test. Stress range and number of loading cycles of the selected members were compared with Wohler Curves for residual fatigue life. On the basis of this comparison, it was concluded that bridge was safe under the loading given in Bridge Rules, 1971 Pakistan Railways & Pakistan Highways Code and residual life has been estimated.**

***Index Terms*—Bridges, Repair, Rehabilitation, Strengthening, Truss Structures, Fatigue Life, Wöhler Curve.**

I. INTRODUCTION

Previous history of loading is almost unknown. Proper design standards have not been used for their design condition of these bridges varies greatly from site to site. Loadings and its number of cycles have no proper record. Interaction of moving vehicles and the type of bridge structures has variable effect on their response and life. Reliable structural behavior, integrality and residual fatigue life assessment become essential for evaluating and addressing these problems.

The multistory station of Kohat and Punjab is connected through a Rail-cum-Road Bridge which crosses the River Indus on four deck truss spans i.e. a 303'-0" anchor arm, a 104'-8" east cantilever (Jand end) , a 261'-0" slung span and a 104'-8" west cantilever (Kohat end) span (Figure 1).

Figure 1 Kohat End Span

The west cantilever is anchored deep into the rock by means of guys. The upper end of the guys is attached to the top boom while the lower end is connected to anchors of size 10'x 7'-6"x 4'. These spans carry broad gauge and were designed for standard B live loading of 1903. The

railway track is at top booms and the roadway is at the bottom booms of the spans. The trusses are 45'-0" high and spaced at 20'-0" c/c.
The roadway on the bridge is 16' wide. The trough plates are laid parallel to track and rest on cross girders that are 25' c/c.
On each end of the bridge there are two stone masonry arches corridors. The road traffic passes through these corridors before entering the bridge. The overburden of the arches also provides support to the guys of 104-ft cantilever on western end of 471 ft. span.
Robertson, one of the Consulting Engineers who had been previously responsible for the erection of the well-known Lansdowne Bridge, described it as the most complicated structure he had ever dealt with.

II. INSPECTIONS OF BRIDGE

On November 26, 2006, a joint team of engineers from Multi-Dimensional Consultants and Pakistan Railways inspected the Khushhal Garh Bridge to assess the physical condition of the bridge for the purpose of the modeling & evaluation. The following worth mentioning points were noted during the inspection:

1) The turnbuckles provided at the top of rail-bridge connecting the two parts of the bridge across an expansion joint were buckled due to expansion and contraction. Similarly, the bracing plates provided in this region on lower side of the railway bridge were also buckled due to the temperature variation.
2) The remedial measures were suggested to provide slots for both turnbuckles and connecting plates to allow movement.
3) The road surface on the lower level bridge was in extremely bad shape. The traffic was still allowed to move on this bridge but due to uneven surface, excessive vibrations and impact loads were produced endangering the safety of the bridge. There seemed to be an urgent need to remove the top surface of the bridge deck for placing new wearing surface besides strengthening of buckled or damaged supporting members.
4) The bearings of the road bridge, at the abutments and at central pier, were required to be repaired to make them functional. These were to be rehabilitated by jacking up the bridge near these supports for their proper oiling & graphing.
5) Curved surfaces at the hinge supports were required to be cleaned and lubricated for its free rotation.
6) The overall condition of the substructure and the steel super-structure was found satisfactory.
7) The lower anchors at the abutments were thoroughly checked, cleaned and painted as these remain submerged during floods. This operation was required to be replaced after every flood season.
8) There is one way traffic system on this bridge. So, traffic signals must be installed to allow smooth movement of traffic.
9) A weigh bridge should be installed near this bridge to avoid overloaded traffic of trucks.

III. FIELD TESTING

Field Testing has been conducted in order to achieve the following objects:

1) To measure stress level at different critical locations.
2) To assess the bridge for its residual life and for rating of the bridge.
3) To recommend suitable measures for enhancing the residual life / capacity through suitable rehabilitation/strengthening measures.
4) To conduct economic feasibility study and prepare rehabilitation / strengthening (accompanied with estimates) for the overstressed/fatigued parts of bridge for making them fit for existing/increased speed of 65 mile/h.
5) To carry out the load and speed rating of the bridge in its existing condition, in case rehabilitation is expensive. Minor repair is accompanied with this option.

For this purpose, location of strain gauges and LVDT were fixed for computer analysis. There were 30 strain gauges. The detail of assignment of strain gauges to different member and locations were marked.
A test train of specified capacity was run to take readings on strain gauges installed at different location as shown in Figure 2.

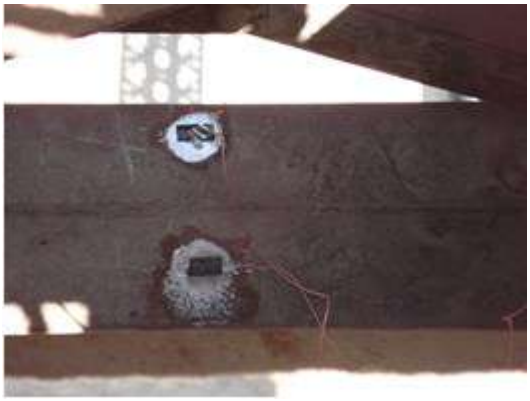

Figure 2 Strain gauges installed at different locations

IV. STRUCTURAL ANALYSIS

Applicable documents

The following documents are used for analyzing the bridge using the design codes mentioned below.
Bridge Rules – Government of Pakistan, Ministry of Communications (Railway Wing), 1971.
Steel Bridge Code - Government of Pakistan, Ministry of Communications (Railway Wing) 1971.

Analysis software

SAP2000 version 8.3.3 was used for analysis of the Bridge. This Software is capable of performing Linear or Non - Linear analysis of concrete and steel structures. The Section Designer wizard has been used to define the section of truss members. The bridge has been analyzed for each load case. The results were reported for each load case so that they can be combined with the required load combinations.

Geometry of structure

The bridge is modeled as a 3D two span continuous frame structure as shown in Figure - 2. The axial releases are given in members L15L16, U16U17, L26L27 and U25U26. The anchor members L16U16 and L26U26 are simulated as tension members (Zero Compression). The inbuilt capability of software for moving load analysis is used for railway and highway loading.

Application of loads

RAILWAY LOADING

TABLE 5.1 Cumulative Data

LOCOMOTIVE GROUP	CROSS GIRDER U29 - U29		BOTTOM CHORD L20 - L21		VERTICAL MEMBER U26 – L26	
	STRESS RANGE	NO. OF CYCLES (10^5)	STRESS RANGE	NO. OF CYCLES (10^5)	STRESS RANGE	NO. OF CYCLES (10^5)
3	0 – 6.45	0.24831	0-3.47	0.24831	0-4.6	0.24831
4	0 – 5.83	0.92994	0-3.13	0.92994	0-4.17	0.92994
Total		**1.17825**		**1.17825**		**1.17825**

VI. MEMBER FATIGUE EVALUATION PROCEDURE

From the actual test train, the variable-amplitude stress spectrum is calculated. The equivalent or constant-amplitude stress is calculated from the calculated variable – amplitudes stress spectrum using AREMA RMC relationship.

$$SR_e = \alpha\left(\sum \gamma_i \times SR_i^3\right)^{\frac{1}{3}}$$

Where,

SR_e = Effective stress range defined for the total number of variable stress cycles to failure (N_v).

SR_i = Stress range of a particular group having number of occurrences n_i.

γ_i = n_i / N_v, ratio of the number of occurrences of SRi to the total number of variable stress cycles N_v.

α = Ratio of stress range either measured from tests or estimated to the stress range calculated by structural analysis.

The calculated effective stress range (SR_e) along with the connection detail type were used to estimate the remaining life of the member using the *WÖLHER CURVE* (S-N curve). In this curve, if the stress range is less than the constant amplitude fatigue limit or the loading cycles are in compression, there is no fatigue and the fatigue life can be considered infinite. If the effective stress range is at or outside the S-N curve, the fatigue life of the member had already exhausted and replacement of part of the structure is required to ensure safety and to further use the bridge for the traffic loading.

Broad Gauge Standard loading of 1926 for Branch Line (B.L) of Bridge Rules 1971, was modeled in software using its bridge load capacity. The train was programmed to run over the bridge length. The each member had been analyzed for maximum and minimum tensile and compressive forces. As per bridge rules Pakistan Railway, the following forces were considered

1. Impact factor for railway loading
2. Racking force
3. Longitudinal loads (tractive and braking)
4. Wind forces

V. ANALYSIS OF TEST DATA

Test data has been analyzed and shown in table 5.1 and also graphically represented (fig. 6.1& 6.2).

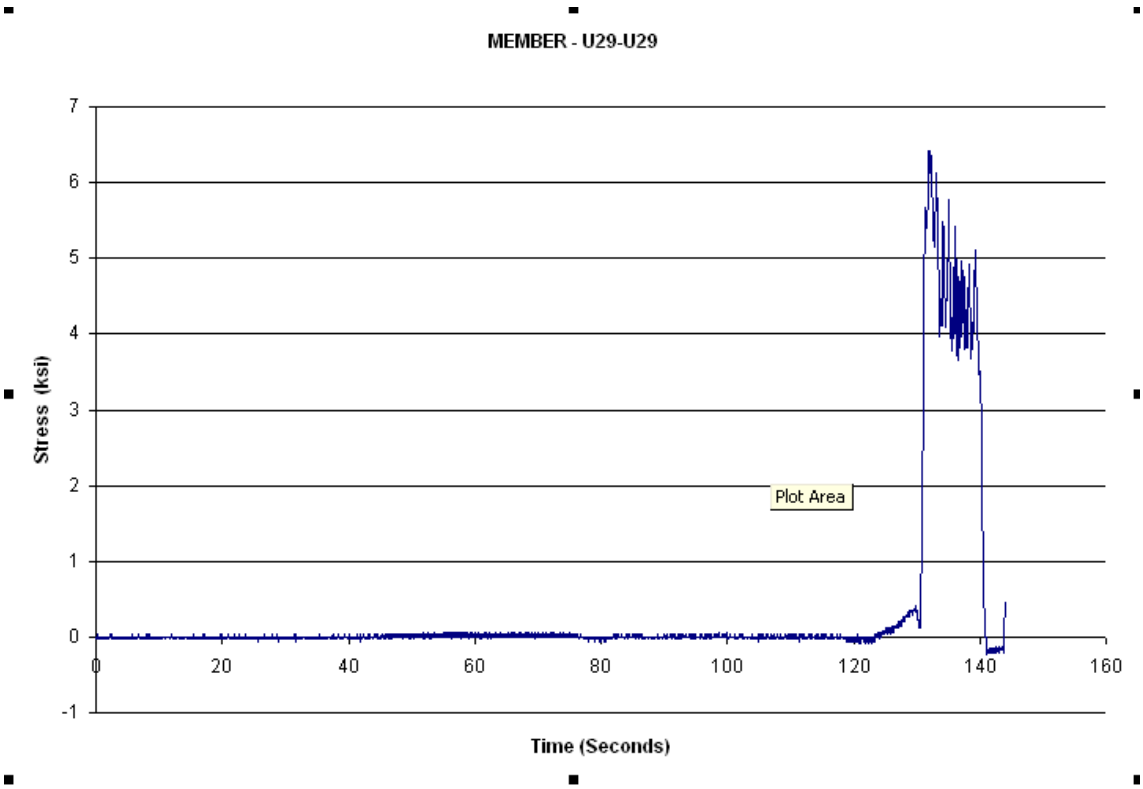

Figure 6.1 Test Train Load Spectrum for Cross Girder U29-U29

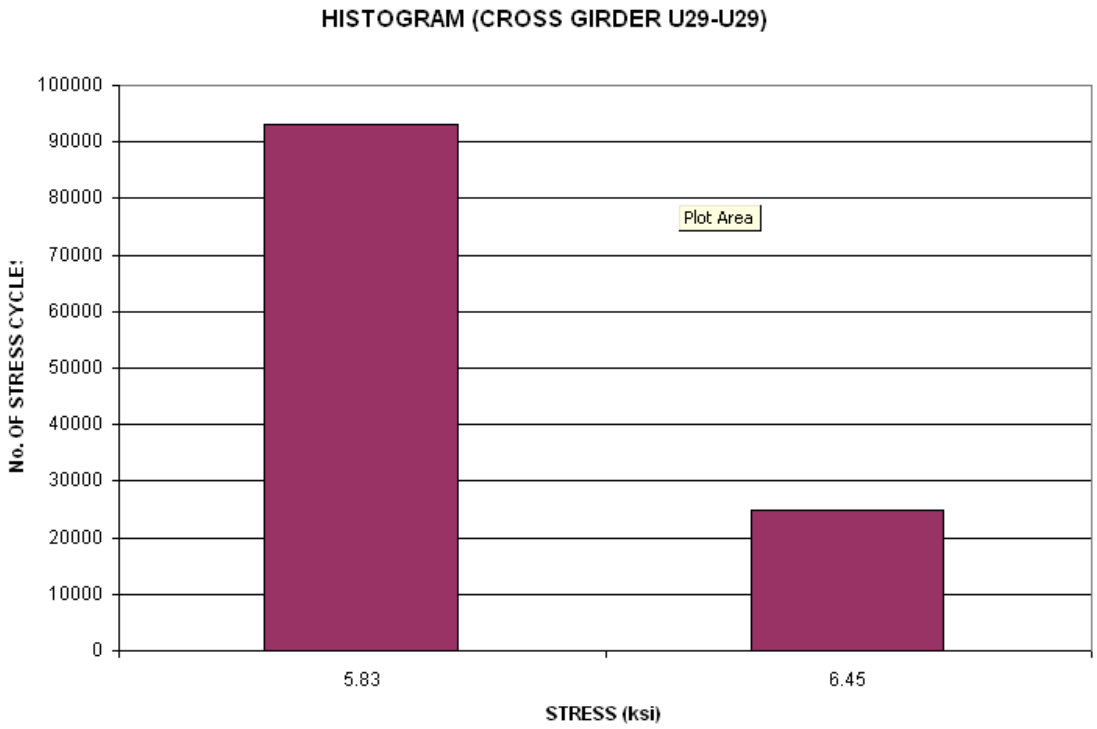

Figure 6.2 Histogram

N_v = 117825
N_1 = 92994`

$\gamma_1 = \frac{92994}{117825} = 0.789$

$SR_1 = 5.83ksi$

$N_2 = 24831$

$\gamma_2 = \frac{24831}{117825} = 0.211$

$SR_2 = 6.45ksi$

$\alpha = \frac{SR_{(measured)}}{SR_{(calculated)}} = \frac{6.64}{4.7} = 1.37$

.

$$SR_e = 1.37\left[(0.789\times 5.83)^3 + (0.211\times 6.45)^3\right]^{1/3}$$

$$= 8.166ksi$$

The calculated effective stress range parameter (SR_e) for member U29-U29 and connection detail category 'D' gave the maximum number of loading cycles equal to about $6x10^6$ = 6,000,000 from *WÖHLER CURVE* (S~N curve) of figure 6.3. Out of these only 117,825 cycles had actually occurred. This showed that significant fatigue life was left for this member.

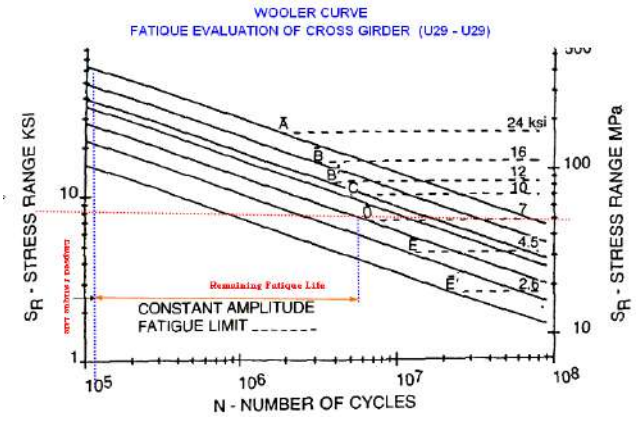

Figure 6.3 *WÖHLER CURVE* (S~N curve)

The same procedure was adopted for the calculation of fatigue life for bottom chord L20-L21 and vertical chord U26-U26.

The resulting applied stress parameter SR_e is compared with fatigue strength *WOOLER CURVE* and member is found safe against fatigue.

VII. CONCLUSIONS

On the basis of inspection, testing and evaluation, the following recommendations were made:

1. On physical inspection the croaked members and members buckled and broken due to expansion or contraction were suggested to be repaired.
2. The road surface on the lower portion bridge being severely in bad shape was recommended to be replaced.
3. The curved surfaces at hinged steel bearing were required to be cleaned and lubricated for free rotation.
4. On analysis of field testing over stressed members were pointed out and assessed for their residual life.
5. The fatigue life of members U29-U29 (cross girder) and member L20-L21 & U26-L26 were assessed using Wohler Curve. It is suggested to carry out regular maintenance to further extend the life of the bridge.

VIII. REFERENCES

1. BS 5400, "Part 10, Code of practice for fatigue, Steel Concrete and Composite Bridges." *British Standard Institutions,* 1980.
2. Fatigue Design of steel structures, Steel Construction, *Journal of the Australian Steel Instituue*.Vol.38, March 2004.
3. Korondi, L., Szittner, A., Kallo, M. and Krisrof, L., "Determination of fatigue safety and remaining fatigue life on a riveted railway bridge by measurement," *Journal of Constructional Steel Research*, Elsevier, 46 (1-3), 430, paper number 327, 1998.
4. Liu, Y., Stratman, B. and Mahadevan, S., "Fatigue crack initiation life prediction of railroad wheels" *International Journal of Fatigue*, Elsevier, 28(7), pp. 747-756, 2006.
5. Manual for Railway Engineering, *American Railway Engineering Association (AREA),* 1991.
6. Ministry of Communications (Railway wing), "Bridge Rules." Government of the Pakistan.
7. Ministry of Communications (Railway wing), "Steel Bridge Code." Government of the Pakistan, Railway Code of Practice for the Design of Steel or Wrought Iron Bridges Carrying Rail, Road or Pedestrian Traffic.
8. Pier and Abutment Standard Code of Practice for the Design of Bridge Pier and abutment.

Pakistan Journal of Engineering and Technology, PakJET
Multidisciplinary | Peer Reviewed | Open Access
Volume: 2, Number: 1, Pages: 36- 40, Year: 2019

Using Carbon Fibre Reinforced Polymer Strips for Recuperation of Originally Fissured Concrete Beams

Ali Ajwad[1, *], Ali Aqdas[2], Muhammad Ali Khan[2], Akhtar Abbas[2] and Zafar Baig[1]

[1]Department of Civil Engineering. University of Management and Technology, Lahore, Pakistan
[2]Department of Civil Engineering, The University of Lahore, Lahore, Pakistan

Corresponding Author: ali.ajwad@umt.edu.pk

Abstract*— Carbon fiber reinforced polymer (CFRP) strips are widely used all over the globe as a repair and strengthening material for concrete elements. This paper looks at comparison of numerous methods to rehabilitate concrete beams with the use of CFRP sheet strips. This research work consists of 4 under-reinforced, properly cured RCC beams under two point loading test. One beam was loaded till failure which was considered the control beam for comparison. Other 3 beams were load till the appearance of initial crack which normally occurred at third-quarters of failure load and then repaired with different ratios and design of CFRP sheet strips. Afterwards, the repaired beams were loaded again till failure and the results were compared with control beam. Deflections and ultimate load were noted for all concrete beams. It was found out the use of CFRP sheet strips did increase the maximum load bearing capacity of cracked beams although their behavior was more brittle as compared with control beam.

***Index Terms*— CFRP, rehabilitation, deflection, brittleness, cracked sections Concrete bonding, Mechanical, Chemical, bonding agent, mix ratio**

I. INTRODUCTION

A staggering seismic tremor, estimating 7.6 on the Richter scale, hit the upper area of Pakistan on eighth October, 2005. With the loss of life of around 90 thousands and wounds in a similar range, it is a fiasco on a scale at no other time found in this district. The seismic tremor likewise brought about annihilation of a wide range of structures and other framework. The structures which survived are likewise experiencing serious significant breaks. The recovery and repair of breaks to make the structure alright for human utilize is a noteworthy issue. To reestablish their basic limit, retrofitting or potentially fortifying are severely required. There are distinctive systems accessible for retrofitting and fortifying of at first split strengthened solid pillars detailed in literature. In this exploration, lab examination with respect to utilization of carbon fiber fortified polymers to fortify a given structure or part of it to reestablish its serviceability and quality is talked about.

From the past research, it is prominent that FRP (Fiber reinforced plates) tend to increase the strength of concrete members in flexure considerably. Carbon fiber reinforced polymer tends to have a satisfactory fatigue performance, extraordinary strength to weight proportion and outstanding confrontation to electrochemical oxidization which makes it essentially aimed at structural solicitation [1]. A study conducted by Alfarabi presented that despite the fact that application of FRP does elevate the maximum load taken by concrete specimens, almost all the beams started to fail at the curtailment zone of the plate [2]. The epoxy that was used to conceal the plate at the soffit of flexural individuals just fizzled at loads considerably higher than the required level [3]. Some studies have also shown that the mode of failure of beams changed from ductile to brittle after the application of Fiber reinforced polymer plates [4]. The likelihood of this change depends to a great extent on the level of FRP being utilized, the area of FRP and the nearness of shear support in the current structures [5]. Researches have also shown that despite this change in behavior of concrete elements from ductile to brittle, an increase in flexural strength ranging from 65%-135% has been seen [6].

In this research work CFRP plates were applied at the soffits of initially cracked RCC beams in different proportions in order to observe their strengthening effect as compared to control beam which was loaded up to its failure load. Besides this investigation centers around the serviceability, quality and flexibility execution for each of the CFRP proportion used to find out their potential application in at first split fortified beams.

II. EXPERIMENTAL SETUP

For investigation of the consequence of repair by using various patterns of CFRP, on the structural response of initially cracked RCC beams, four Reinforced cement concrete beams were cast, cured and tested. All beams were designed by ultimate strength method as under-reinforced and having dimensions 3000 x 200 x 275 mm and singly strengthened by 3 # 4 bars, without using shear reinforcement. All specimens were tested under two pint loading. One beam, designated by A1, was named as Control Beam and was loaded till failure. During loading of A1 specimen, deflection gauges were used to measure the deflection in the beam which were installed at middle and quarter points and finally in the end its failure load was also noted. Other three specimens were loaded till they had reached three-quarters of maximum load taken by A1 specimen. Subsequently, the load was removed and specimens removed from the testing frame, so that repairs may be carried out.

A total of three concrete beams were rehabilitated with use of altered amounts of Carbon fiber reinforced polymer plates and when repair process was over, they were again tested by the same loading arrangement till failure and deflections noted. The response of each of the three retrofitted specimens in terms of Stiffness, deflection, ultimate load, cracking load and also analyzed in the experiment were their failure patterns. Beam strengthened with one CFRP strip, are designated as B1. Similarly beam strengthened with one 1.5 meter length of strip is designated as B2 and beam strengthened by two CFRP strip is designated by B3.

A. Materials used in the beam

Cement that was used in this research was of type 1 ordinary Portland cement. Sand from Lawrencepur (Pakistan), free from deleterious substances was used. Gradation of sand was carried out in accordance with ASTM Standards. Fineness Modulus was found as 2.62. Coarse Aggregate consisted of hard, clear, sound, strong, and uncoated crushed stones quarried from Margalla hills, best source of aggregate in Pakistan near Islamabad. ASTM standard complied gradation was done for coarse aggregates. Water fit for drinking, as proved by water quality tests, was used for making of concrete elements. Beams were casted with the help of moulds of steel formwork.
1:2:4 mix design was used in making of concrete for beams with a water to cement ratio of 0.5. The average slump that was obtained from fresh concrete prepared was of 45 mm. Maximum cube crushing strength obtained from experimentation was 28 MPa. Surface of concrete was properly cleaned as the bond strength of epoxy greatly depends on the cleanliness of the surface of finished concrete

B. Materials for retrofitting

1) Sika Carbudur Laminates

Type used was S812, 1.2 mm in thickness and 80 mm in width having a cross sectional area of 96 mm^2, Black color, having base of carbon fiber reinforced with an epoxy matrix. Fiber volumetric content is greater than 68%. Main properties for this type as provided by manufacturer are as under:

Unlimited (no exposure to direct sunshine) Total life

> 165,000 N/mm^2	**Young's modulus**
> 28,000 N/mm^2	**Strength in tensile**
> 1.7 %	**Elongation at break**
1.5 g/cm^3	**Density**

2) Sikadur-30 Adhesive

For bonding Sika Carbudur laminates on the prepared substrate of beams, Sikadur-30 adhesive was used. It has following properties as per manufacturer technical data:

0.04 %	**Shrinkage**
12,800 N/mm^2	**Static E-Modulus**
Failure of concrete (4.5 N/mm^2)	**Adhesive Strength**
Failure of concrete (15.5 N/mm^2)	**Shear Strength**

C. Strengthening of beams

Three beams were retrofitted at their soffits as under:

- One S812 cover was attached along the length of beams right in the center as shown in Fig. 1.
- One 1.5 meter portion of S812 cover was attached over mid span right in the centre, shown in Fig. 2.
- Two S812 laminates were bonded along the length of beams right in the center. The schematic diagram is shown in Fig. 3.

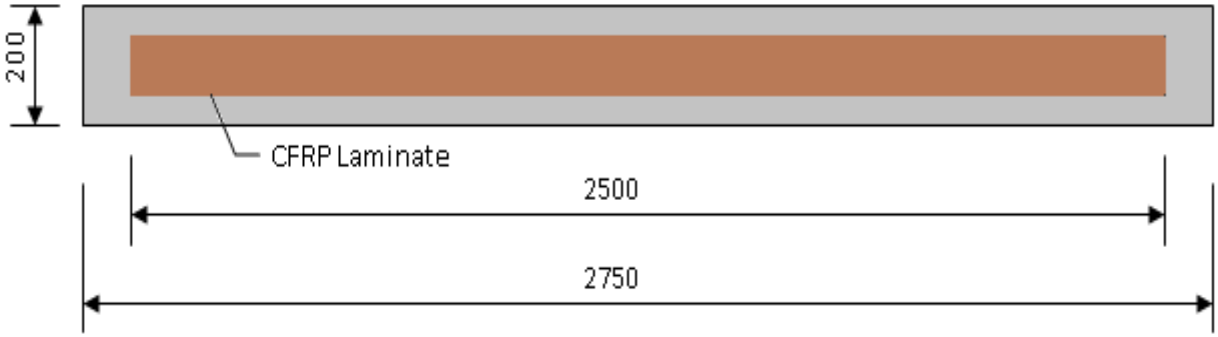

Fig. 1. Strengthening by one strip of full beam length

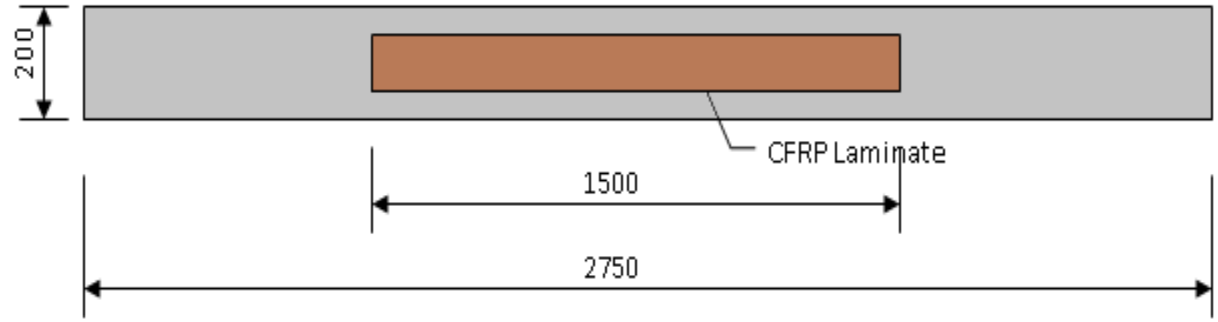

Fig. 2. Strengthening by one strip of 1.5 m length

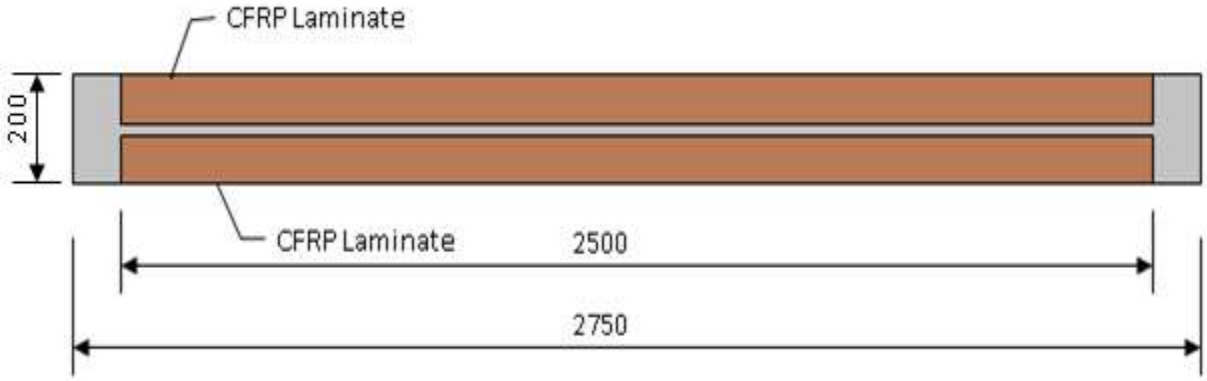

Fig. 3. Strengthening by two strips of full beam length

III. Results and Discussion

Fig. 4, 5 and 6 show load-deflections curves of specimens B1, B2 and B3 before and after repair. For plotting these curves only, deflections measured at the midspan were used. It can be seen from the plotted graphs that specimens showed more of a brittle behavior after application of CFRP laminates as competed to ductile behavior before application of CFRP. The decrease in deflection is more prominent at advanced stages of loading. Beams strengthened with one 1500 mm CFRP plate show least deflection at the highest ultimate load i.e., 180 KN, which reveals that these beams are more brittle as compared to control as well as other repaired beams. A comparison of ultimate loads, taken by control and repaired beams, is shown in fiG. 8.

In case of control beam, failure load was 201 KN. First crack appeared at 136 i.e., 68 % of the ultimate load. Crack pattern showed that failure mode was tension failure.

In case of B1, failure load of repaired beams was 220 KN, which is greater than that of control beam. First crack appeared at an average load of 152 KN i.e., 69% of failure load. After strengthening, ultimate load bearing capacity increased by 10%. Failure mode was CFRP plates end interfacial de-bonding.

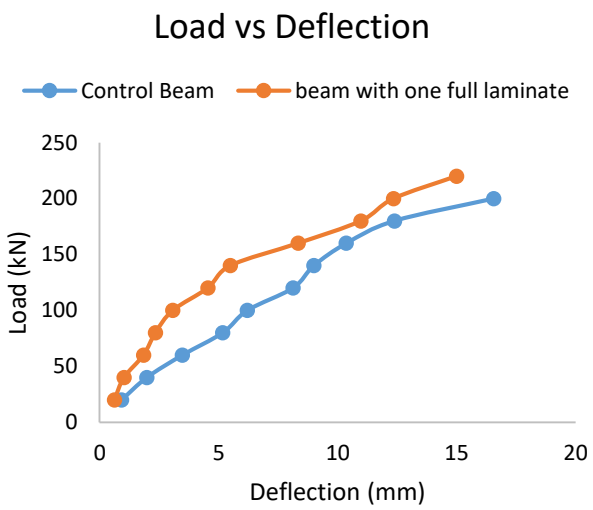

Fig. 4. Load vs Deflection graph for B1.

In case of B2, beams failed at a failure load of 180 KN. Ultimate load bearing ability for repaired beams decreased at a number of 10 % in comparison with the control beam. Failure was flexural tension failure near ends of CFRP laminates. Both tested beams failed in the same manner with CFRP plates intact with bottom.

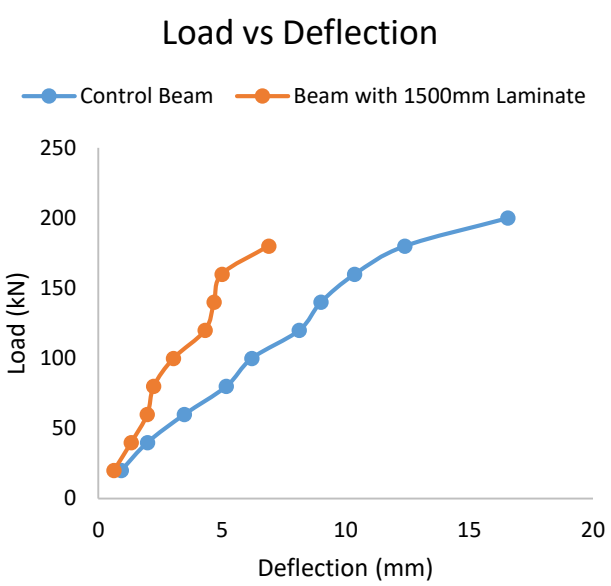

Fig. 5. Load vs Deflection graph for B2.

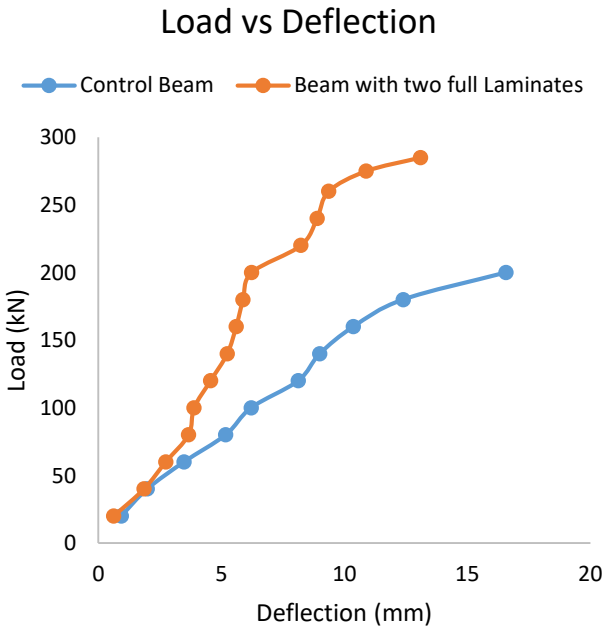

Fig. 6. Load vs Deflection graph for B3

When two CFRP laminates of full beam's length were used for repair of cracked beams, more favorable results were found. Both beams failed at 285 KN load. Ultimate load bearing capacity increased by 42% over the control beam. This ultimate bearing capacity is 29 % more than B1 and 58 % more than B2. Cracks started at load of 220 KN, which is 77 % of the ultimate failure load. Mode of failure involved the concrete cover separation (peeling off) along with laminate from one end.

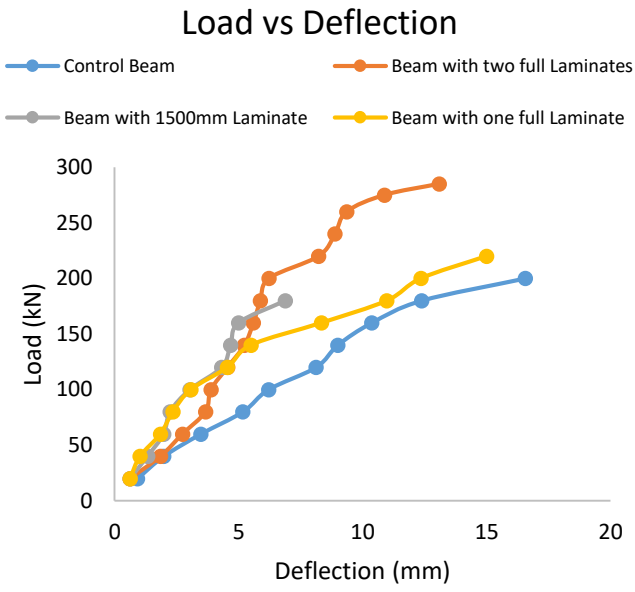

Fig. 7. Comparison for control beam and strengthened beams

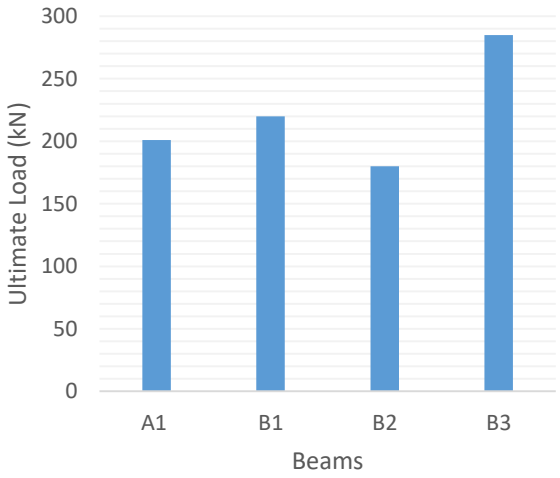

Fig. 8. Comparison of ultimate loads taken by all beams

IV. Conclusions

Based on this study, the following conclusions can be made:

- Except one repair method, all other methods proved to be effective when it comes to ultimate flexural strength and an increase was noticed in ultimate bearing capacity of beams in flexure.
- Beams rehabilitated with CFRP laminates showed more of a brittle behavior as deflection for beams considerably reduced which resulted in shear tensile failure of concrete cover when two laminates were used in soffit.

- Best results regarding ultimate failure load were achieved in case of two CFRP strips having lengths equal to full beam's length. On the other hand, the same is associated with high cost of CFRP strips used. This factor should be kept in mind while finally selecting this mode of repair.

REFERENCES

[1]. Renata, K. and S. Cholostiakow. (2015) New Proposal for Flexural Strengthening of Reinforced Concrete Beams Using CFRP T-Shaped Profiles, *Polymers* (7), 2461-2477.

[2]. Alfarabi, S., Alsulaimani, G.J., Basunbul, I.A., Bamch, M.H. & Ghaeb, B.N. (1994), Strengthening of initially loaded reinforced concrete beams with using FRP plates, *ACI Struct Journal*, 160-168.

[3]. El-Mihimly, M.T. & Tedesco, J.W. (2000), 'Analysis of reinforced beams strengthened with FRP laminates', *J Struct Eng*, 684-691.

[4]. Kim, M., Pokhrel, A., Jung, D., Kim, S. and Park, C. (2017). The Strengthening Effect of CFRP for Reinforced Concrete Beam, *Procedia Engineering (*210), 141-147.

[5]. Obaidat, Y.T, Heyden, S. and Dahlblom, O. (2010) The effect of CFRP and CFRP/concrete interface models when modelling retrofitted RC beams with FEM, *Composite structures* (92), 1391-1398.

[6]. Razali, M., Kadir, A. & Noorzaci J. (2005), Repair and structural performance of initially cracked reinforced concrete slabs, *Construction and Building Material J*, (19), 595-603.

Pakistan Journal of Engineering and Technology, PakJET
Multidisciplinary | Peer Reviewed | Open Access
Volume: 2, Number: 1, Pages: 41- 43, Year: 2019

Study of Crack Repair in Reinforced Concrete Structures Using Suitable Materials

Muhammad Ali Khan[1,*], Akhtar Abbas[1], Ali Ajwad[2], Ali Aqdas[3]

[1]Department of Civil Engineering, The University of Lahore;
[2]University of Management and Technology
[3]Governent College University, Faisalabad

*Corresponding author: Muhammad Ali Khan (email: muhammad.alikhan@ce.uol.edu.pk

***ABSTRACT*—Out of numerous serious problems that occur in reinforced concrete, formation of cracks and their propagation has its own say. Different types of cracks can form due to numerous reasons which include reinforcement corrosion, environmental effect, load impact and settlement of framework which can then affect the useful lifetime of any structure hence making the reinforced concrete structure less durable. Crack repairs, with the help of suitable materials, need to be done in order to reinstate the original strength of the structure. Water penetration test besides compression test were used to study the effectiveness of different materials used for repair work in current study. Results elaborated that polymer injection with materials available in local market can restore the actual strength of reinforced concrete elements and works more effectively as compared to other additives. It was found out through Water penetration test that water resistance was shown by all polymer injection materials.**

***Index Terms*—Repair, reinforced concrete, cementitious materials, cracks.**

I. INTRODUCTION

Reinforced concrete structures are a standout amongst the most prevalent on the planet. They are regularly utilized as a part of common and water driven designing. Amid their administration time, such type of structures have a tendency to disintegrate. Cracks are one of the most concerning issues showing up in strengthened concrete. The reasons that reason cracking of structures could be unique: reinforcement corrosion, impact of load, flimsy settlement of framework, effects from the environment, and so on. Cracks cause the diminishing of the structure's sturdiness and life span [1-3]. Consequently, it is imperative to repair these harmed structures. Diverse repair strategies have been effectively created to fortify a given structure or part of it to reestablish its serviceability and quality. It is likewise judicious to consider the toughness viewpoint when repair or reinforcing is completed. The last determination of a reasonable and best strategy for the most part relies upon straightforwardness, speed of use, basic execution and aggregate cost [4]. The correct repair of splits relies upon knowing the causes and choosing the repair systems that consider these causes; generally, the repair may just be brief. Effective long haul repair systems must assault the reasons for the breaks and additionally the splits themselves. These days all makers of repair materials endeavor to enhance their items so as to give more general and innovatively less complex repair materials for the market. It is of extensive enthusiasm to contrast financially accessible infusion materials and cementitious materials and to appraise the reasonableness of them for the cracks repair in various conditions.

Considerable amount of research has been done on use of different materials for crack repairs. Bester assessed the got to Elevate Quality Control and Quality Affirmation for Specialized Concrete Split Repair within the South African Development Industry and his comes about uncovered that there's exceptionally small dialog among the partners with respect to quality control and acknowledgment criteria when performing concrete fix repairs, not one or the other for the distinguishing proof of fix repair disappointment specifically after the completion of the fix repair, nor for long term execution of the fix repairs [5]. Kruger examined Concrete Split Repair with Polymer Altered Materials. The Require for Specialized Preparing of Implements, Providers, Experts and Clients and proposed that in spite of the fact that there's assertion that polymer-modified concrete patch repair could be a profoundly specialized field; there's an unacceptably low level of preparing in each of these segments with respects to the proper choice, application and care of such repair materials. Off base detail, improper fabric determination, misconception of the fabric properties and lacking quality control are results of this need of information and understanding which along these lines may lead to untimely disappointments and/or under-performance of the repair. In

expansion, the overview comes about moreover demonstrate that the workforce performing the physical repair work, is primarily incompetent and a few genuine intercession is required to redress this circumstance [6]. Ahn worked on Modern Surface-Treatment Method of Concrete Structures Utilizing Break Repair Adhere with Mending Fixings and concluded that water spillage can be avoided which the strength of a concrete structure can be made strides through self-healing. Too, it was confirmed that the splits were superbly closed after 28 days due to application of the split repair adhere. These comes about demonstrate the ease of use of the break repair adhere for concrete structures, and its self-healing effectiveness [7].

II. MATERIALS USED

The materials used in this research included three cementitious mortars which were prepared in three different ways; No additive was added in first mix, expansive additive was used in second and third mix was modified with polymer additive. Cement, aggregate and water used in preparation of concrete specimens were according to ASTM standards.

III. METHODOLOGY

For checking the flexural and compressive strength of mortars, specimens were prepared with dimensions of 40mm x 40mm x 160mm. Test specimens were then splitted into two parts from the center at an angle of 60 degrees to the horizontal and then they were repaired with the materials mentioned. Afterwards, compressive strength tests were performed to the check the overall decrease or increase in compressive strength compared to the control sample.

IV. RESULTS AND DISCUSSION

Effect of additives on mortar strength

For checking the effects of additives in the mortar mix, flexure and compressive strength tests were performed after a period of 28 days. Table 1 and figure 1 show the different values obtained for all the specimens tested.

Table 1 Flexural and compressive strength of mortar

Mortar type	Compressive strength (MPa)	Flexural Strength (MPa)
Mortar with no additive	22.12	3.9
Expansive additive Mortar	23.91	4.78
Polymer additive mortar	28.89	4.32

It can be seen from the table that addition of additives did have some effects on the mortar strength. In case of compressive strength, polymer additive proved to be the best modification as increase of 27% was noticed whereas in case of flexural loading, modification by expansive additive proved to be more fruitful with an increase of 23% in overall flexural strength

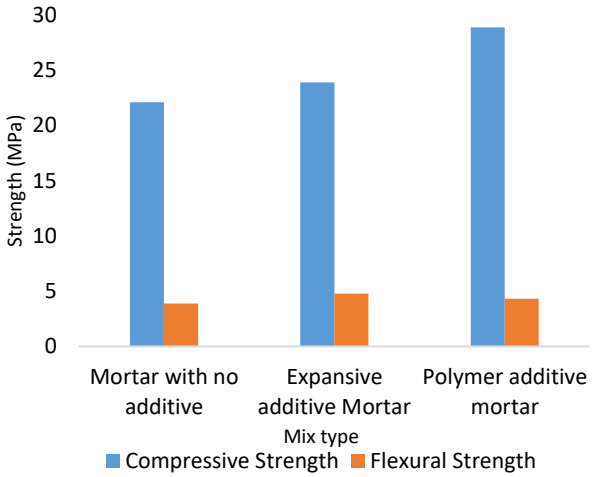

Fig 1 Flexural and compressive strength for mortar

Effect of additives on mortar strength

When repaired samples were put to compressive loading, the following results were obtained which is demonstrated by figure 2 below.

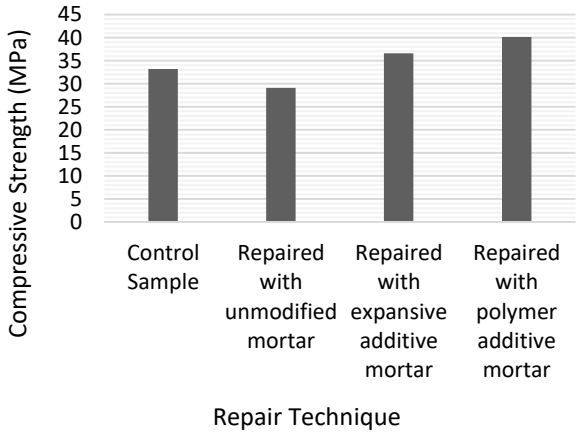

Fig 2 Compressive Strength of repaired samples

It can be seen from figure that samples repaired with polymer additive mortar displayed best results with an increase of strength of around 18%. Strength also increased with expansive additive mortar but decreased than control sample when only cementitious mortar was used.

Penetration of water in repaired samples

Table 2 shows the time taken for the water to penetrate the specimens.

Table 2 Water Penetration time (min).

Mix type	Time taken
Mortar with no additive	15
Expansive additive Mortar	31
Polymer additive mortar	18

From the above table it can be seen that expansive additives showed most resistance against water penetration when added in mortar.

V. CONCLUSION

- In case of compressive strength, polymer additive proved to be the best modification as increase of 27% was noticed.
- In case of flexural loading, modification by expansive additive proved to be more fruitful with an increase of 23% in overall flexural strength. Expansive additive mortar also showed more resistance against water penetration.

REFERENCES

[1] C.Q. Ye, R.G. Hu, S.G. Dong, X.J Zhang, R.Q. Hou, R.G. Du, C.J. Lin and J.S. Pan. EIS analysis on chloride-induced corrosion behavior of reinforcement steel in simulated carbonated concrete pore solutions. Journal of Electroanalytical Chemistry, vol. 688, pp. 675-681, 2013.

[2] E. Serri, M.Z. Suleiman and M.A.O Mydin. The Effect of Curing Environment on Oil Palm Shell Lightweight Concrete Mechanical Properties and Thermal Conductivity. Advances in Environmental Biology, vol. 9(4), pp. 222-225, 2015.

[3] P. Chindaprasirt and W. Chalee. Effect of sodium hydroxide concentration on chloride penetration and steel corrosion of fly ash-based geopolymer concrete under marine site. Construction and building materials, vol. 63, pp. 303-310 2014.

[4] R. Eadie, M. Browne, H. Odeyinka, C. Mckeown and S. Mcniff. BIM implementation throughout the UK construction project lifecycle: An analysis. Automation in construction, vol. 36, pp. 136-141, 2013.

[5] J. Bester and D. Kruger. The Need to Uplift Quality Control and Quality Assurance for Specialized Concrete Crack Repair in the South African Construction Industry. Advanced Materials Research, vol. 1129, pp. 416-421, 2015.

[6] D. Kruger and J. Bester. Concrete Crack Repair with Polymer Modified Materials. The Need for Specialized Training of Applicators, Suppliers, Consultants and Clients. Advanced Materials Research, vol. 1129, pp. 409-415, 2015.

[7] T.H. Ahn, H.G. Kim and J.S Ryou. New Surface-Treatment Technique of Concrete Structures Using Crack Repair Stick with Healing Ingredients. Materials, vol. 9(8), pp. 3-8, 2016.

Pakistan Journal of Engineering and Technology, PakJET
Multidisciplinary | Peer Reviewed | Open Access
Volume: 2, Number: 1, Pages: 44- 50 Year: 2019

Fiscal Management In Public Sector

Ch. Karamat Ali[1,*], Muhammad Masood Ashiq[1]

[1]Department of Civil engineering, The University of Lahore
*Corresponding author: Ch. Karamat Ali (email: chkaramatali108@gmail.com)

ABSTRACT— Fiscal management and financial discipline are the key indicators of the resource utilization, economic development and sustained investment. It is a proven reality that the investment cannot be productive and sustainable, till the same is utilized economically, efficiently and prudently. The research paper under consideration, differs from routine and is not much engineering oriented rather it mainly focused on financial and fiscal management in the Government Departments. How professional and competent an engineer may be, but he cannot be a good financial manager and administrator, till he has a command over latest financial rules, codes and the management tools. However, generally the engineers lack in this area, depends upon the subordinate and resultantly face serious consequences. Their ignorance in the financial matter leads to misclassification, embezzlement and doubtful expenditure.

The paper deliberates in detail, different accounts parameters, derived from New Accounting Model (NAM) introduced by World Bank to enforce strict financial management in the government departments. Detailed framework of account classifications and different elements of New Accounting Model have been deliberated and coding of different transactions presented through examples for guidance/ understanding of financial managers. The paper will be particularly helpful for the SDOs and the DDOs (XENs) to exercise and implement these latest financial tools within their jurisdictions. Implementation of this latest coding technique will ensure strict financial discipline and transparency in disbursements. This fiscal prudency will not only lead to satisfaction among DDOs but they will also feel protected against any subsequent implications and embarrassment before auditing authorities/ donner agencies. The paper will be equally helpful for the functionaries working in the private sector/organization.

Index Terms—Accounts Classifications, Financial Management, Fiscal Prudency, Budgetary Transaction and Disbursements, Accounting Element, Drawing and Disbursement Officers (DDOs).

I. INTRODUCTION

Financial resources are very instrumental towards the infrastructural development and economic growth of any country. It is the established fact and proven reality that no nation could exist, progress and sustain without technological advancement and economic development. Contrary to the general education, the engineers stimulate, activate and accelerate the process for achieving the above national targets. Based upon their professional education in a specific field, computer expertise in modeling, they can conceive, prepare and execute the development projects / activities in an efficient, effective and sustainable manner. They can also very well apprehend the fate of the investment to be made for the infrastructural and technological development.

The financial resources of any nation are generated through public contribution in the form of taxes and other liabilities. Evidently the authority and competency for utilization of these resources must lie and entrusted to the 'public representative'. Under this principle, public representatives' functions as 'policy makers' and identify the area for utilization of the resources. However, the professionals are associated in this process and their role is not only limited to project execution but they are also made responsible for disbursement and account's maintenance.

The alarming part of story is that neither the engineers are educated in the field of accounting at undergraduate level nor their capacity is properly built on joining the Govt. Departments, whereas they are given such important portfolio of financial disbursement. Their status is very synonymous to the untrained and unprofessional bus driver, who is seated on the driving seat and given the control of the bus. What could be the fate of passenger? They can only be survived but with the blessing of God. On the same analogy, untrained financial manager (Engineers), when given the authority of fund utilization, they misappropriate and mishandles the Government resources, leading to serious consequences in terms of inquiries, suspension and their terminations.

II. BUDGET AND ACCOUNT CYCLE

In Pakistan's scenario, the financial cycle comprises of three major Authorities. The public representative function as 'policy maker' to allocate the available resources in the priority sector of Government. The Provincial Administrative Depts. (PADs) executes the given policies and disburse the resources. The expenditure such incurred is audited and monitored by 'DG/AG

Audit & Accounts'. The Accounts of departments are finally presented to the public representative through PACs to assess whether the given resources to PADs are utilized and disbursed in line with the policy directives, rules and regulation. The financial cycle being implemented in Pakistan and the financial flow hierarchy within the Departments is shown below (Fig 1 & 2):

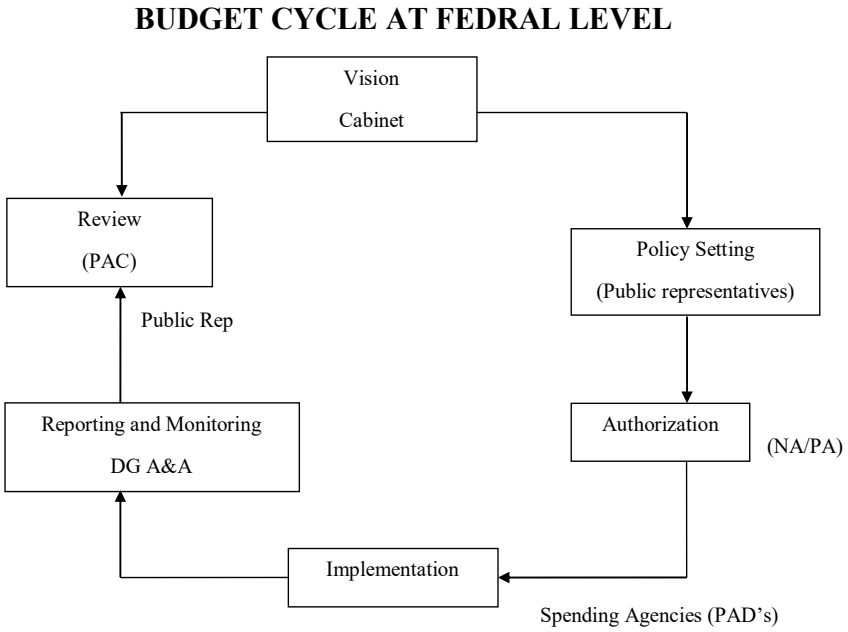

Figure 1: Budget cycle at Federal Level

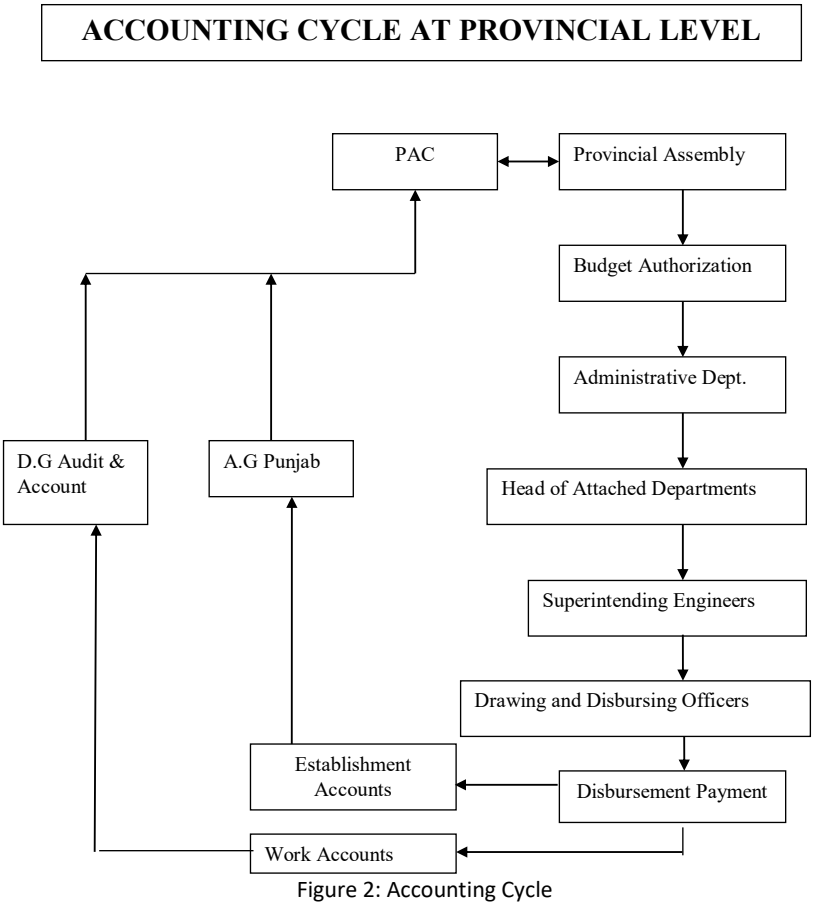

Figure 2: Accounting Cycle

From the above it is evident that the public resources/funds are allocated and controlled by the Public Representative in line with their Government policies and priorities. Under the given policy directive projects are prepared by the Administrative Departments (ADs) and authorized by the public representative institutions i.e. 'National Assembly' (NA) and 'Provincial Assembly' (PA). The allocated resources are then spent by the administrative departments and monitored/audited by the Audit Departments. The accounts of the spending by ADs are ultimately presented to the Public Accounts Committee (PAC) to ensure that the spending is transparent, equitable and in accordance with rules & regulations.

In order to exercise a better financial control over the resources different type of delegations, codes and accounts manual have been prepared specifically indicating the detail accounts classification for the guidance of Drawing and Disbursing Officers (DDOs). The resources are supposed to be utilized under the defined 'Head of Account' and within the budgetary limits. Drawing and Disbursing Officers (DDOs) are required to reconcile their expenditure within their own hierarchy and also with the Audit Department at districts, divisions & provincial level. Any discrepancy needs to be reconciled and rectify at that level. However, what I observed during my decade long association with the Irrigation Department, there is a lot of variations, misclassifications and misappropriations in the spending along with the bookings, particularly at provincial level (AG, DG, A&A). The consequences are obvious. Due to lack of coordination and reconciliation the department suffer and ultimately feel very embarrassing situation before PAC.

Historically, accounting system in Pakistan remained so weak and misclassified that during 80's World Bank conducted audit of its loan and there were million-dollar difference and misclassified when accounts were reconciled. The expenditure figure booked by GOP, substantially varies from the World Bank in terms of allocation, utilization, booking and particularly in the classifications. Resultantly World Bank put a huge plenty on GOP for this financial mismanagement and irregular spending. This irresponsive attitude on the part of DDOs and supervisory authorities not only brought a bad name for Pakistan but World Bank also decided to control and limit the further loaning. Under this drive the project of PIFRA was launched and New Accounting Model (NAM) introduced in Pakistan so that the DDO's could exercise better financial management within their respective jurisdiction. The new 'Chart of Account' under NAM indicating very detailed accounts classification is as under:

III. CHART OF ACCOUNTS

The chart of "Accounts" provides a "Frame–Work" for organizing accounting transaction to provide number of views of a particular transaction. The various views are indicated with elements comprising of alpha and numeric characters. The chart of account applies to all accounting entities and responsibilities for "Its" updating and maintenance lies with the Auditor-General of Pakistan.

Preciously speaking, the new chart of account will be a 'Phrase' comprising of some alpha character (A, B, C) and the numeric character (1, 2, 3…). However, each alpha and numeric character will refer to a particular element and the activity. The chart of the account will ultimately identify and indicate the detailed 'Account Classification' under which the expenditure will be booked/managed. This can be elaborated through an example that in the language of chemistry Carbon and Oxygen when differently related change their characteristics altogether CO (carbon monoxide), CO2 (Carbon dioxide), CO3 (Carbon trioxide) hence by changing CO to CO2 and CO2 to CO3, the characteristics of carbon changes, similar is the behavior of chart of accounts in the New Accounting Modal (NAM). By changing any alpha or 'Numeric Character' the account classification is changed. The main framework of chart of account are as under:

IV. ELEMENTS OF CHART OF ACCOUNTS

1) Entity elements.
2) Object elements.
3) Fund elements.
4) Functional elements.
5) Project elements.

1) Entity Element:

Under the entity element the DDOs, particular Department and the District where the office of DDOs is located are identified. In addition, the District Account Office (DAO) with which the DDO is drawing its disbursement is identified. It contains a phrase of 'eleven characters' (three alpha and eight numeric). Alpha character indicates the province and District Account Office whereas the numeric character indicate department, attached department and the DDOs. Each DDO will be allocated a unique account number in Pakistan (i.e. like ID of each individual).

Under this element one can have an access to DDO of a particular department, the province and the DAO. However, the activity which the DDO is making is not traceable. The hierarchy of this entity element is shown below (Fig 3): *2) Object Element:*

There are following two broad classification of this element

i. Accounting element
ii. Account number

The accounting element indicate the nature of transection/voucher which the DDO is performing i.e. whether the DDO is making expenditure or receiving the amount on behalf of Government. Each type of activity is indicated by one 'alpha character'. Likewise, the 'account number' is further classified into three sub heads i.e. major object, minor object and the detail object. The major object indicates the type of expenditure/receipt. The minor & detailed object further elaborate the specific & particular area where the activities are to be performed and expenditure is being made. The structural hierarchy of this element is shown below (Fig 4)

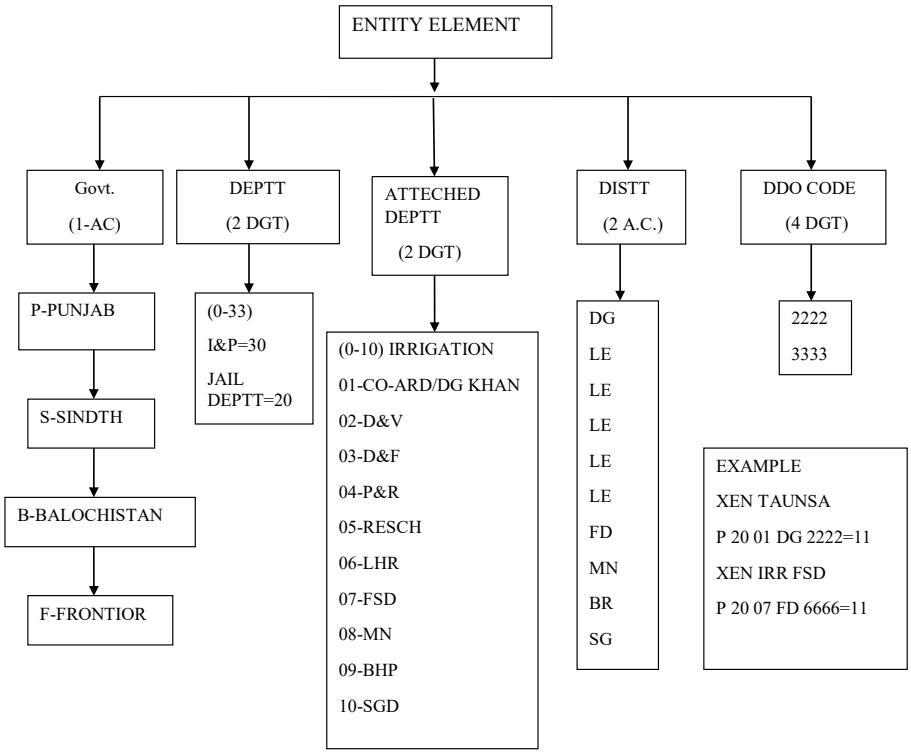

Figure 3: Entity Element

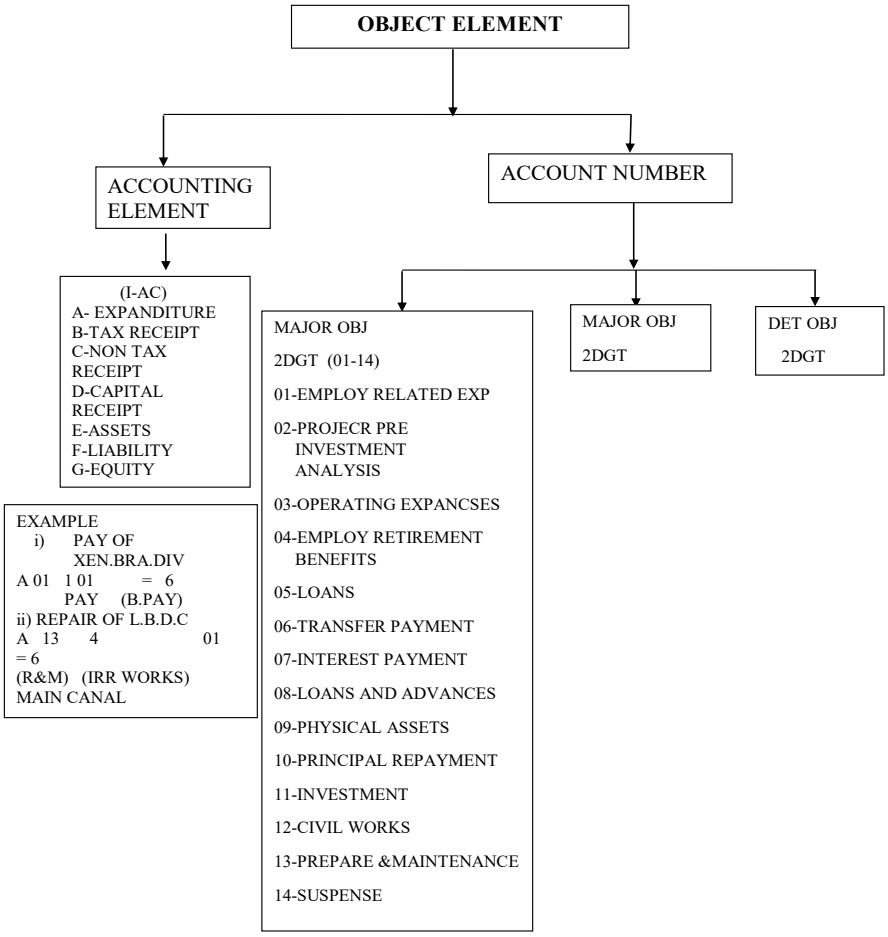

Figure 4: Object Element

3) Fund Element:

The fund element indicates the source of funding i.e. consolidated or public accounts. Furthermore, whether the funds being utilized is a 'voted' or 'charged expenditure' (presented & approve by assembly or otherwise)

The fund element comprises of six characters i.e. one alpha and five numeric. The alpha character only indicates the type of funding (consolidated or public funds) and numeric character indicate the source and nature of approval. Furthermore, each department is given a particular 'grant number' indicated by three digits. The classification of fund elements narrated as under (Fig 5):

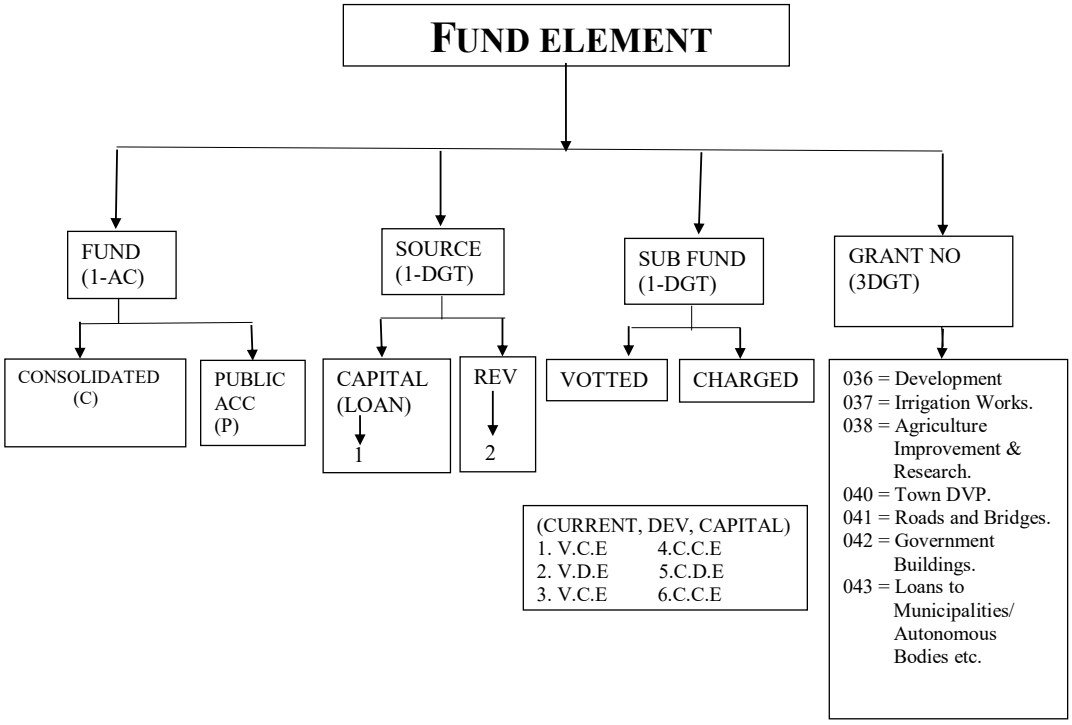

Figure 5: Fund Element

4) Functional element

This element is divide into following major classification

i. Major function (2DGT)
ii. Minor function (1DGT)
iii. Detailed function (1DGT)
iv. Sub detailed function (2DGT)
v. Program (3DGT)

The functional element indicates the role, responsibility and function of the organization where DDO is either making expenditure or receiving amount from public and private organization on behalf of Government. The total departments/organization of Pakistan have been divided into ten major functions. Then each major function is divided into series of minor function. Each minor function is divided into detailed function and ultimately each detail function is further divided into sub detailed function.

If the project is identified and executed under a program (National drainage program) then each program is allocated three digits.

This element comprises of eleven characters and all are numeric. However, each digit in these eleven characters will refer to a particular organization, department and further subsections. The functional element clearly takes you to the lowest formation, account classification minimizing the chance of misclassification and ids very effective tool for financial management. The hierarchy of function element is as under:

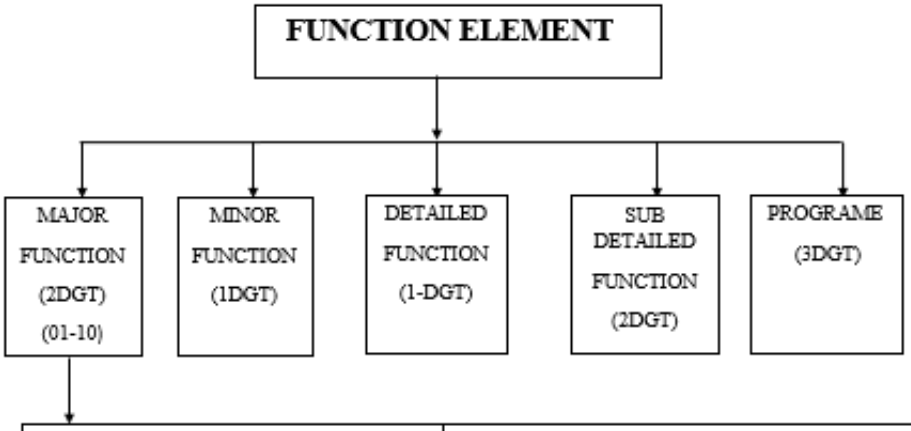

Major Function	Minor Function
01- GENERAL PUBLIC SERVICE	011. Executive and Legislative Organs Financial and Fiscal Affairs, External Affairs. 012- Foreign Economic Aid 013- Public Debt Transactions 014- Transfers 015- General Services 016- Basic Research 017- Research and Development General Public Services. 018- Administration of General Public Services 019- General Public Services not Elsewhere defined.

Detailed coding of 1 Major Function relevant to Irrigation Department

MAJOR FUNCTION	MINOR FUNCTION (1-8)	DETAILED FUNCTION	SUB DETAILED FUNCTION
ECONOMIC AFFAIRS (04)	1-COMMERCIAL & LABOUR AFFAIR 2- AGRICULTURE, FOOD & IRRIGATION. 3- FUEL AND ENERGY 4- MINNING AND MANUFACTURING 5- CONSTRUCTION AND TRANSPORTATION 6- COMMUNICATION 7- OTHER INDUSTRIES 8- RURAL DEVELOPMENT	0421 AGRICULTURE 0422 IRRIGATION 0423 LAND RECLAMATION	0422 01 ADMN 0422 02 DAMS 0422 03 CANAL IRRI 0422 04 TUBEWELLS 0422 05 EQUIPMENT & MACHINERY WORKSHOP 0422 06 IRRIGATION RESEARCH & DESIGN 0422 07-50 OTHERS **0423 01 ADMINISTRATION** 0423 02 WATER LOGING & SALINITY 0423 03-50 OTHERS

The new chart of account under NAM is very effective tool and provides a detailed framework through is different elements to manage the accounts under details subhead and the classifications. The coding under various transaction through this is revised and new modal is deliberated with the following examples:

The one transection (technical pay of chief engineer Faisalabad zone and basic pay of superintendent jail Sargodha) is classified under all the elements i.e. entity, object fund and functional elements. This example is good guideline/ tool for the learner who is involved and practicing the NAM.

Coding of all Elements under NAM:

EXAMPLE (PREPAIR IRRI DAM)

04	2	2	02	009 =	9
MAJOR FUNCTION	MINOR FUNCTION	DET FUNCTION	SUB DET FUNCTION	PROGRAMME	

EXAMPLE. TECH. PAY OF C.E IRRIGATION FAISALABAD ZONE.

P 20 07 FD 2222 — ENTY ELE

A 01 1 04 — OBJECT ELE

C 2 1 333 — FUND ELE

04 2 2 01 — FUNC ELE

EXAMPLE. Basic Pay of Superintendent Jail Sargodha

P13 01 SG 7777 — ENTY ELE

A011 01 — OBJECT ELE

C 1 1 444 — FUND ELE

0341 01 — FUNC ELE

Project Element: Every project will be allotted an independent No of four digit code.

V. CONCLUSION

1. Previously the Account's classification were comparatively broad based and were not well defined. Resultantly the expenditure were mis-booked and mishandled. This lose control on the budgetary transections leads to misuse of authority by DDOs, corruption and the embezzlement. Contrary to this, detail classification under NAM has been introduced, which provides excellent tool and framework for DDOs to manage and book the expenditures under proper 'head of account'. This new system has substantially controlled and managed the financial mismanagement and misuse of powers in the Govt. Departments.
2. Due to relaxed classification under traditional system, expenditure was booked under irrelevant head within and intra Departments (expenditure of irrigation was booked in agriculture department). This was the common phenomena at district and particularly at provincial level (AG Punjab). This scenario, creates a lot of problems in 're-conciliation of accounts'. Now every transaction has been regulated and defined under specific head of account. Therefore the chances of misclassification has substantially minimized. Consequently, the issue of re-conciliation of accounts has been much streamlined at all level. The officers feel more relaxed and don't face any embarrassment before PAC.
3. New Accounting Model (NAM) present a good frame work and road map for spending, managing and booking the accounts transections. The new system is very useful for young engineers (SDOs) and particularly DDOs (XENs). Now they feel more confident and comfortable in spending and managing the 'budget allocation' up to the grass root level. Due to usage of 'Budgetary allocation' efficiently, affectivity and prudently, officers have been much relaxed and protected against inquires, suspension and termination, enjoying a good growth and development in their professional carriers.

VI. REFERENCES

1. "Chart of Accounts." *PIFRA Pakistan*, http://www.pifra.gov.pk/docs/nam/05-Chart-of-Accounts.pdf. Accessed 15 Jun. 2019.
2. "Financial Accounting & Budgeting System." *FABS CGA Pakistan*, https://fabs.gov.pk/. Accessed 14 Jun. 2019.
3. "New Accounting Model." *PIFRA Pakistan*, http://www.pifra.gov.pk/nam.html. Accessed on 10 Jun. 2019.
4. "PIFRA Brochure – FABS." *PIFRA Pakistan*, Brochure/PIFRA-broucher.pdf. Accessed on 19 Jun. 2019.

Pakistan Journal of Engineering and Technology
Multidisciplinary | Peer Reviewed | Open Access
Volume: 2, Number: 1, Pages: 51- 58, Year: 2019

Variational Regularization for Multi-Channel Image Denoising

Muhammad Wasim Nawaz[1], Abdesselam Bouzerdoum[2], Senior Member, IEEE, and Son Lam Phung[2], Member, IEEE

[1] Department of Computer Engineering, The University of Lahore, Lahore, 54000, Pakistan
[2] School of Electrical, Computer and Telecommunications Engineering, Northfields Avenue, Wollongong, Australia

Corresponding author: Muhammad Wasim Nawaz (e-mail: Muhammad.wasim@dce.uol.edu.pk).

Abstract- **Image restoration from noisy observations is an inverse problem. Total variation (TV) is widely used to regularize this problem. TV preserves object boundaries better than a quadratic regularizer; however, it performs poor in low-textured image regions because it generates undesirable staircase artefacts. Furthermore, TV can preserve sharp horizontal and vertical edges; however, it causes the unnecessary smoothing of edges at an angle other than 0° or 90°. This problem arises because TV minimizes the gradient magnitude. Therefore, to preserve sharp boundaries, the design of an efficient variational regularizer is crucial. This paper presents a novel regularizer for the denoising of multi-channel vector valued image. The proposed regularizer uses horizontal, vertical as well as diagonal derivatives, and imposes the intensity continuity of partial image derivatives at each pixel of the underlying image. Experiments reveal that the proposed regularizer preserves edges and object boundaries better than TV based regularizers. This regularizer is also able to reduce undesirable staircase artefacts produced by TV in flat image regions.**

Index Terms -- **Image denoising, Regularization, Sparsity, Total variation, Multi-channel images.**

I. INTRODUCTION

Most of image processing tasks are inverse problems where the aim is to find the solution of an unknown signal from noisy observations. Variational methods stabilize the solution of these ill-posed problems by regularizing unknown signals [15]. The regularization is required to obtain physically plausible solutions. A good regularizer ensures a stable estimation of the unknown signal; therefore, the design of an efficient variational regularizer is crucial.

Variational methods impose a smoothness constraint to regularize ill-posed image processing tasks. A quadratic regularizer blurs strong edges and object boundaries by penalizing intensity variations at or across them. To protect sharp edges and boundaries, robust norms are used with the smoothness constraint [4]. The ℓ_1 norm is of particular interest because it makes the variational functional convex. TV regularization has been successfully used in numerous image processing tasks such as image denoising [2, 12, 23, 28], image restoration [18, 19], image deconvolution [8] and image de-blurring [2, 20]. The TV regularizer promotes the sparsity of the computed solution. It preserves object boundaries better than a quadratic regularizer; however, it performs poor in low-textured image regions because it generates undesirable staircase artefacts. Thus, this paper proposes a novel sparsity enhancing regularizer, which aims to overcome shortcomings of the TV regularizer.

The rest of the paper is organized as follows. Section 2 reviews regularization techniques for variational methods. Isotropic, anisotropic and higher order total variation regularizations are focused in this review. Section 3 proposes a novel regularizer that enforces the continuity of partial derivatives of the underlying image. The rotational invariance of the proposed regularizer is proved. Section 4 embeds the proposed regularizer into a variational framework to denoise multi-channel images. It also gives algorithmic details of the proposed method. Section 5 presents experimental results to show the superiority of the proposed regularizer over total variation for noisy image restoration. Section 6 concludes the paper.

II. SPARSITY PROMOTING TV REGULARIZATION

This section presents sparsity promoting isotropic, anisotropic and higher order TV regularizers.

A. ISOTROPIC TOTAL VARIATION

An isotropic quantity does not change its value regardless of its direction of measurement. An isotropic regularizer applies the same amount of regularization in each direction [6]. Let a digital image. *F(i, j)* be defined for the horizontal and vertical co-ordinates *i* and *j*, respectively, over a domain $\mathfrak{D}$. The discrete isotropic TV (iTV) of *F(i, j)* can be defined as the sum of the magnitude of the image gradient at each pixel:

$$\|\nabla F(i,j)\|_{\mathrm{iTV}} := \sum_{i,j\in\mathfrak{D}} |\nabla F(i,j)| = \sum_{i,j\in\mathfrak{D}} \sqrt{[\nabla_x F(i,j)]^2 + [\nabla_y F(i,j)]^2}. \quad (1)$$

The sum of the gradient magnitude makes TV a semi ℓ_1 norm. It is well-known that ℓ_1 norm of the gradient promotes the sparsity of the image in the gradient domain [5]. Therefore, a piecewise smooth image is obtained by minimizing (1). An isotropic TV can preserve sharp horizontal and vertical edges; however, it causes the unnecessary smoothing of edges at an angle other than 0^o or 90^o. This problem arises because isotropic TV minimizes the gradient magnitude. This problem can be reduced by using variants of TV, for example, anisotropic TV [13, 25, 26], nonlocal TV [16, 21] or higher order TV [7, 27].

B. ANISOTROPIC TOTAL VARIATION

Anisotropic TV applies a direction dependent regularization to the underlying image. It imposes the smoothing along strong intensity structures but not across them [26]. For a discrete image *F(i, j)*, the anisotropic TV (aTV) can be defined as the sum of the absolute difference of partial image derivatives:

$$||\nabla F(i,j)||_{\text{aTV}} := \sum_{i,j\in\mathfrak{D}} |\nabla_x F(i,j)| + |\nabla_y F(i,j)|. \quad (2)$$

Anisotropic TV regularization performs better than isotropic TV at strong intensity structures such as edges and object boundaries. However, unlike isotropic TV, it is not rotationally invariant to the pixel grid. Thus, it produces suboptimal solutions in the presence of rotations of the camera or the pixel grid [17].

Discontinuities in an image occur along object boundaries where the image gradient is high. Therefore, making the regularization adaptive to the image structure can preserve sharp boundaries better than a non-adaptive regularization. To this end, anisotropic TV regularization is sometimes weighted by an image-driven weight function $w(|\nabla I|)$ as

$$E_{\text{reg}}(F(i,j)) = \sum_{i,j\in\mathfrak{D}} w(|\nabla I|)\big(|\nabla_x F(i,j)| + |\nabla_y F(i,j)|\big). \quad (3)$$

For small positive numbers α and β, $w(|\nabla I|)$ can be chosen as $w(|\nabla I|) = \exp(-\alpha|\nabla I|^{\beta})$. Anisotropic TV is easier to minimize than its isotropic counterpart. Therefore, numerous convex minimization methods can be used to minimize anisotropic TV. These include gradient methods [3, 14], primal dual methods [6], iterative shrinkage or thresholding-based methods [2, 4], and graph cuts based methods [11, 17].

C. HIGHER ORDER TOTAL VARIATION

Mathematically, higher order total variation (HOTV) can be given as

$$||\nabla F(i,j)||_{\text{HOTV}} := \sum_{i,j\in\mathfrak{D}} |\nabla F(i,j)| + \alpha|\nabla^k F(i,j)|, \quad (4)$$

where *k* represents the order of the regularization, and a positive constant α balances the effect of gradient and higher order derivatives. The idea of using higher order derivatives has been modified to include Laplacian Δ with the gradient for the regularization of unknown images as

Isotropic and anisotropic TV produce staircase artefacts in low-textured and flat image regions. To reduce this undesirable effect, higher order total variation regularization has been proposed [7].

$$||\nabla F(i,j)||_{\text{Lap-TV}} := \sum_{i,j\in\mathfrak{D}} |\nabla F(i,j)| + \alpha|\Delta F(i,j)|. \quad (5)$$

The use of higher order derivatives may result in the blurring of sharp image boundaries. Thus, higher order TV regularization uses an adaptive functional which makes the regularizer act as ordinary TV at sharp boundaries, whereas it uses higher order derivatives in textured and flat image regions.

Total generalized variation (TGV) has been proposed as a generalization of higher order TV regularization [22, 27]. By changing the order of the regularizer, TGV allows to reconstruct piecewise smooth, affine and quadratic images. The TGV regularizer can be used to obtain a globally optimal solution because, similar to the TV regularizer, it is also convex. TGV and HOTV are computationally more expensive than the ordinary TV because of the calculation of higher order derivatives.

III. PROPOSED REGULARIZER

This section proposes a novel regularizer capable of avoiding the shortcomings of TV based regularizers. The proposed regularizer is based on the variational measure introduced in [24], which imposes the intensity continuity of partial image derivatives at each pixel in a small neighborhood. The variational measure is defined for scalar images only. However, the proposed regularizer is designed to handle multi-channel vector valued images. This regularizer, in contrast to TV based regularizers, can preserve edges and object boundaries which are not either horizontal or vertical. It is also able to reduce undesirable staircase artefacts produced by TV in flat regions where there is a little intensity change. First, the regularizer is formulated for multi-channel images. Second, the rotational invariance of the proposed regularizer is proved for multi-channel images.

A. THE FORMULATION

Let $\mathbf{F} = [F_1\, F_2 \cdots F_c]^{\mathrm{T}}$ be a multi-channel image with *c* number of channels. Discrete partial derivatives of this image **F** at pixel location (*i, j*) can be given as forward differences:

$$\nabla_{x(i,j)}\mathbf{F}(i,j) = \mathbf{F}(i+1,j) - \mathbf{F}(i,j),$$

and

$$\nabla_{y(i,j)}\mathbf{F}(i,j) = \mathbf{F}(i,j+1) - \mathbf{F}(i,j).$$

Now, for each channel of **F**, let us consider the continuity of its partial derivatives in a 2 × 2 neighborhood. Partial

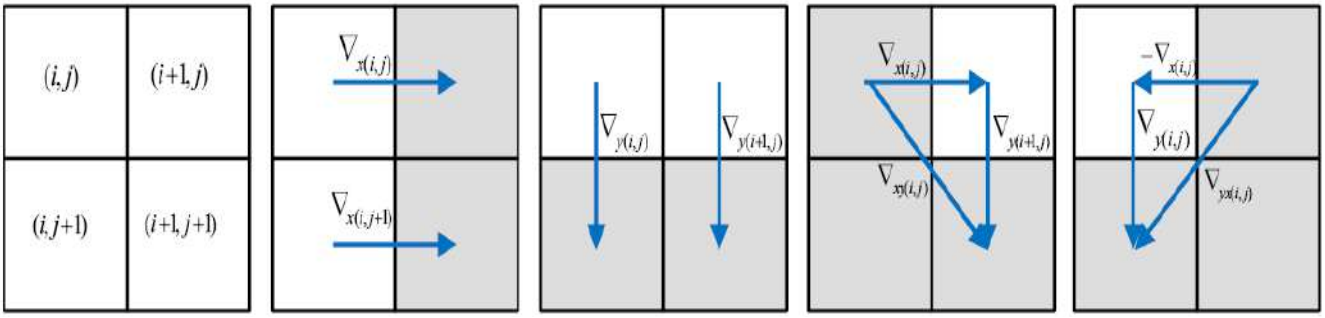

Figure 1: The gradient continuity: (a) a 2 × 2 neighbourhood showing pixel positions, (b)-(e) the vertical, horizontal, diagonal 45° and diagonal 135° boundaries, respectively. Required derivatives for the gradient continuity are shown in blue colour in (b)-(e), for each direction of the boundary.

derivatives $\nabla_{x(i,j)}$ and $\nabla_{y(i,j)}$ can be continuous along all directions except their own directions because they are desired to be discontinuous to preserve sharp edges and boundaries. For example, $\nabla_{x(i,j)}$ enforces the continuity along all directions except the horizontal direction. The continuity of partial derivatives depends upon the direction associated with the boundary. Continuity constraints for different boundary directions in a 2 × 2 neighborhood are as follows:

- vertical, $\nabla_{xx(i,j)} = \nabla_{x(i,j+1)} - \nabla_{x(i,j)} = 0;$
- horizontal, $\nabla_{yy(i,j)} = \nabla_{y(i+1,j)} - \nabla_{y(i,j)} = 0;$
- diagonal 45°, $\nabla_{xy(i,j)} = \nabla_{x(i,j)} + \nabla_{y(i+1,j)} = 0;$
- diagonal 135°, $\nabla_{yx(i,j)} = \nabla_{y(i,j)} - \nabla_{x(i,j)} = 0.$

Figure 1 shows these four boundaries along with associated image derivatives in a 2 × 2 neighborhood. For vertical, horizontal, diagonal 45◦ and 135◦ boundaries, the directional continuity of partial derivatives ∇_x and ∇_y is enforced by minimizing $\nabla_{xx(i,j)}$, $\nabla_{yy(i,j)}$, $\nabla_{xy(i,j)}$ and $\nabla_{yx(i,j)}$, respectively. To regularize the multi-channel image $\mathbf{F}$, we minimize the $\ell 1$ norm of aforementioned partial derivatives as

$$E_{\text{reg}}(\mathbf{F}) = ||(\nabla_x \mathbf{F})||_1^2 + ||(\nabla_y \mathbf{F})||_1^2 + ||(\nabla_{xy} \mathbf{F})||_1^2 + ||(\nabla_{yx} \mathbf{F})||_1^2 + ||(\nabla_{xx} \mathbf{F})||_1^2 + ||(\nabla_{yy} \mathbf{F})||_1^2. \quad (6)$$

A careful inspection of continuity constraints reveals that

$$\nabla_{xx} \mathbf{F} = \mathbf{F}(i+1, j+1) + \mathbf{F}(i,j) - \mathbf{F}(i+1,j) - \mathbf{F}(i,j+1) = \nabla_{yy} \mathbf{F}. \quad (7)$$

Given the goal to recover sparsest partial derivatives, $\nabla_{xx(i,j)} = 0$ or $\nabla_{yy(i,j)}, = 0$ implies zero partial derivative along the horizontal or vertical direction, respectively. This is equivalent to $\nabla_{x(i,j)} = 0$ or $\nabla_{x(i,j)} = 0$. In this case, the minimization of $\|\nabla_{xx} \mathbf{F}\|_1$ and $\|\nabla_{yy(i,j)} \mathbf{F}\|_1$ is redundant under the minimization of either $\|\nabla_x \mathbf{F}\|_1$ or $\|\nabla_y \mathbf{F}\|1$. Therefore, these two terms can be omitted in (6). Since $\mathbf{F} = [F_1\, F_2 \cdots F_c]^{\mathrm{T}}$, we penalize the magnitude of

Horizontal, vertical and diagonal derivatives of each channel, and denote this regularizer as HVD ($\mathbf{F}$):

$$\begin{aligned} \text{HVD}(\mathbf{F}) &:= E_{\text{reg}}(\mathbf{F}) \\ &= ||\sqrt{(\nabla_x F_1)^2 + (\nabla_x F_2)^2 + \cdots + (\nabla_x F_c)^2}||_1^2 \\ &+ ||\sqrt{(\nabla_y F_1)^2 + (\nabla_y F_2)^2 + \cdots + (\nabla_y F_c)^2}||_1^2 \\ &+ ||\sqrt{(\nabla_{xy} F_1)^2 + (\nabla_{xy} F_2)^2 + \cdots + (\nabla_{xy} F_c)^2}||_1^2 \\ &+ ||\sqrt{(\nabla_{yx} F_1)^2 + (\nabla_{yx} F_2)^2 + \cdots + (\nabla_{yx} F_c)^2}||_1^2. \end{aligned} \quad (8)$$

The regularizer HVD($\mathbf{F}$) enforces the continuity of partial image derivatives at each pixel, and minimizes their $\ell 1$ norm separately.

Therefore, regularizing an image using (8) is expected to preserve sharp horizontal, vertical as well as diagonal edges. Furthermore, the inclusion of diagonal derivatives along with the horizontal and vertical derivatives in a neighborhood around each pixel imposes more constraints on the image to be restored. Consequently, the HVD regularizer reduces staircase artefacts in flat regions. In addition, it is more robust against outliers than traditional TV regularizer. The separate minimization of partial derivatives favors a solution which is sparser than the solution obtained by using TV. As an implication, HVD($\mathbf{F}$) requires fewer number of measurements than TV for the estimation of unknown signals.

B. ROTATIONAL INVARIANCE

We prove the rotational invariance of the proposed regularizer given in (8) for multi-channel images. We use 2D rotations to give proof for 2-channel images; nevertheless, by using higher dimensional rotations, it is easy to show that the regularizer is invariant to rotations for multi-channel images. Let $\mathbf{R}$ be a 2D rotation matrix for a 2- channel image $\mathbf{F} = [F_1\, F_2]^{\mathrm{T}}$. When the camera is rotated by an angle θ, the rotated image $\mathbf{RF}$ is given as

or $$\mathbf{RF} = \begin{pmatrix} \cos(\theta) & -\sin(\theta) \\ \sin(\theta) & \cos(\theta) \end{pmatrix} \begin{pmatrix} F_1 \\ F_2 \end{pmatrix} \quad (9)$$

$$\mathbf{RF} = \mathbf{R}_1 F_1 + \mathbf{R}_2 F_2, \quad (10)$$

where $\mathbf{R} = (\mathbf{R}_1 \ \ \mathbf{R}_2)$. For the proposed regularizer, we will prove that HVD(**F**) = HVD(**RF**). Considering the first term in the square root of (8), i.e., $(\nabla_x F_1)^2 + (\nabla_x F_2)^2$, and substituting rotated image **RF** into this term, we get

$$\begin{aligned}(\nabla_x \mathbf{R}_1 F_1)^2 + (\nabla_x \mathbf{R}_2 F_2)^2 &= (\nabla_x F_1 \cos\theta - \nabla_x F_2 \sin\theta)^2 \\ &+ (\nabla_x F_1 \sin\theta + \nabla_x F_2 \cos\theta)^2, \\ &= (\nabla_x F_1 \cos\theta)^2 + (\nabla_x F_2 \sin\theta)^2 \\ &- 2(\nabla_x F_1 \cos\theta)(\nabla_x F_2 \sin\theta) \\ &+ (\nabla_x F_1 \sin\theta)^2 + (\nabla_x F_2 \cos\theta)^2 \\ &+ 2(\nabla_x F_1 \sin\theta)(\nabla_x F_2 \cos\theta).\end{aligned}$$

By canceling common terms and after some rearrangements, we obtain

$$\begin{aligned}(\nabla_x \mathbf{R}_1 F_1)^2 + (\nabla_x \mathbf{R}_2 F_2)^2 &= (\nabla_x F_1)^2(\cos^2\theta + \sin^2\theta) \\ &+ (\nabla_x F_2)^2(\cos^2\theta + \sin^2\theta), \\ &= (\nabla_x F_1)^2 + (\nabla_x F_2)^2,\end{aligned}$$

which is identical to the image without rotation. The similar proof can be provided for terms involving ∇_y, ∇_{xy} and ∇_{yx}. Hence the proposed regularizer is invariant to camera rotations.

IV. IMAGE DENOISING USING PROPOSED REGULARIZER

In this section, we apply the proposed regularizer to the problem of image denoising. Let $\mathbf{f} = [\mathbf{f}_1 \ \mathbf{f}_2 \cdots \mathbf{f}_c]^T$ be the lexicographically vectorized multi-channel image **F**, **g** be the degraded version of **f** and S be a linear matrix operator that represents the degradation process. The image restoration model can now be given as

$$\mathbf{g} = S\mathbf{f} + \eta, \tag{11}$$

where η denotes multichannel noise. One popular example of the restoration process is image denoising. When the matrix S is assumed to be an identity matrix I_n of size n × n, we get **g** to be a noisy version of the original image **f**. We denoise (11) using the proposed regularizer. The variational energy $E(\mathbf{f})$ incorporating (11) and the proposed regularizer can now be given as

$$E(\mathbf{f}) = \min_{\mathbf{f}} ||\mathbf{f} - \mathbf{g}||_1^2 + \lambda[\mathrm{HVD}(\mathbf{f})], \tag{12}$$

where λ is a regularization parameter. The first term in (12) represents the data fidelity term that enforces the restored image to be close to the noisy image. We have used the robust ℓ_1 norm with the data fidelity term to handle outliers in the restoration process. Note that both data and regularization terms in (12) are convex; thus, convex optimization methods can be used to solve for f from the resulting energy $E(\mathbf{f})$. Here, we demonstrate how a fast algorithm, NESTA, presented in [3] can be modified to solve Equation (12). NESTA has been used to solve large-scale variational problems [9]. We give the algorithmic details for the image denoising. NESTA uses a differentiable Huber norm approximation to the ℓ_1 norm; therefore, it can handle smooth as well as non-smooth convex functionals. We modify NESTA to solve image restoration problem.

Table 1: The proposed algorithm for image restoration

Initialization: $\mathbf{f}^0 = 0$.
Set iteration index $k = 1$.
while(not converged & $k \leq$ max_iter)
1. compute $\partial_{\mathbf{f}^k} E(\mathbf{f}^k)$ from (14),
2. compute $\gamma^k = \frac{1}{2}(k+1)$ and $\tau^k = \frac{2}{k+3}$,
3. compute $\mathbf{p}^k = \mathbf{f}^k - \frac{1}{L}\partial_{\mathbf{f}^k} E(\mathbf{f}^k)$,
4. compute $\mathbf{q}^k = \mathbf{f}^0 - \frac{1}{L}\sum_i^k \gamma^i \partial_{\mathbf{f}^i} E(\mathbf{f}^i)$,
5. update $\mathbf{f}^k = \tau^k \mathbf{p}^k + (1-\tau^k)\mathbf{q}^k$,
$k = k + 1$.
end while

The Huber norm is given as

$$||x||_\epsilon = \begin{cases} \frac{x^2}{2\epsilon}, & \text{if } |x| \leq \epsilon, \\ |x| - \frac{\epsilon}{2}, & \text{otherwise.} \end{cases}$$

The derivative of the Huber norm is given by

$$\frac{\partial}{\partial x}||x||_\epsilon = \frac{x}{\max(\epsilon, |x|)}.$$

We use differentiable Huber norm in place of the ℓ_1 norm in (12). The combined data and the regularization energy $E(\mathbf{f})$ is now given as

$$\begin{aligned}E(\mathbf{f}) = \min_{\mathbf{f}} &||\mathbf{f} - \mathbf{g}||_\epsilon^2 \\ &+ \lambda\Big(||\sqrt{(\nabla_x \mathbf{f}_1)^2 + (\nabla_x \mathbf{f}_2)^2 + \cdots + (\nabla_x \mathbf{f}_c)^2}||_\epsilon^2 \\ &+ ||\sqrt{(\nabla_y \mathbf{f}_1)^2 + (\nabla_y \mathbf{f}_2)^2 + \cdots + (\nabla_y \mathbf{f}_c)^2}||_\epsilon^2 \\ &+ ||\sqrt{(\nabla_{xy} \mathbf{f}_1)^2 + (\nabla_{xy} \mathbf{f}_2)^2 + \cdots + (\nabla_{xy} \mathbf{f}_c)^2}||_\epsilon^2 \\ &+ ||\sqrt{(\nabla_{yx} \mathbf{f}_1)^2 + (\nabla_{yx} \mathbf{f}_2)^2 + \cdots + (\nabla_{yx} \mathbf{f}_c)^2}||_\epsilon^2 \Big),\end{aligned} \tag{13}$$

where $\boldsymbol{\nabla}_x$, $\boldsymbol{\nabla}_y$, $\boldsymbol{\nabla}_{xy}$ and $\boldsymbol{\nabla}_{yx}$ are sparse difference matrices to calculate derivatives of vectorized images. An iterative scheme is used to find the minimum of (13) at iteration k as

$$\begin{aligned}\partial_{\mathbf{f}^k} E(\mathbf{f}^k) = \Big[&2(\mathbf{f}^k - \mathbf{g}) \\ &+ \lambda\Big(\boldsymbol{\nabla}_x^{\mathrm{T}} \frac{(\boldsymbol{\nabla}_x \mathbf{f}^k)}{\max(\epsilon, |\boldsymbol{\nabla}_x \mathbf{f}^k|)} + \boldsymbol{\nabla}_y^{\mathrm{T}} \frac{(\boldsymbol{\nabla}_y \mathbf{f}^k)}{\max(\epsilon, |\boldsymbol{\nabla}_y \mathbf{f}^k|)} \\ &+ \boldsymbol{\nabla}_{xy}^{\mathrm{T}} \frac{(\boldsymbol{\nabla}_{xy} \mathbf{f}^k)}{\max(\epsilon, |\boldsymbol{\nabla}_{xy} \mathbf{f}^k|)} + \boldsymbol{\nabla}_{yx}^{\mathrm{T}} \frac{(\boldsymbol{\nabla}_{yx} \mathbf{f}^k)}{\max(\epsilon, |\boldsymbol{\nabla}_{yx} \mathbf{f}^k|)} \Big) \Big],\end{aligned} \tag{14}$$

where $\partial_{\mathbf{f}^k} E(\mathbf{f}^k) = \partial E(\mathbf{f}^k) / \partial \mathbf{f}^k$. The algorithm computes two auxiliary variables p_k and q_k at each iteration from $\partial_{\mathbf{f}^k} E(\mathbf{f}^k)$. It then combines both auxiliary variables to get next estimate $\mathbf{f}^k$. The choice of ε plays an important role in the algorithm. The speed of the convergence is shown to have direct relationship with this approximation constant [3]. A small value of ε gives

good accuracy at the cost of slow convergence and vice versa. The proposed algorithm uses Lipschitz continuity; therefore, a Lipschitz constant L is required for the computation of auxiliary variables from (14). Lipschitz constant L depends on λ, Huber norm parameter ε, and the norms of sparse difference matrices.

To compute the Lipschitz constant L, we need to find the upper bound for the norm of HVD. It has been shown in [10] that difference matrices used to calculate TV are bounded above by 8. A similar analysis can be made for difference matrices used in HVD. The ℓ_1 norm of any matrix is maximum absolute column sum of that matrix.

HVD consists of four sparse difference matrices: ∇_x, ∇_y, ∇_{xy} and ∇_{yx}, which are used to compute discrete differences. These matrices have exactly two nonzero entries +1 or −1. Therefore, they satisfy $\|\nabla_x\|1 = 2$, $\|\nabla_y\|1 = 2$, $\|\nabla_{xy}\|1 = 2$ and $\|\nabla_{yx}\|1 = 2$. Since we minimize the magnitude of each partial flow derivative in HVD,

$$||\nabla_x^{\mathrm{T}}\nabla_x||_1 + ||\nabla_y^{\mathrm{T}}\nabla_y||_1 + ||\nabla_{xy}^{\mathrm{T}}\nabla_{xy}||_1 + ||\nabla_{yx}^{\mathrm{T}}\nabla_{yx}||_1 = 4+4+4+4 = 16.$$

Hence, difference matrices used in HVD are bounded above by 16. Lipschitz constant L is then given as $L = 16\lambda/\varepsilon$. The algorithm runs for a fixed number of iterations or until it reaches the convergence. The summary of the algorithm is shown in Table 1.

V. EXPERIMENTAL RESULTS

The proposed regularizer has been tested on several images to evaluate its performance under noise. For the validation of the proposed regularizer, a comparative analysis is conducted with isotropic [6], anisotropic [26] and higher order TV [27] regularizers by assessing the quality of the denoised images. First, the experimental setup, describing images used in experiments, is presented. Second, the performance is analyzed on images corrupted by a controlled amount of noise.

A. EXPERIMENTAL SETUP

All experiments have been performed on publically available real world images which are used as benchmarks for various vision and image processing tasks. The image dataset used in these experiments comprises of greyscale images *Cameraman*, *Barbara*, *Boat* and *Man*, and colour images *Baboon*, *House*, *Monarch* and *Pepper*. These images are corrupted by a controlled amount of noise. The quality of denoised images have been assessed by calculating the peak signal to noise ratio (PSNR), which is given as

$$\mathrm{PSNR} = 20 * \log(\frac{f_{\max}^2}{\mathrm{MSE}}),$$

where $f_{\max}$ = 255 for an 8 bit image and MSE is the mean squared error:

$$\mathrm{MSE} = \frac{1}{n}\sum_n (\mathbf{f}-\mathbf{g})^2.$$

To conduct a fair comparison, the energies of proposed regularizer and the three TV regularizers are minimized using NESTA ([3]). It should be mentioned that the use of different regularizers alter the variational energy to be minimized. Consequently, the values of optimum regularization parameters for these regularizers also change. In these experiments, we have manually tuned regularization parameters of these regularizers to get best denoising results for all of these regularizers. These experiments are conducted using $\lambda_{\mathrm{iTV}} = 0.05$, $\lambda_{\mathrm{aTV}} = 0.05$, $\lambda_{\mathrm{HVD}} = 0.01$ and $\lambda_{\mathrm{HOTV}} = 0.006$.

B. IMAGE DENOISING

These experiments have been conducted to test the capability of the proposed regularizer to denoise images. A controlled amount
of Gaussian noise is added to images described above. Since clean images are available, performances of the proposed and TV based regularizers have been measured quantitatively by calculating the PSNR for denoised images. The influence of the controlled noise is also analyzed qualitatively on denoised images.

Table 2 shows quantitative results for all four regularizers on eight images. These results have been taken for a standard deviation of noise $\sigma = 25$. Optimum values of regularization parameters are used for all regularizers. It can be observed that the HOTV regularizer performs better than both isotropic and anisotropic TV regularizers. However, the proposed HVD regularizer outperforms the HOTV for most of images.

Figure 2 demonstrates the denoising of the greyscale image *Cameraman* when it is contaminated with a noise of $\sigma = 25$. Highlighted parts of images in Figure 2 (c) and (d) show staircase artefacts, whereas highlighted parts in Figure 2 (e) and (f) show a significant reduction in these artefacts. However, the image denoised by the HVD has a higher value of PSNR = 30.21 as compared to the image denoised by the HOTV regularizer with a PSNR = 29.38, as given in Table 2. Highlighted parts of Figure 2 are also shown in Figure 3 as 3D plots for a better visualization of staircase artefacts.

Denoising results on the colour image *Monarch* are shown in Figure 4. A qualitative comparison of images in Figure 4 (b) and (c) with (d) and (e) reveals that HVD and HOTV regularizers outperform anisotropic and isotropic TV especially in highlighted textured regions of denoised images. The image denoised by the HVD regularizer in Figure 4 (d) has a higher PSNR = 30.92 than anisotropic, isotropic and higher order TV regularizers with PSNR = 28.58, 28.07 and 30.15, respectively. Moreover, staircase artefacts can be observed in highlighted parts of images in Figure 4 (b) and (c). HVD and HOTV regularizers do not show noticeable staircase artefacts.

Figure 5 presents PSNR as a function of standard deviation of noise σ for all four regularizers. An average PSNR has been calculated over all eight images, and the results are reported in Figure 5 (a). These results clearly indicate that the proposed regularizer outperforms TV based regularizers for increasing values of standard deviation of noise. Similar kind of results can be observed for *Cameraman* and *Pepper* in Figure 5 (b) and (c), respectively

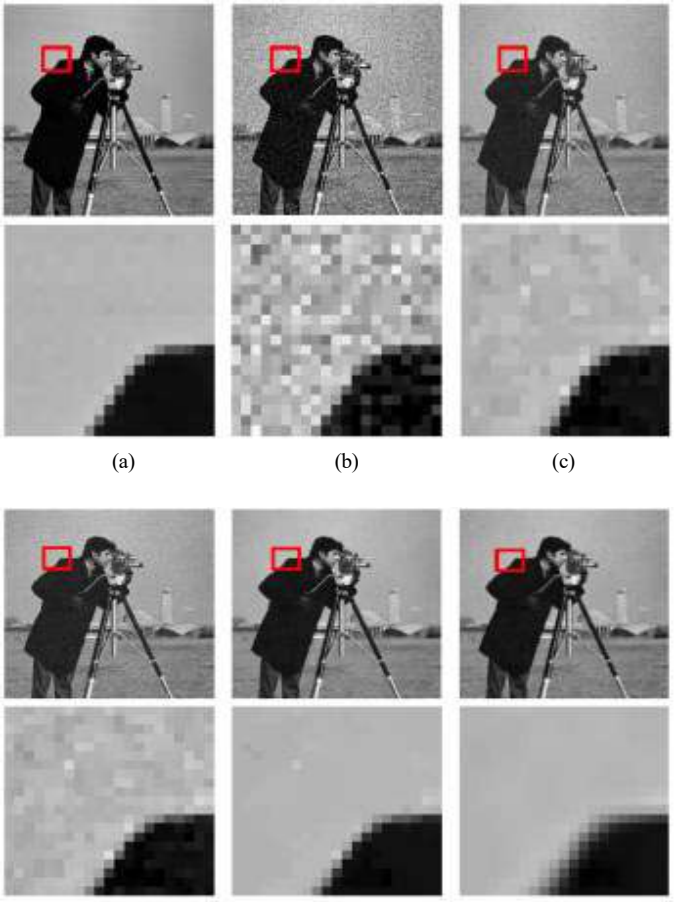

(a) (b) (c)

(d) (e) (f)

Figure 2: The denoising of the greyscale image *Cameraman*. (a) Original image, (b) image corrupted by a Gaussian noise of σ = 25, image denoised by (c) anisotropic TV, (d) isotropic TV, (e) the proposed HVD and (f) higher order TV regularizers. Highlighted parts of these images are also given in the bottom.

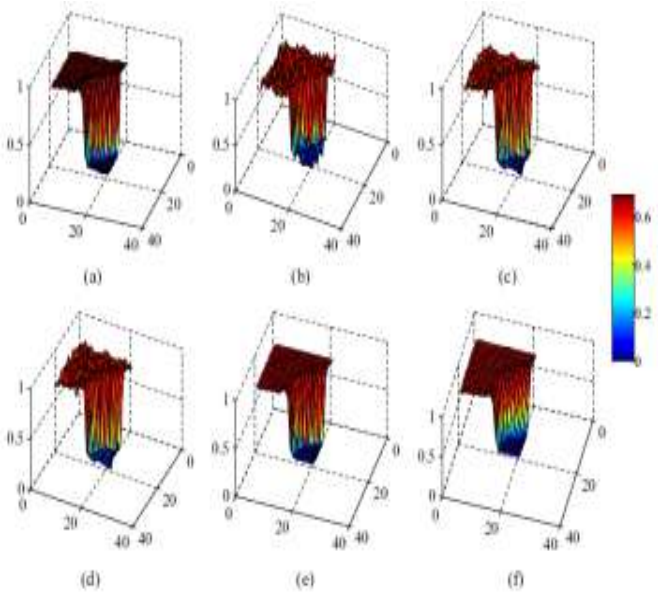

(a) (b) (c)

(d) (e) (f)

Figure 3: Highlighted parts of Figure3 shown as 3D plots for the visualization of staircase artefacts.

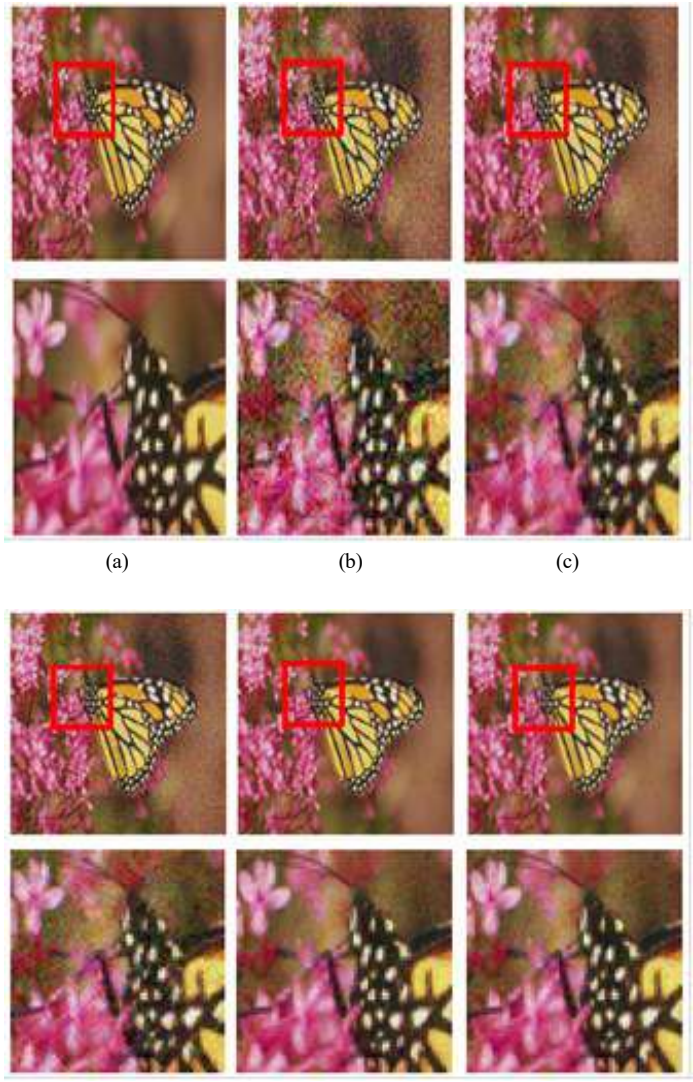

(a) (b) (c)

(d) (e) (f)

Figure 4: The denoising of the colour image *Monarch*. (a) Original image, (b) image corrupted by a Gaussian noise of σ = 25, image denoised by (c) anisotropic TV, (d) isotropic TV, (e) the proposed HVD and (f) higher order TV regularizers. Highlighted parts of these images are also given in the bottom.

VI. CONCLUSION

This paper presented a novel sparsity enhancing variational regularizer for multi-channel image denoising. It investigated sparsity enhancing regularizers in the context of variational methods. The proposed HVD regularizer was proven to be rotationally invariant to camera motions. TV regularizer is known to generate staircase artefacts in the computed solution. However, the HVD regularizer was shown to reduce these artefacts significantly. The proposed regularizer was applied to the problem of image denoising. Experiments were conducted to show that the proposed regularizer can produce results better than TV based regularizers in terms of higher PSNR and better visual quality.

Table 2: PSNR results for the denoising of all eight images using optimum values of regularization parameters.

Image	Anisotropic TV	Isotropic TV	Proposed HVD	Higher order TV
Cameraman	27.85	27.18	**30.21**	29.38
Barbara	28.65	28.27	30.28	**30.43**
Boat	26.6	26.94	**30.46**	30.07
Man	27.36	27.02	**31.09**	30.42
Baboon	26.95	26.15	29.84	**30.67**
House	27.61	27.09	**30.48**	30.12
Monarch	28.58	28.07	**30.92**	30.15
Pepper	28.64	28.56	**30.67**	29.81

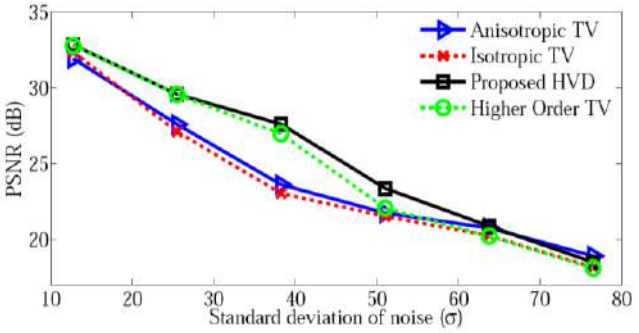

(a)

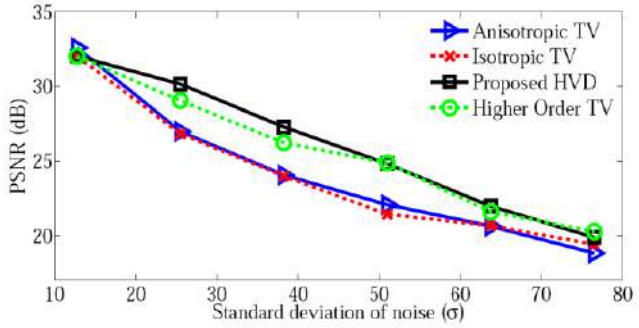

(b)

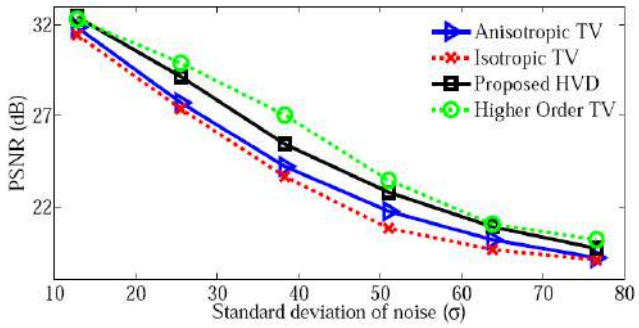

(c)

Figure 5: The PSNR as a function of the standard deviation σ of noise for anisotropic TV, isotropic TV, proposed HVD and higher order TV regularizers. Results for (a) the whole dataset of 8 images (b) *Cameraman* and (c) *Pepper*. Regularization parameters of all four regularizers have been tuned to get best PSNR performances.

REFERENCES

1. D. Bappy, I. Jeon, 'Combination of hybrid median filter and total variation minimization for medical x-ray image restoration', *IET Image Processing*, 2016, 57, (11), pp 1413-1457.
2. A. Beck, M. Teboulle, 'Fast Gradient-Based Algorithms for Constrained Total Variation Image Denoising and Deblurring Problems', *IEEE Transactions on Image Processing*, 2009, 18, (11), pp 2419-2434.
3. S. Becker, J. Bobin and E. J. Candes, 'NESTA: a fast and accurate first-order method for sparse recovery', *SIAM Journal on Imaging Sciences*, 2011, 4, (1), pp 1-39.
4. J. Bioucas-Dias, M. Figueiredo, 'A New TwIST: Two-Step Iterative Shrinkage/ Thresholding Algorithms for Image Restoration', *IEEE Transactions on Image Processing*, 2007, 16, (12), pp 2992-3004.
5. E. J. Candes, M. B. Wakin and S. Boyd, 'Enhancing Sparsity by Reweighted L1 Minimization', *Journal of Fourier Analysis and Applications*, 2008, 14, (5), pp 877-905.
6. A. Chambolle, T. Pock, 'A First-Order Primal-Dual Algorithm for Convex Problems with Applications to Imaging', *Journal of Mathematical Imaging and Vision*, 2011, 40, (1), pp 120-145.
7. T. F. Chan, A. Mulet, 'High-order total variation-based image restoration', *SIAM Journal on Scientific Computing*, 2000, 22, (2), pp 503-516.
8. T. F. Chan, A. M. Yip and F. E. Park, 'Simultaneous total variation image inpainting and blind deconvolution', *International Journal of Imaging Systems and Technology*, 2005, 15, (1), pp 92-102.
9. K. Choi, J. Wang, L. Zhu, T-S. Suh, S. Boyd and L. Xing, 'Compressed sensing based cone-beam computed tomography reconstruction with a first-order method', *Medical Physics*, 2010, 37, (9), pp 5113-5125.
10. J. Dahl, P. C. Hansen, S. H. Jenson and T. L. Jensen, 'Algorithms and software for total variation image reconstruction via first-order methods', *Numerical Algorithms*, 2009, 53, (1), pp 67-92.
11. J. Darbon and M. Sigelle, 'Image restoration with discrete constrained total variation, Part I: fast and exact optimization', *Journal of Mathematical Imaging and Vision*, 2006, 26, (3), pp 261-276.
12. M. Elad M. and M. Aharon,'Image denoising via sparse and redundant representations over learned dictionaries', *IEEE Transactions on Image Processing*, 2006, 15, (12), pp 3736-3745.
13. S. Esedoglu and S. Osher, 'Decomposition of Images by the Anisotropic Rudin-Osher-Fatemi Model', *Communications on Pure and Applied Mathematics*, 2004, 57, (1), pp 1609-1626.
14. M. A. T. Figueiredo, R. D. Nowak and S. J. Wright, 'Gradient projection for sparse reconstruction: Application to compressed sensing and other inverse problems', *IEEE Journal of Selected Topics in Signal Processing*, 2006, 1, (4), pp 586-597.
15. I. M. Gelfand and S. V. Fomin, *'Calculus of Variations*', Courier Dover Publications, 2005.

16. G. Gilboa and S. Osher, 'Nonlocal operators with applications to image processing', *Multiscale Modeling and Simulation*, 2008, 7, (3), pp 1005-1028.
17. D. Goldfarb and W. Yin, 'Parametric Maximum Flow Algorithms for Fast Total Variation Minimization', *SIAM Journal on Scientific Computing*, 2009, 31, (5), pp 3712-3743.
18. M. A. Kitchener, A. Bouzerdoum and S. L. Phung, 'Adaptive regularization for image restoration using a variational inequality approach', *In Proceedings of the IEEE International Conference on Image Processing*, Sep. 2010, pp 2513-2516.
19. A. Matakos, S. Ramani, J. A. Fessler, 'Accelerated edge-preserving image restoration without boundary artifacts', *IEEE transactions on image processing*, 2013, 22, (5), pp 2019-2029.
20. J. P. Oliveira, J. Bioucas-Dias and M. Figueiredo, 'Adaptive total variation image deblurring: A majorization-minimization approach', *Signal Processing*, 2009, 89, (9), pp 1683-1693.
21. G. Peyre, S. Bougleux and L. Cohen, 'Non-local Regularization of Inverse Problems', *In Proceedings of the European Conference on Computer Vision*, 2008, pp 57-68. Springer Berlin Heidelberg.
22. R. Ranftl, K. Bredies and T. Pock, 'Non-local total generalized variation for optical flow estimation', *In Proceedings of the European Conference on Computer Vision*, 2014, pp 439-454.
23. Z. F. Pang, Y. M. Zhou, T. Wu and D. J. Li, 'Image denoising via a new anisotropic total-variation-based model', *Signal Processing: Image Communication*, 2019, 74, 140 – 152.
24. X. Shu and N. Ahuja, 'Hybrid compressive sampling via a new total variation TVL1', *In Proceedings of the European Conference on Computer Vision*, Sep. 2010, pp 393-404.
25. Y. Wang, J. Yang, W. Yin and Y. Zhang, 'A New Alternating Minimization Algorithm for Total Variation Image Reconstruction', *SIAM Journal on Imaging Sciences*, 2008, 1, (3), pp 248-272.
26. L. Wanga , L. Xiaoa , J. Zhang and Z. Weia, 'New image restoration method associated with tetrolets shrinkage and weighted anisotropic total variation', *Signal Processing*, 2013, 93, (4), pp 661-670.
27. L. Xinwu, 'Weighted total generalised variation scheme for image restoration', *IET Image Processing*, 2016, 10, (1), pp 80 - 88.
28. A. B. Said,; R. Hadjidj.and S. Foufou, 'Total Variation for Image Denoising Based on a Novel Smart Edge Detector: An Application to Medical Images', *Journal of Mathematical Imaging and Vision*, 2019, 61, 106-121.